UCSF
UC San Francisco Electronic Theses and Dissertations

Title
Ornithine decarboxylase in the African trypanosome

Permalink
https://escholarship.org/uc/item/34f66254

Author
Phillips, Margaret A.

Publication Date
1988

Peer reviewed|Thesis/dissertation

eScholarship.org Powered by the California Digital Library
University of California

ACKNOWLEDGMENTS

I would first like to thank my advisor Dr. C.C. Wang for his guidance throughout my graduate work. His help while I was preparing for my oral qualifying exam and his expert scientific advice while I was engaged in the research that makes up this thesis were essential to my success. I am grateful also to Dr. Phil Coffino for his valuable technical and scientific assistance during the ornithine decarboxylase cloning, sequencing and expression experiments. I also extend thanks to all my laboratory associates for their friendship throughout my graduate studies: Dr. Susan Aldritt, Dr. Alice Wang and Dr. Rashid Aman for teaching me basic laboratory techniques; Dr. Liz Hedstrom, Dr. Rich Miller, and Mr. Rick Dovey for their advice on protein purification and enzyme kinetics; Dr. Patsy Babbit and Ms. Madhu Macrae, for their advice on cloning and sequencing techniques; Ms. Heidi Louie for purifying bloodstream form trypanosomes for me and Ms. Kathy Bass for helping me verify the ODC sequence after mutagenesis. I would also like to thank my family, Dr. Dan Garwood and my parents Dr. and Mrs. Theodore Phillips for their support throughout my graduate education.

ABSTRACT African trypanosomes, the causative agents of sleeping sickness in man and nagana in cattle, remain a health threat despite available chemotherapy. DL-α-difluoromethylornithine (DFMO) is an irreversible inhibitor of ornithine decarboxylase (ODC), a key enzyme in polyamine biosynthesis. Inhibition of trypanosomal ODC by DFMO results in cessation of cell growth and clearing of the parasite from the bloodstream while no serious effects on the host occur. The importance of polyamine biosynthesis to the trypanosome, exemplified by the antitrypanosomal action of DFMO, prompted us to initiate a thorough study of ODC.

In mammals the isolation of DFMO resistant mutants that overproduce ODC facilitated study of this low level protein. A trypanosome mutant resistant to DFMO was therefore isolated. The mutant, unfortunately, contained the same level of ODC activity as the wild-type, while drug accumulation was significantly decreased.

The gene encoding *Trypanosoma brucei brucei* ODC was identified by cross hybridization to mouse ODC cDNA. The *T. brucei* gene has an open reading frame of 445 amino acids that shares 61.5% identity with the mouse enzyme. The major differences were the addition of a 20 amino acid N-terminal peptide and the deletion of a 36 amino acid C-terminal peptide in the *T. brucei* ODC. The absence of this C-terminal peptide, which contains a PEST sequence, predicts a slow *in vivo* turnover for the parasite enzyme. This was supported by our data. Slow turnover of ODC in trypanosomes may explain the basis of the selective antitrypanosomal action of DFMO.

Recombinant *T. brucei* ODC was produced in *Escherichia coli* and purified 2200 fold to apparent homogeneity. The recombinant protein has a specific activity of 3.2×10^6 nmol CO_2/hr/mg protein, two identical subunits each of 45 kdal, and a P_I of 5.0. The K_m for ornithine is 303 μM, the K_I for DFMO is 154 μM with a halflife of inactivation at infinite DFMO concentration of 3.9 min. These values are in excellent agreement with the results we obtained for purified authentic *T. brucei* ODC.

TABLE OF CONTENTS:

Title	Page
Introduction	1
Chapter 1: A *Trypanosoma brucei* mutant resistant to α-difluoromethylornithine.	20
Materials and Methods	21
Results	23
Discussion	26
Chapter 2: Cloning and sequencing of the ornithine decarboxylase gene from *Trypanosoma brucei. Implications for enzyme turnover and selective difluoromethylornithine inhibition.*	38
Materials and Methods	39
Results	42
Discussion	45
Chapter 3: Purification and characterization of ornithine decarboxylase from *Trypanosoma brucei.*	61
Materials and Methods	62
Results and Discussion	65
Chapter 4: Expression of *Trypanosoma brucei* ornithine decarboxylase in *E. coli*: *Purification and characterization of the recombinant enzyme.*	77
Materials and Methods	78
Results	81
Discussion	84
Conclusion	102
References	104

LIST OF TABLES

Table	Page
3.1) Native *T. brucei* ODC purification scheme.	67
3.2) Comparison of the physical and kinetic characteristics of mouse and *T. brucei* ODC.	68
4.1) Expression of *T. brucei* ODC activity in *E. coli* HT298 cells.	86
4.2) Recombinant *T. brucei* ODC purification scheme.	87
4.3) Comparison of physical and kinetic characteristics of *T. brucei* native and recombinant ODC.	88

LIST OF FIGURES:

Title	Page
I.1) Life cycle of *T. brucei.*	3
I.2) Infection course of *T. brucei.*	5
I.3) Polyamine biosynthetic pathway.	10
I.4) Inhibitors of polyamine biosynthesis.	14
1.1) Growth inhibition of *T. brucei* procyclic forms by DFMO.	29
1.2) Selection of a DFMO resistant *T. brucei* mutant.	30
1.3) Ornithine metabolism in procyclic forms of *T. brucei.*	31
1.4) DFMO uptake by wild-type and DFMO resistant *T. brucei* procyclic cells.	32
1.5) A. Ornithine uptake by wild-type and DFMO resistant *T. brucei* procyclic cells.	33
B. Putrescine uptake by wild-type and DFMO resistant *T. brucei* procyclic cells.	34
1.6) Stability of DFMO resistant *T. brucei* mutant phenotypes.	35
1.7) Competition of analogs for ornithine uptake in *T. brucei* wild-type cells.	36
1.8) The effects of transport inhibitors and temperature on DFMO uptake in wild-type *T. brucei* cells.	37
2.1) Molecular weight determination of *T. brucei* ornithine decarboxylase.	
A. Native	48
B. Subunit	50
2.2) Southern blot analysis of *T. brucei* genomic DNA probed with mouse ornithine decarboxylase cDNA.	52
2.3) Southern blot analysis of *T. brucei* cosmid DNA probed with mouse ornithine decarboxylase cDNA.	54
2.4) Restriction map of the *T. brucei* ornithine decarboxylase gene.	55
2.5) Northern blot analysis of *T. brucei* poly(A)$^+$ RNA probed with the *T. brucei* ornithine decarboxylase gene.	57
2.6) Nucleotide sequence of the ornithine decarboxylase gene from *T. brucei.*	58

Title	Page

2.7) Comparison of the amino acid sequences between *T. brucei* ornithine decarboxylase and the mouse ornithine decarboxylase. 59

2.8) Measurement of the turnover rate of *T. brucei* ornithine decarboxylase. 60

3.1) Native *T. brucei* ODC purification, pyridoxamine phosphate affinity column elution profile. 69

3.2) Native *T. brucei* ODC purification, Mono Q column elution profile. 70

3.3) Native *T. brucei* ODC purification, Superose 6 column elution profile. 71

3.4) SDS-PAGE analysis of purified *T. brucei* ODC. 73

3.5) K_m determination for *T. brucei* ODC. 74

3.6) DFMO inactivation of *T. brucei* ODC, time dependence and K_I. 75

3.7) Native *T. brucei* ODC purification, Mono P column elution profile, PI determination. 76

4.1) *In vitro* translation and immunoprecipitation of *T. brucei* ODC. 90

4.2) Construction of the *T. brucei* ODC gene expression vector pQtODC.8. 91

4.3) Turnover of *T. brucei* ODC expressed in *E. coli* HT289 cells. 93

4.4) Recombinant *T. brucei* ODC purification, pyridoxamine phosphate affinity column elution profile. 94

4.5) Recombinant *T. brucei* ODC purification, mono Q column elution profile. 95

4.6) SDS-PAGE analysis of purified recombinant *T. brucei* ODC. 97

4.7) Recombinant *T. brucei* ODC purification, superose 6 column elution profile. 98

4.8) K_m determination for recombinant *T. brucei* ODC. 99

4.9) DFMO inactivation of recombinant *T. brucei* ODC, time dependence and K_I. 100

4.10) Recombinant *T. brucei* ODC purification, Mono P column elution profile, PI determination. 101

INTRODUCTION

Trypanosomiasis

The African trypanosomes are a family of parasitic protozoa that cause African sleeping sickness in man and nagana in cattle. Two species, *T. brucei gambiense*, found mainly in western and central Africa, and *T. brucei rhodesiense*, found in east Africa, are responsible for the disease in man(1). Both species, as well as the species affecting livestock, are transmitted by the tsetse fly. Approximately 250,000 people are affected by this disease which, both epidemic and endemic, is almost always fatal if untreated(1). The organism is deposited into the dermal connective tissue by the tsetse fly and from there enters the draining lymphatics, the bloodstream and in later stages crosses the choroid plexus into the brain and cerebrospinal fluid(2). The initial infection results in a nodular lesion, a chancre, developing at the site of the fly bite where the dividing trypanosome remains localized for several days before traveling to the bloodstream. For *T.b. gambiense* it may take years before early symptoms appear and months to years more before late symptoms emerge. However, for *T.b. rhodesiense* a fulminent early stage infection can occur within 2 to 3 weeks followed by onset of the late stage disease within another 2-3 weeks(1). The early infection, caused by circulating organisms in the blood stream, is characterized by fever and lymphadenopathy. Heart failure and jaundice may also occur in Rhodesian sleeping sickness(3). The trypanosome then invades the central nervous system causing symptoms characteristic of the late stage of the disease(3). These include behavioral and personality changes, hallucinations and delusions. Headache and drowsiness are also common. If the patient is not treated, their level of consciousness deteriorates until they lapse into a coma and die(3).

Treatment of African trypanosomiasis classically falls into two courses. Early stage trypanosomiasis can be treated with suramin, a relatively non toxic drug. It is, however, ineffective against late stage infection. Late stage infection is treated with an arsenic containing compound melarsoprol B, which is very toxic, causing myocarditis, renal damage and encephalopathy. Up to 5% of patients will die from the disease or drug-related encephalopathy when treatment is not initiated prior to onset of late stage disease(3). A new chemotherapeutic agent, difluoromethylornithine(DFMO), has recently been tested successfully against trypanosomiasis in mice(4) and in man(5). DFMO, a mechanism based inhibitor of ornithine decarboxylase (ODC), is able to cure both early and late stage infections of *T. gambiense* in clinical trials in man and does not appear to be particularly toxic(5). Thus it may be the drug of choice for the treatment of trypanosomiasis in the future. Its mechanism of action will be discussed in detail below.

Despite the prevalence of trypanosome infections in man, the major problem caused by the trypanosome is the infection of livestock. Cattle trypanosomiasis, caused by *T. brucei brucei*, has prevented cattle ranching in most of tropical Africa to date and has been a major cause of malnutrition and suboptimal economic growth in the region(1). Despite the use of several methods for control of livestock trypanosomiasis including chemotherapy, insecticides to remove the vector and use of trypanotolerent livestock no real progress has been made. Clearly, additional methods for control of this pathogen are still needed.

The trypanosome life cycle

The trypanosome is a uniflagellete with a width of 1.5 um and a length of 10-40 um depending on the life cycle stage(3). It is a member of order kinetoplastida, and as such contains a prominent kinetoplast, a network of interlocked circular DNA molecules encoding mitochondrial DNA(2). The kinetoplast DNA consists of two circular species, maxicircles(20-40kb) of which there are 25-50 copies, and minicircles(0.5-2.3kb), of which there are 5000-10000 copies per cell(2). The maxi circles contain genes for cytochrome oxidase, cytochrome b,9S rRNA, 12S rRNA and NADH dehydrogenase, whereas the minicircles do not appear to be transcribed(2). Two morphological stages of *T. brucei*, the trypomastigote which has a postnuclear kinetoplast and the epimastigote which has a prenuclear kinetoplast, have been described(2). In addition, the size, shape and biochemistry of these two morphological species vary greatly at different stages of the parasites' life cycle. The morphological changes of the cattle parasite *T. brucei brucei* are outlined in Figure I-1. The most striking biochemical changes occur in the single mitochondrion and the surface membrane of the organism as it prepares to adapt to life in the second of its two hosts.

There are two bloodstream stages of the trypanosome, the long slender trypomastigote and the short stumpy trypomastigote. The long slender trypomastigote divides by binary fission, as do all dividing forms of the organism. Its sole source of energy is derived from glycolysis. The parasite is extremely efficient at glycolysis and is able to obtain a rate of glycolysis that is 50 times higher than its mammalian host(7). The glycolytic enzymes are located in a membrane bound organelle termed the glycosome of which there are approximately 200 copies in the long slender form. The single mitochondrion lacks cristae and does not perform cytochrome mediated electron transport. Oxidation of NADH does occur, but it is linked to a glycerol 3-phosphate dehydrogenase-glycerol-3-phosphate oxidase shuttle system(2). While the bloodstream parasite is able to take advantage of the glucose rich environment of the mammalian host to consolidate its energy producing machinery, it could not survive without having evolved a complex mechanism for protecting itself from the host immune response. The long slender trypomastigote has an electron dense layer 12-15 nm thick, made up of 10^7 identical

The Life Cycle of T. Brucei

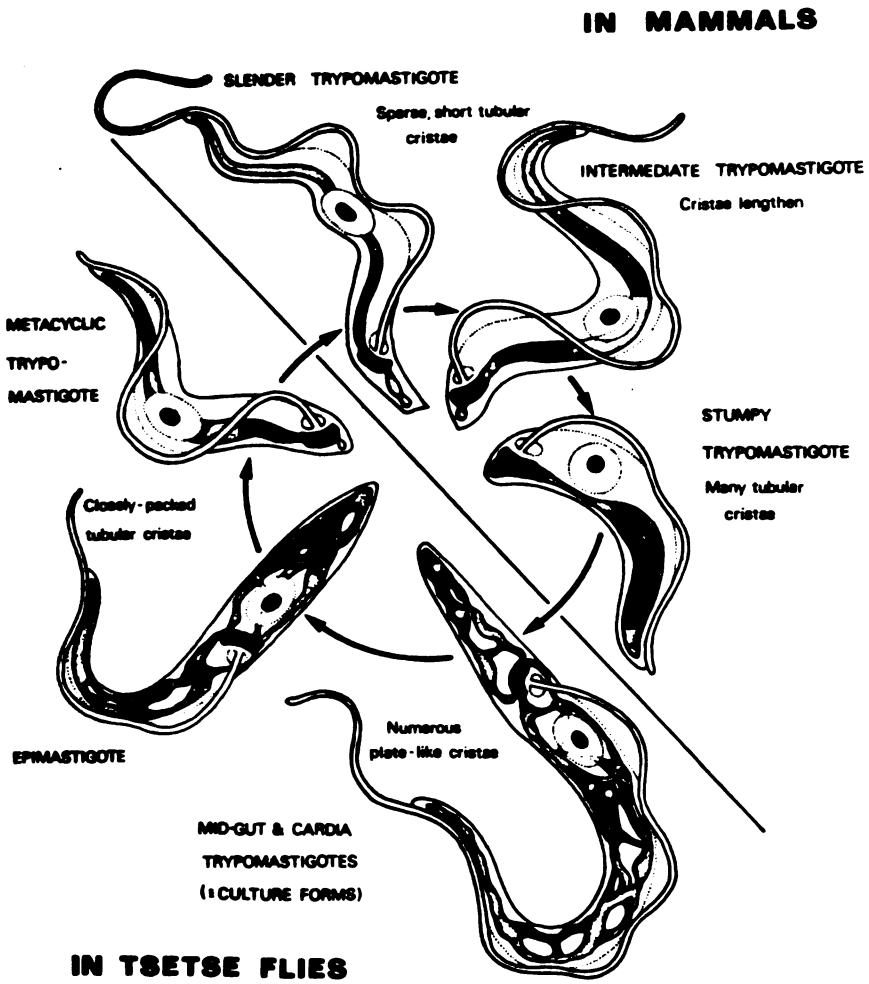

FIG. 2-6. Scheme showing changes in the form of the mitochondrion and its cristae during the life cycle of *Trypanosoma brucei*. (Vickerman, *in* Ecology and Physiology of Parasites, 1971. Courtesy University of Toronto Press.)

Figure I-1. Life cycle of *Trypanosoma brucei*.

glycoproteins(10% of the cell protein), termed variant surface glycoprotein(VSG), on its membrane surface(2). The trypansosome contains up to1000 separate genes which encode antigenically distinct VSG. In a population of dividing trypanosomes most will be expressing the same VSG on their surface. In addition to this major population, immunofluorescence shows that some of the organisms will be expressing a different VSG on their surface. When the host mounts an IgM response to the major VSG, parasitemia declines and the long slender trypomastigotes with the major VSG die(2). The organisms that express a different VSG can continue to multiply during remission until one overgrows the others and again parasitemia may peak(2). This fluctuation of parasitemia, the result of antigenic variation through the sequential expression of genes encoding immunologically distinct VSG, will continue over the entire course of the infection as illustrated in Figure I-2(8).

The short stumpy bloodstream form is the non dividing blood form that emerges from the long slender trypomastigote as it begins to undergo the biochemical and morphological changes necessary to prepare itself for life in the insect vector. The mitochondrion swells and develops cristae, and proline and α–ketoglutarate oxidase appear. When the tsetse fly takes a blood meal, short stumpy trypamastigotes are brought to the mid gut of the fly where they transform to the dividing procyclic form. This is accompanied by the loss of VSG, an increase in body length, a further expansion of the mitochondrion into a branched network and a change in shape of the glycosome(2). Proline instead of glucose becomes the major energy source. This is followed by the appearance of fully functional cytochrome mediated mitochondrial respiration(2).

The procyclic trypomastigotes migrate to the salivary gland of the fly where they transforms to the dividing epimastigotes that attach by the flagellum to the microvilli of the epithelial cells lining the gland lumen. The epimastigote then transforms to the metacyclic trypomastigote. This transformation is accompanied by a change back to an unbranched mitochodrion and the appearance of functional spherical glycosomes (2). The nondividing metacyclic form also has VSG on its membrane surface. The metacyclic trypomastigote is deposited into the dermal connective tissue of the mammalian host by the fly where it transforms to the long slender blood stream form(2).

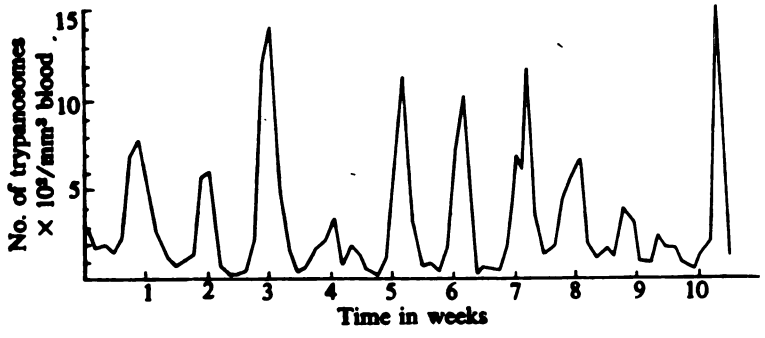

Figure I-2. The infection course of *T. brucei* in the host blood stream.

Molecular Biology

A. VSG

VSG is a glycoprotein that fully covers the entire cellular surface of the blood stream stages of the African trypanosome thereby protecting it from the host immune response (2). VSG has a molecular weight of approximately 60 kdal, composed of 450 amino acids and 7-17% carbohydrate(9). The molecule is arranged into two domains, the N-terminal domain which is variable among the different VSG's, and the C-terminal domain, which is relatively constant(9). A 20 amino acid N- terminal signal sequence that directs the protein to the membrane is cleaved off in the mature protein. In addition, a hydrophobic C-terminal peptide is cleaved and replaced by a glycophospholipid that attaches VSG to the membrane via the α carboxyl of the C- terminal amino acid,either serine or aspartate (10). The attachment of the carbohydrate anchor, through the diacylglycerol moiety of phosphatidylinositol, was initially thought to be very novel, but has since been reported for a number of non trypanosomal proteins(11). Osmotic shock or mechanical disruption of the cell membrane results in the release of soluble VSG by a membrane bound glycan-phosphatidylinositol specific phospholipase C(12). The physiological role of the phospholipase C is unknown, but is speculated to be involved in release of VSG during transformation from short stumpy to procyclic trypomastigotes(12).

X-ray crystallographic study of two separate VSG clones, ILTat 1.24 and MITat 1.2, has revealed that despite the lack of homology in the first 350 amino acids of the N-terminal domain, there are strong structural similarities between them(13). The existence of an underlying structural motif within the VSG's would allow for the easy replacement of one for another at the parasite's surface. Thus, it appears that the primary selection pressure for the survival of a VSG sequence may be their ability to fulfill the three dimensional structural requirements.

There are as many as 1000 separate VSG genes in *T. brucei*, yet only one is expressed at any given time. Thus, an intriguing aspect of *T. brucei* is the genetic mechanism by which the organism undergoes antigenic variation. Much has been learned about this process through the cloning and sequencing of numerous VSG genes. Despite this knowledge, the trigger that initiates the VSG change is still unknown. Many of the 1000 genes are clustered at internal positions on the chromosome and many others are found at positions near one of the over 200 chromosome ends(14). These genes are the silent or basic copy VSG genes. The active gene always has a telomeric location in one of several VSG gene expression sites. The mechanism by which a particular expression site becomes activated is unknown, but a basic copy gene can be activated for expression by being transferred to one of these active telomeric sites via several

mechanisms. A basic copy gene can undergo duplicative transposition to the expression site, which involves replication of an extra gene copy(14). Alternatively, reciprocal exchange of telomeres or telomere conversion may occur(14).

Maturation of mRNA in the trypanosome occurs through trans splicing of two exons that are transcribed from separate genes. The 5' exon, common to all the gene transcripts, contributes a capped 35 nucleotide exon and will be discussed in detail later. The VSG gene transcript is a 60 kb polycistronic unit from which VSG mRNA and several other mature mRNAs are generated by trans splicing to the 5' exon(16). The expression site for VSG is a telomere containing regulatory regions which control the synthesis of the polycistronic transcript. The expression site contains from 5' to 3' several expression site associated genes, as much as 10 kb of a 70 bp imperfect repeat and the transposed segment containing the VSG gene(14).

B. Discontinuous transcription and formation of mature messenger RNA in the Trypanosome.

Maturation of mRNA in the trypanosome is unlike that described for other eukaryotic mRNA. All trypanosome mRNA's are derived from two separate exons, initially transcribed from separate genes and spliced together in a trans splicing event(15). The 5' end is a 35 nucleotide exon contributed by a 140 base long medRNA (mini-exon-derived) which is transcribed from a 1.35 kb gene found as tandem repeats of 200 copies within the genome. The medRNA contains a cap structure and is synthesized by RNA polymerase II. It is spliced onto the acceptor RNA(transcript of the structural gene) in an event that has a lot in common with the typical eukaryotic mRNA processing. The acceptor splice sites at the intron-exon boundary are identical to the normal eukaryotic cis- splicing sites($(C/T)_N$NNAG)(15). Trans splicing involves cleavage of the mini-exon intron boundary, followed by trans-esterification of the 5' phosphate on the 100 nucleotide intron and joining of this intron through a 2'-5' phosphodiester bound to the donor RNA to form a Y-shaped branched RNA. This is analogous to the formation of the lariat in typical cis-splicing event. Trans-esterification with the 3' hydroxyl group of the 35 nucleotide mini exon to the intron boundary of the acceptor RNA releases the branched RNA which contains both introns, and forms the mature mRNA in the process. Introns within structural genes and thus, the typical cis-splicing event seen in other eukaryotic cells, have never been described in trypanosomes.

Traditional eukaryotic promotors for transcription initiation have not been described for any trypanosome gene. Most of the genes studied so far are found in the genome as tandem arrays. There is now overwhelming evidence that a number of genes are transcribed initially as polycistronic messages, which through addition of the mini exon in the trans-splicing event, are separated into unique, capped mature messages(15). VSG mRNA, for example, is initially produced as a 60 kb transcript, which yields upon processing, at least 8 stable mature

mRNAs(16). Transcription promotors will only be required at the start of each polycistronic transcript, explaining why a consensus promotor sequence has not been found directly preceding any of the studied genes.

C. Analysis of Genes.

Trypanosoma brucei contains approximately 2.5×10^7 base pairs of DNA per haploid genome (6). Genes encoding four glycolytic enzymes (87), calmodulin (88), α and β tubulin (89), heat shock protein (73),VSG (17) and, as will be detailed in this thesis, ornithine decarboxylase (ODC), have been cloned and sequenced at this point. The trypanosome contains multiple copies of most of these genes organized as tandem repeats. With the exception of VSG, the cloning of these genes was achieved through cross hybridization to their counterpart eukaryotic genes. There are two copies of the aldolase (ALDO) (87) and glyceraldehyde phosphate dehydrogenase (GAPDH) (87) genes, three copies of phosphoglycerate kinase (PGK)(87) and calmodulin genes, seven copies of the heat shock gene and 14-17 copies of the tandem unit that contains both the α and β tubulin genes (89). Triosephosphate isomerase (TIM) and ODC are the only genes studied that are believed to exist as single copy in the genome (87). In addition, the sequence of a number of mitochondrial genes and genes encoding rRNA have been identified on the maxi circle DNA (17).

The number of genes that have been well characterized in *T. brucei* is quite limited. As discussed above, with the exception of the mini-exon splice site, no similarities in the 5' and 3' untranslated regions of the genes have emerged . The transcription initiation site and the polyadenylation signal are both unknown at this time(17). Codon usage in the trypanosome genes is similar to that in other organisms, in that there is a bias. For the house keeping genes C is favored over A at the third position of the triplet, particularly for GAPDH, ALDO, TIM, α and β tubulin and calmodulin(18), but is not pronounced for PGK or ODC. This preference for C is unique to the third base as the distribution of the four nucleotides is constant at the first two positions. In contrast, VSG preferentially uses A in all positions where T is rarely found in any(18), implying that VSG codon usage is not biased. The fact that VSG is a very abundant protein(10% of cellular protein) but shows no codon preference is somewhat unusual since codon biases seem to play a role in the efficiency of translation, and are usually most pronounced in abundant proteins.

ORNITHINE DECARBOXYLASE

A. Characteristics and regulation in mammalian cells

Ornithine decarboxylase (ODC) is the initial and rate limiting step in the biosynthesis of the aliphatic cations known as the polyamines(19). ODC catalyses the conversion of ornithine to putrescine, the first polyamine formed in the pathway. In mammalian cells this reaction provides the sole source of putrescine as illustrated in Figure I-3. Plants and *Escherichia coli* are also able to produce putrescine via the decarboxylation of arginine to form agmatine as a precursor to putrescine(34). Putrescine is then combined with decarboxylated S-adenosyl-L-methionine to produce first spermidine and then, with the addition of a second decarboxylated S-adenosyl-L-methionine, spermine. The polyamines are thus normal cell constituents and they are required for normal cell growth. ODC, as the rate limiting enzyme in their formation, is a highly regulated essential enzyme for normal cell growth. Mammalian ODC has a very short halflife of 15-30 min (20) which may contribute to its ability to rapidly increase or decrease its levels in response to a number of extra- and intracellular factors. ODC activity peaks at specific points in the cell cycle, its activity is induced by all known classes of hormones acting on their specific target organs and by a variety of tumor promoting agents(19). ODC and the gene encoding it have both been well characterized. The protein has been purified from a number of mammalian tissues (19) as well as from *E. coli*, yeast, and *Physarum polycephalum* (20). The cDNA coding for ODC has been cloned and sequenced from two mammalian sources, mouse (21-23) and human (24). Genomic clones of ODC from yeast (25) and from mouse (26) have also been analyzed. The yeast ODC gene contains no introns whereas the mouse ODC gene contains 11 introns.

Trophic polypeptide and amine hormones all induce ODC in their target tissue resulting in an increase in polyamine synthesis (19). The induction requires both new RNA and protein synthesis. Induction of ODC is accompanied by induction of RNA polymerase I resulting also in an increase in rRNA levels (19). Growth hormone stimulates ODC in liver, adrenal, heart, kidney, thymus and developing brain while folical stimulating hormone induces ODC activity in the ovary and testis. cAMP has been postulated by some to mediate these hormonal inductions of ODC activity through the stimulation of cAMP dependent protein kinases (19). A potential cAMP binding site has also been found 48 nucleotides upstream of the transcription initiation site of the mouse ODC gene (26). ODC is induced in regenerating liver after partial hepatectomy. The process is dependent on both new protein and RNA synthesis while the turnover of the enzyme is unaffected (19).

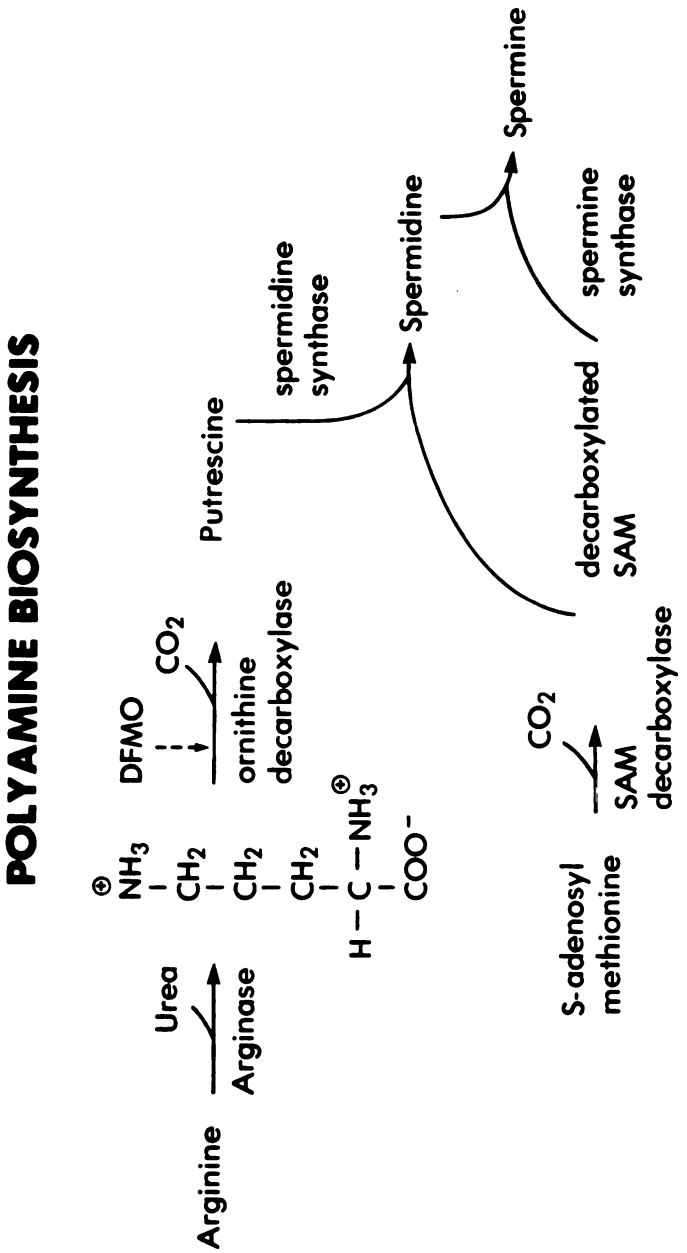

Figure I-3. Polyamine metabolism in mammals and trypanosomes.

Steroid hormones also induce ODC activity in certain tissues. The best documented example of this type of ODC induction is the effect of testosterone on mouse kidney. Unlike the effect of trophic hormones the regulation of steroid ODC induction may be transcriptional, translational or both. Currently, three molecular mechanisms are believed to account for the fluctuations in ODC activity ; transcriptional regulation, translational regulation and post translational regulation(effecting enzyme stability or activity). Testosterone treatment of male mice resulted in an increase in immunoreactive ODC from 0.004% to 0.05% of cytosol protein(28). This induction is mediated by an androgen receptor-dependent mechanism because the induction does not take place in kidneys of mice lacking functional androgen receptors. It can be accounted for in part by an increase in the halflife of the immunoreactive ODC from 16 min to 140 min(28). A similar change in halflife was observed when actual enzyme activity was measured(28). This change in ODC halflife implies that post translational modification may regulate ODC activity . The increase in ODC is also in part due to a 10 to 20 fold increase in the steady state level of ODC mRNA(22).

Tumor promoting agents, most notably the phorbol esters, induce a rapid increase in ODC activity, followed by eventual formation of tumor in the exposed region (19). These observations have led to the postulate that ODC may play a fundamental role in tumor promotion. For example, 12-o-tetradecanoyl phorbol-13-acetate (TPA), a potent tumor promotor when applied to mouse skin, increases ODC activity 230 fold within 4 hrs. This induction requires protein but not RNA synthesis. When a related class of phorbol esters is compared, one finds the magnitude of the ODC induction is directly related to their relative tumor promoting capacity (19). DFMO can block the ODC induction and reduce tumor incidence. TPA induction of ODC also appears to be related to changes in ODC mRNA levels. They were increased by 20-50 fold in murine 3T3 cells treated with TPA(29). A four fold increase in transcription rate was observed but this could not account for the entire increase. Stable ODC transcripts that were increased by TPA could be detected in cycloheximide pretreated fibroblasts (29), implying that TPA induction of ODC mRNA levels may in part be due to an increased halflife of ODC mRNA(29).

A series of DFMO resistant mouse lymphoma S49 cells has also been thoroughly characterized(30). Gene amplification, resulting in increased ODC levels in the mutants, was shown to account for the resistance to high levels of DFMO (10 mM). However, in cells resistant to lower levels (0.1 mM) several other mechanisms were observed. An increase in the synthetic rate of ODC accounted at least in part for the resistance of two of the cell lines(30). Two other cell lines were resistant to 0.1 mM DFMO because of increases in the steady state ODC mRNA levels. Yet, none of the DFMO resistant cell lines showed changes in ODC stability(30).

ODC levels are also affected by the addition of exogenous polyamines to cells in culture. In mouse lymphoma S49 cells,10 μM putrescine causes a 7-12 fold reduction of ODC activity. Since the ODC mRNA levels remain unchanged, the polyamines apparently do not regulate ODC at the transcriptional level. The drop in ODC activity is caused by a combined decrease in the enzyme stability and in the rate of ODC mRNA translation (30). Additional evidence that polyamines regulate ODC by decreasing the synthetic rate of ODC and/or increasing the rate of enzyme degradation have been found by several other laboratories in Ehrlich ascites tumor cells(31) and Chinese hamster ovary cells(32,33).

B. The role of Polyamines

In this section the potential mechanism by which polyamines actually influence cell growth and differentiation will be discussed. The discovery of ODC inhibitors and the selection of polyamine deficient mutants have been crucial to the study of the role of polyamines. Several potent inhibitors of polyamine biosynthesis exist (27). The most interesting class of inhibitors are the inhibitors of ODC of which there are two types, competitive inhibitors like α-methylornithine (Figure I-4) and mechanism based inhibitors like α-difluoromethylornithine (DFMO)(Figure I-4). Treatment of cells with ODC inhibitors, such as DFMO, results in a decrease in putrescine and spermidine that is accompanied by cessation of cell growth (20). Notably these effects can be reversed by addition of exogenous putrescine to the cells. The second class of inhibitors that have been used are inhibitors of S-adenosylmethionine decarboxylase, a key enzyme for the formation of spermidine and spermine(Figure I-3). The most widely studied inhibitor in this class is methylglyoxal bis(guanylhydrazone) (MGBG) (Figure I-4) (27). Treatment with MGBG inhibits spermidine and spermine biosynthesis while putrescine accumulates (20). MGBG inhibits cell growth and the effects are reversible by the addition of spermidine or spermine (20). These studies on polyamine depleted cells have proven that ODC, and hence, the polyamines are essential for cell growth (27). However, despite a wealth of data, results are difficult to interpret and the exact role of these essential cations remains obscure.

The effect of polyamines on DNA synthesis. Cells that are depleted of polyamines through the use of ODC inhibitors become arrested in either the G1 or G2 phase of the cell cycle (27). When cells in a quiescent (Go) state are stimulated to grow, a dramatic increase in ODC activity occurs as the cell enters the G1 phase (27) and again in late G1-early S phase. Cells in the G1 phase undergo several events which are essential to the initiation of DNA synthesis. The increase in ODC which leads to an increase in polyamine levels is one of these essential events. The late G1 activation of ODC is also observed in continuously dividing cells (27). There is a temporal correlation between the increase in ODC activity and the time of onset of DNA replication, implying strongly that polyamines are required before the cell can initiate DNA synthesis (27). Studies to define this polyamine requirement in mammalian cells showed that polyamine starvation decreased the rate of DNA synthesis by decreasing the initiation rate of DNA synthesis (20,27). This decrease could, in turn, account for the growth inhibition by polyamine starvation. However, in polyamine deficient *E. coli* mutants, whose growth rate is only 30% of that obtainable in the presence of polyamines, polyamines were shown to inhibit the rate of DNA synthesis, a fact that is inconsistent with the observed effect on the growth rate of *E. coli* (20).

1. α-DL-difluoromethylornithine

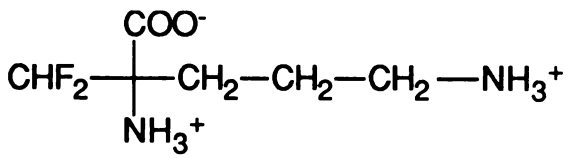

2. α-methylornithine

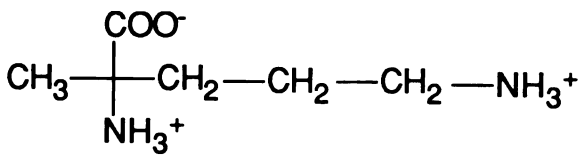

3) Methylglyoxalbis(guanylhydrozone)

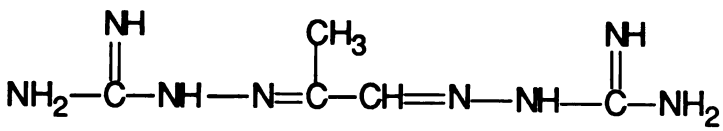

Figure I-4. Inhibitors of Polyamine biosynthesis.

Bacteriophage have been shown to contain polyamines in the mature virus, but the effects of polyamine deficiency on bacteriophage replication have been inconsistent (20). Bacteriophage T4 can be formed in the absence of polyamines but bacteriophage lamda cannot be formed when grown in polyamine deficient *E. coli* mutant cells (20). Polyamines appear to be required early in the course of phage infection as well as late for optimal packaging of phage heads (34). A role for polyamines in phage DNA packaging is supported by the observation that polyamines can condense and precipitate DNA *in vitro* (20) when 90% of the negative charges of DNA have been neutralized.

The effect of polyamines on RNA synthesis. Polyamines are postulated to be involved in almost every step of RNA synthesis and degradation (20). Many of these results are based on *in vitro* studies and the actual role of polyamines *in vivo* remains completely obscure. Polyamines are required for the maintenance and replication of yeast killer double-stranded RNA virus but the actual step that is effected is unknown. Spermidine also appears to increase the extent and accuracy of intron excision during mRNA processing (20).

The role of polyamines in protein synthesis. Polyamines facilitate the association of ribosomal subunits. Ribosomes isolated from polyamine deficient *E. coli* are less active in a protein biosynthesis system and are apparently defective in the 30S ribosomal subunit(20). Polyamines also increase the fidelity of *in vitro* translation(20), potentially by increasing the accuracy of the initial binding of aminoacyl-tRNA to the ribosome. Supporting this, spermidine is known to bind to tRNA *in vitro* (20). Fewer full length proteins are formed in the absence of polyamines implying they may also have a role in termination of protein synthesis(20). This is further supported by the inability of polyamine deficient *E. coli* cells to serve as host for certain amber mutants of T4 and T7(20).

The role of polyamines in cell division. ODC activity peaks prior to mitosis implicating the polyamines in this process as well (27). It has been postulated that polyamines are required for the chromosome condensation of interphase nuclei (27). The antimitotic agents, colchicine and vinblastine, which affect microtubular structure, both inhibit ODC activity *in vivo* but not *in vitro* lending further support to the likelihood that ODC plays a role in mitosis (27).

Polyamines and cell differentiation. Polyamines are required for proper embryonic development. Treatment of developing eggs of the polychaete *Ophryotroch lbronica* with α-methylornithine resulted in the arrest of development just prior to gastrulation(27). This inhibition is consistent with interference in rRNA synthesis, a process which begins at this stage of development. Sea Urchin eggs treated with α-methylornithine were arrested in the late blastula stage, an effect that was reversible by the addition of polyamines (27). Mutant yeast cells that are deficient in

polyamine biosynthesis are unable to grow or sporulate in the absence of exogenous polyamines(34). DFMO treatment of both chick embryo and mouse embryo arrested development very early at the stage of gastrulation(27). Development of nervous tissue also requires polyamines(35). ODC expression has a unique pattern in different regions of the brain with the highest levels being associated with the time periods of most rapid growth. DFMO arrests brain cell maturation and interferes with neuronal migration, axonogenesis and synatptogenesis, leading to the disruption of cytoarchitectural organization of the brain.

Thus, despite the inherent difficulties in defining the exact nature of polyamine involvement in cell growth and differentiation, their fundamental importance to normal cell growth in all organisms is apparent. It is,thus, not surprising that the polyamine biosynthetic pathway has become a chemotherapeutic target for treatment of cancer and African trypanosomiasis. The success of DFMO as an antitrypanosomal agent can further be attributed to the exhibited selective toxicity of the drug toward the parasite over the mammalian host. The possibility that polyamines play some unique roles in the growth of *T. brucei* has only recently been addressed and until initiation of the work described here in little was known about the *T. brucei* ODC. Thus, the mechanism by which DFMO is selectively toxic to the parasite over the host was not understood.

C. Polyamines and ODC in T. brucei

The make up of the polyamine pools and the synthetic pathways to their production in the trypanosomatids is fairly well understood (36). All three polyamines, putrescine, spermidine and spermine were found in *T. brucei* and their production appears to follow the same metabolic pathway observed in mammalian cells (Figure I-3), where ODC provides the sole source of de novo putrescine(36). Spermidine and putrescine levels are the highest in early log growth of the long-slender bloodstream *T. brucei* thus, as with mammalian cells, the polyamines appear to be required for *T. brucei* growth. As a result, inhibition of polyamine biosynthesis reduces polyamine levels and inhibits trypanosome growth(36).

DFMO, the mechanism based inhibitor of ODC, has received a lot of attention for its ability to deplete trypanosomes of polyamines and arrest cell growth. As discused previously, DFMO has been shown to be an effective antitrypanosomal agent(4). When administered in a 2% solution in the drinking water to *T. brucei* infected mice, DFMO was able to cure the trypanosome infection as illustrated by mouse survival time of longer than 30 days(4). Blood smears from the mice were free of trypanosomes from 5 days to 2 months after the treatment. No relapse of infection occured. Control mice that had received no DFMO died from trypanosomiasis within 2 days. The drug did not cure the trypanosome infection in immunosuppressed mice (41). It is only cytostatic to the parasite and apparently, to be effective, an antibody response to VSG is required to clear the drug-arrested parasite from the blood(41). DFMO completely inhibits ODC activity within 12 hours after the *in vivo* treatment and depletes the trypanosomes of up to 90% of their putrescine and of up to 50% of their spermidine(40). Spermine concentrations were slightly increased(40). After 12 hrs of DFMO treatment DNA synthesis was inhibited by 45-90%, RNA synthesis was inhibited by 50-80%while protein synthesis was actually enhanced by 50-100%(40). Parasites from mice treated with DFMO for 36 hrs were abnormal in appearance and resembled the short stumpy blood forms rather than the long slender forms. Many of the cells had multiple nuclei and kinetoplasts implying that cytokinesis had been inhibited (40). This information, taken with the fact that intraperitonealy injected putrescine was able to reverse the growth inhibitory effects of DFMO (42), implies strongly that DFMO acts on *T. brucei* by inhibiting its ODC. Thus, the general biochemical effects of DFMO on *T. brucei* appear similar to that seen on mammalian cells. The parasite, however, appears to be more sensitive to the toxic effects of DFMO as illustrated by the low toxicity of DFMO on the human host and the effectiveness of DFMO in clearing the parasite from the blood (5).

ODC was partially characterized in crude extracts of *T.brucei* (37,38). The trypanosomal enzyme was found to have a native molecular weight of 107 kdal (37) very similar to that observed

for mammalian ODC (19). The K_m for ornithine was 161 μM (36)and the K_I for DFMO was found to be 130 μM (38), again very similar to the values reported for mammalian ODC of 75-160 μM (19)and 39 μM (39) respectively. It appears from this information that intrinsic differences in the catalytic properties of ODC between the parasite and the host do not account for the selective toxicity of DFMO and, if the mechanism of selective toxicity is to be understood, a more thorough analysis of the role of polyamines and ODC in *T. brucei* will be required.

The polyamine requirement for cell differentiation has been discussed for a number of cell types. Recently, Giffin et al discovered that polyamines may play a role in regulating the essential transformation of long slender trypomastigotes to intermediate and short stumpy trypomastigotes prior to ingestion by the tsetse fly(45). DFMO causes the transformation of long-slender forms to intermediate and short stumpy-forms (45) allowing for the possibility that polyamine depletion could be a trigger for the transformation under natural circumstances. The morphological change is accompanied by an increase in NAD diaphorase activity, a mitochondrial marker enzyme (45). Mitochondrial genes are known to be differentially transcribed between the long-slender and short-stumpy form parasites, with most of the major mitochondiral transcripts being more abundant in the short-stumpy form (44). A similar pattern of differential transcript production is also observed in the DFMO-inducued short-stumpy parasites, implying again that DFMO has caused a normal transformation event (44). Fairlamb, et al discovered that a unique cofactor for glutathione reductase, containing two glutathiones conjugated to spermidine, existed in *T. brucei* (43). This cofactor, termed trypanothione, is believed to be important for the maintenance of intracellular thiols in the correct redox state and in the removal of hydrogen peroxide (43). DFMO depletes trypanothione by 66% in the trypanosome after a 12 hr treatment of the infected mice (43). Depletion of trypanothione, thus may be another factor in the selective toxicity of DFMO.

REAEARCH GOALS

The importance of ODC to the normal growth and differentiation of African trypanosomes and the significance of ODC inhibitors as promising antitrypanosomal agents underscore the need for further characterization of the trypanosomal ODC, its regulation and of the role of polyamines in the trypanosome. The goal of my research was to characterize the ODC from *T. brucei*. We anticipated that this would provide insight into the mechanism of selective DFMO toxicity , while additional studies on the regulation of ODC might lead to the discovery of additional therapeutic targets. ODC is present at less than 0.001% of the total *T. brucei* cell protein, making extensive characterization of the enzyme through conventional protein purification techniques very difficult. To overcome this problem I first attempted to select a DFMO resistant strain of *T. brucei* with the hope of achieving an increased level of ODC production, as has been observed in mammalian cells resistant to DFMO . A DFMO resistant strain was obtained but the resistance was due to a decreased drug accumulation rather than an increase in ODC levels. The characterization of this mutant is discussed in Chapter 1. The next approach was to assess the feasibility of cloning the trypanosomal ODC gene for the later expression in *E. coli*, where sufficient levels of trypanosomal ODC may be obtained for thorough enzyme characterization. I discovered that through cross hybridization to mouse ODC cDNA it was feasible to clone the *T. brucei* ODC gene. Chapter 2 describes the cloning and sequencing of the *T. brucei* ODC gene. As a result of this work, we discovered a potential mechanism for the selective toxicity of DFMO on the trypanosome over the mammalian host. The *T. brucei* ODC gene sequence predicted that *T. brucei* ODC would have a much longer intracellular halflife than the mammalian enzyme. This was confirmed experimentally and led to the conclusion that the difference in enzyme turnover rates may explain the greater DFMO toxicity to the trypanosome. Chapter 3 describes the purification and characterization of ODC from *T. brucei*. The *T. brucei* ODC gene was successfully expressed in *E. coli* (Chapter 4) The recombinant enzyme was purified to apparent homogeneity and characterized (Chapter 4). No differences in any of the measured characteristics between the authentic and recombinant *T. brucei* ODC were found.

CHAPTER ONE

A *Trypanosoma brucei* Mutant Resistant to α-Difluoromethylornithine

MATERIALS AND METHODS

Cell cultures. T.brucei strain 366D bloodstream forms, a gift from Dr. Larry Simpson of the Department of Biology, University of California Los Angeles, were propagated in Wistar rats, harvested and purified by a standard procedure (46). The bloodstream trypomastigotes were transformed to the procyclic forms in the modified Steiger's medium pH 7.3 (47) plus 5 mM cis-aconitate at 26°C (12). The procyclic forms, cultivated at 26 °C (48) in the modified Steiger's medium with 10% dialyzed fetal calf serum, reach the mid-log phase of 4×10^6 cells/ml after 4 days and the stationary phase of 1×10^7 cells/ml after 7 days, when inoculated with a 5% mid-log phase culture.

The ODC assay. T. brucei, washed and resuspended in 50 volumes of 60 mM phosphate buffer pH 7.8, 44mM NaCl, 1 mM dithiothreitol (DTT), 1 mM EDTA and 0.05 mM pyridoxal phosphate, were freeze-thawed three times in a dry ice bath. The suspension was centrifuged at 27,000 x g for 20 min. to remove cell debris. Protein concentrations of the crude extracts were determined by the method of Lowry et al. (49) using bovine serum albumin as a standard.

The ODC activity of the extract was monitored by the release of CO_2 from radiolabeled ornithine as described by Janne and Williams-Ashman. (50). Briefly, a 250 µl reaction mixture containing 100 mM glycylglycine pH 7.2, 4 mM DTT, 0.2mM pyridoxal phosphate, 0.4 mM [1 -^{14}C]ornithine (5mCi/mmol) and the enzyme was incubated at 37 °C in an enclosed vial with a hanging strip of filter paper previously soaked in 200 µl of hyamine hydroxide (New England Nuclear, Boston, MA). The reaction, initiated by the addition of enzyme, was ordinarily continued for one hour and stopped by an injection of 1 ml of 40% TCA to the reaction mixture. The incubation was continued for another 30 min to assure a complete trapping of the CO_2 by the filter paper. The filter paper was then removed, and the radioactivity measured by scintillation counting. The enzyme activity was linear over a protein concentration range of 0.24 mg/ml to 1.2 mg/ml and throughout the 60 min. assay time. Data was collected within this linear range. A unit of activity was defined as 1 nmole $C0_2$/hr/mg protein.

The substrate uptake assays. Freshly harvested *T. brucei* were pelleted, washed and resuspended in phosphate buffered saline (PBS) pH 7.5 and 0.05% glycerol to a final concentration of 1×10^8 cells/ml. A radiolabeled substrate was added to the cell suspension incubated at 26°C, and 100 µl aliquots were taken at designated time intervals, layered onto 200 µl of dibutylphthalate (density = 1.04 gm/ml) in a 500 µl Eppendorf tube and centrifuged immediately in an Eppendorf microfuge for 2 min. The aqueous layer was siphoned off and replaced with 100 µl of PBS. Both the aqueous and oil phase were removed, the cell pellets were

lysed with 50 µl of 17% perchloric acid and the radioactivity measured by scintillation counting. The zero time point was obtained by removing cells immediately after the addition of the radiolabeled compound. This value was subtracted from all prior time points.

Each uptake experiment was repeated at least twice with different batches of cells. The reproducibility of data points taken with the same cell batch was within 15%. Data taken on different batches could differ up to 30% when examining the actual uptake of radioactivity, but the relative differences within the same experiment remain constant.

Chemicals. [1-^{14}C]-DL-ornithine (59 mCi/mmol), [5-^{14}C]-DL-ornithine (60 mCi/mmol), [5-^{3}H]-L-arginine (25 Ci/mmol), [1,4-^{14}C]-putrescine (118 mCi/mmol), [5-^{14}C]-DL-DFMO (59 mCi/mmol) and [U-^{14}C] tetraphenylphosphonium bromide (31.4 mCi/mmole) were purchased from Amersham, Arlington Heights, Il. DFMO was a gift from Dr. P.P. McCann of Merrill Dow Research Institute, Cincinnati, OH. The L-amino acids were from Sigma, St. Louis, MO. All other chemicals used were of the highest purity commercially available.

RESULTS

Growth inhibition by DFMO. DFMO was tested in the *in vitro* cultures of *T. brucei* 366D procyclic forms at varying concentrations and found to be cytostatic. It has an ED_{50} value (effective dose for 50% growth inhibition) of 225μM (Figure 1-1). This growth inhibition could be totally reversed by the simultaneous presence of 1 mM putrescine, but was completely unaffected by the addition of 1 mM L-ornithine (Figure 1-1).

Selection of a DFMO resistant mutant. Culture medium containing 400 μM DFMO was inoculated with a mid-log phase culture of *T. brucei* 366D procyclic forms. Cells were allowed to grow back to the stationary phase over a prolonged period of incubation at 26 °C (Figure 1-2), and were then serially passaged to fresh culture media containing the same concentration of DFMO. When the growth rate returned to the normal range of 0.3 to 0.4 day doubling time, the serial transfers were repeated five times in order to stabilize the new trait of drug resistance. These serial passages were then continued at increasing concentrations of DFMO in a stepwise fashion to 1.0 mM, 4.0 mM, 11.0 mM and 20.0 mM, until the cells were capable of growing at a normal rate in 20 mM DFMO.

This DFMO-resistant mutant of *T. brucei* 366D, obtained after 50 serial transfers (Figure 1-2) is very stable. It could be serially transferred in the absence of DFMO for at least 10 passages without losing its resistance to 20 mM DFMO. Specific ODC activities in the cell-free extracts of wild-type and DFMO-resistant cells grown in the absence of DFMO were similar, 5.7 and 3.4 nmol/hr/mg protein, respectively. The basis of DFMO resistance in the mutant is thus unlikely to be due to an increase in ODC activity. Relatively little ODC activity (0.3 nmol/hr/mg protein) was detectable in the mutant when cultivated in the presence of 4 mM DFMO even when the cells were washed before lysis. This low activity was attributable to the difficulty in removing all the cell associated drug molecules by washing. Freshly harvested wild-type cells pre-incubated in 4 mM DFMO for 2 hrs were washed and lysed as above, the specific activity of ODC was similarly only 0.1 nmol/hr/mg protein.

DFMO uptake by the mutant. The lack of change in ODC activity in the DFMO resistant mutant led to further examination of the rate of L-ornithine decarboxylation by the intact mutant cells grown in the absence of DFMO. The procedure of uptake assay (materials and methods) was adopted, in the absence of DFMO, for comparing the rates of uptake of radioactivity derived from 54 μM of [1-^{14}C] ornithine versus that from 54 μM of [5-^{14}C]ornithine. The former was taken as the uptake of

ornithine which was not immediately decarboxylated upon entering the cells, whereas the latter represented both the intact ornithine and the decarboxylated ornithine found in the cells. The difference between these two rates should reflect the rate of uptake of ornithine which was destined to be converted to polyamines. The results shown in Figure 1-3 suggest no appreciable difference between the mutant and the wild type cells in their abilities to take up exogenous ornithine and convert it to polyamines. Thus differences in ornithine metabolism do not account for the DFMO resistance.

Next, DFMO uptake by the resistant and wild type cells was studied. Cells that had been grown in the absence of DFMO for three passages were used for these uptake experiments. The wild type cells take up DFMO at a linear rate for the initial 60 min (Figure 1-4) which is in good agreement with the previous observation by Bitonti et al (51). The mutant, however, takes up DFMO at a much lower initial rate and becomes saturated at a final level of 0.01 nmol DFMO per 10^7 cells after 15 min (Figure 1-4). Assuming a cellular volume of 54 μm^3 for *T. brucei* procyclic trypomastigotes (52), the steady state intracellular level of DFMO in the mutant is 18 μM, well below the K_i value of DFMO on *T. brucei* ODC (130 μM) (38).

It is thus likely that DFMO resistance, in this particular mutant, is the result of the failure of the cell to accumulate intracellular DFMO.

Characterization of the DFMO uptake mutant. Membrane potentials of the wild-type and mutant *T. brucei* 366D procyclic forms were estimated from the cellular uptake of [U-^{14}C]-tetraphenylphosphonium bromide (TPP)(53). TPP was rapidly taken up by both the wild type and the mutant cells at a very similar initial rate. Intracellular TPP reached a steady state level of 1.5 nmol/10^7 wild-type or mutant cells, representing an intracellular concentration of 0.8 mM (52) after a 20 min incubation with 11 μM TPP. This level reflects a membrane potential of -110 mV for both cell types and is in excellent agreement with the value reported for *T. brucei* by Midgley (53).

Uptake of [5-^{14}C]-ornithine and [1,4-^{14}C]-putrescine were then compared between the wild-type and mutant cell lines. A 14-fold increase in the rate of ornithine uptake by the mutant grown in 20 mM DFMO when compared to the wild type grown in the absence of DFMO was observed (Figure 1-5A). Growth of the wild type cell line in 400 μM DFMO had no effect on the rate of ornithine uptake. A 3 to 4 fold increase in the rate of putrescine uptake was observed for the mutant cell when compared to the wild type cell. However, when wild-type cells were grown with 400 μM DFMO a similar enhancement in putrescine uptake was observed.

Thus, it appeared that the mutant cell line had three characteristics that distinguished itself from wild type cells; a decrease in DFMO uptake and an increase in ornithine and putrescine uptake.

The stability of these traits in the absence of DFMO was measured. The mutant cells were serially passaged five times in the absence of DFMO. The cells were harvested after each passage and the uptake of DFMO, ornithine and putrescine was measured. The reduced DFMO uptake is a stable trait of the mutant (Figure 1-6). However, the enhanced uptake of ornithine and putrescine is not, as levels are returned to normal after a single passage of the mutant strain in the absence of DFMO (Figure 1-6). The enhanced ornithine and putrescine uptake could be restored to the mutant after one passage in the presence of 20 mM DFMO but not if the cells were merely preincubated with 20 mM DFMO for 2 hrs before the uptake assay was performed. The enhancement of putrescine uptake in wild -type cells grown with 400 μM DFMO was also eliminated after one passage without the drug. It, therefore appears that the three observed phenotypic changes in the mutant cell line cannot be associated as a single stable genetic trait.

Further examination of the uptake of DFMO and L-ornithine by T. brucei. The uptake of [5-^{14}C]-L-ornithine by the *T. brucei* 366D wild-type procyclic forms was examined more thoroughly. It was apparently unaffected by an excessive concentration of DFMO (20 mM) or putrescine in the assay solution, and was only partially reduced by the presence of 20 mM arginine (Figure 1-7). More thorough analysis of the kinetics of ornithine and arginine uptake by Lineweaver-Burk plots provided K_m values of 3.9±1.7 μM and 6.2 ±3.7 μM for the two amino acids, respectively. Arginine was a competitive inhibitor of ornithine uptake with an estimated K_i value of 1.2 mM, whereas ornithine inhibited arginine uptake competitively with a K_i value of 5.6 mM. These extraordinarily high K_i values make it unlikely that arginine and ornithine compete with each other for the same transporter in *T. brucei.*

The uptake of DFMO (54 μM) was relatively unaffected by the presence of 20 mM putrescine, arginine or ornithine(data not shown). Nor was it significantly influenced by the addition of 1 mM iodoacetamide, 0.02% azide or 0.5 mM salicylhydroxamic acid (SHAM) (Figure 1-8). However, when the assay temperature was dropped from 26°C to 4°C, no DFMO uptake could be detected (Figure 1- 8), which suggests that although the drug uptake may not be energy dependent, it may rely on a temperature-dependent process. A Lineweaver-Burk analysis of the kinetics of DFMO uptake by *T. brucei* 366D wild-type procyclic form suggested a K_m value of 244 μM.

Discussion

In our present investigations, we have successfully isolated a DFMO resistant procyclic *T. brucei* 366D mutant. The mutant strain exhibited a change in drug sensitivity from an ED_{50} of 225 μM to a total resistance to 20 mM DFMO; an increase in drug resistance of at least 100 fold.

This drug resistant mutant strain has apparently neither enhanced its ODC activity nor lowered the sensitivity of its ODC toward DFMO inhibition. It has the normal rate of converting exogenous ornithine to endogenous polyamines. It has not amplified its ODC gene (unpublished observation), but, instead, altered its ability to accumulate exogenous DFMO to a very low saturating level of 0.01 nmol DFMO/10^7 cells. This low intracellular drug concentration of 18 μM has apparently prevented DFMO from exerting its inhibitory effect on the growth of *T. brucei* procyclic forms.

The uptake of a drug is not equivalent to the transport of a drug. It represents a combination of drug transport in and out of the cell, intracellular distribution, binding to various cellular components, incorporation and possible metabolism. Though we have determined that the mechanism of drug resistance is due to decreased DFMO uptake, the exact reason for this decrease remains unknown. The selection of a DFMO uptake mutant can be disappointing for the purpose of further understanding the mechanism of antitrypanosomal action of DFMO. But it is helpful in furthering our knowledge on the mechanism of DFMO uptake by *T. brucei*. Previous studies with the bloodstream forms of *T. brucei* by Bitonti et al. (51) indicated a linear relationship between the exogenous DFMO concentrations up to 10 mM and the intracellular DFMO levels in 60 min. uptake assays. The drug uptake was not significantly affected by ornithine, lysine or arginine. It was inhibited approximately 30% by SHAM but was markedly inhibited at 0°C. Our observations are in good agreement with these previous findings. The only exception we found was that SHAM did not affect DFMO uptake by the procyclic forms. This, however, may be due to the differences in energy metabolism between the two forms of *T. brucei* (54). The conclusion reached by the previous workers that DFMO uptake by *T. brucei* is by passive diffusion (51) may be difficult to reconcile with our selection of a DFMO uptake mutant strain. Clearly, all the data accumulated by Bitonti et al. and us have not ruled out the possible involvement in *T. brucei* of a specific transporter protein(s) for DFMO uptake. The function of this protein(s) could be lost in our mutant strain and the low level of 0.01 nmol DFMO taken up by 10^7 of the mutant cells may represent the drug uptake by passive diffusion at 26°C. An alternative explanation may attribute

the decline in intracellular accumulation of DFMO to an increase in efflux of DFMO out of the cell. In the multi-drug resistance(mdr) phenotype, tumor cells become resistant to a broad range of structurally unrelated chemotherapeutic drugs such as anthracyclines and vinca alkaloids when initially challenged with only one compound. This phenotype has been demonstrated for Chinese hamster ovary cells which, selected for initial resistance to colchicine, are also resistant to a number of unrelated drugs(55). Uptake of colchicine by the cells is by passive diffusion, a characteristic that is common to drugs exhibiting the mdr phenotype(55). Cells exhibiting the mdr phenotype have also in common the overproduction of a class of high molecular weight membrane glycoproteins, the result of gene amplification(56). The gene for one of these glycoproteins has been cloned and sequenced(57,58). The deduced amino acid sequence reveals that the mdr protein is likely to be an integral membrane protein with two potential ATP binding sites. It has strong homology to a class of bacterial transport proteins that are ATP dependent. Thus, the mdr protein appears to be an energy dependent transport protein that may decrease drug accumulation by increasing the rate of drug efflux from the cell. There is no information on possible glycoproteins of this sort in the membranes of the trypanosome, nor has there been any indication of multiple drug-resistance in our DFMO-resistant mutant. Genomic Southerns containing wild type and DFMO-resistant mutant cell DNA were probed with the Chinese hamster ovary gp-170 cDNA. No changes in the hybridization pattern between the wild type and mutant DNA were found, (unpublished observation) implying that amplification of a gene with significant homology to the gp-170 cDNA had not occurred. Another way of examining the possible involvement of multi-drug resistance in the DFMO-resistant mutant would be to test for the reversal of drug resistance by ATPase inhibitors (57,58). Further studies are needed to clarify these points.

One of the more interesting observations made in the present study concerns the interrelationships of ornithine, arginine, putrescine and DFMO uptake in *T. brucei* procyclic forms. The uptake of ornithine, arginine and putrescine is undoubtedly an indication of the capability of procyclic *T. brucei* to transport, incorporate and metabolize these compounds. The uptake of DFMO was not, however, inhibited by excessive ornithine, arginine or putrescine, which is in agreement with the observations by other workers on *T. brucei* bloodstream forms (51) and mammalian cells (58). The lack of effect of DFMO on the uptake of ornithine, arginine and putrescine by the procyclic cells is also apparent (Figure 1-7). However, when the DFMO-resistant strain was cultivated in the presence of DFMO, the uptake of ornithine was significantly enhanced (Figure 1-5A). This enhancement of ornithine uptake is not tied in with an increased conversion of ornithine to putrescine because the latter reaction remained at a normal rate in the mutant

grown in the presence of DFMO (Figure 1-3). It is not a genetic trait of the mutant, since one passage of the mutant in the absence of DFMO reduces the ornithine uptake to the original rate and extent without affecting its drug resistance (Figure 1-6). Nor does DFMO have any direct enhancing effect on ornithine uptake by the originally drug-free mutant, because neither preincubation of the mutant with DFMO nor the inclusion of DFMO in the assay of the mutant exerts any detectable effect on the ornithine uptake. This transient increase of ornithine uptake by growing the DFMO-resistant mutant in the presence of DFMO for a few generations is not observed on the wild-type procyclic forms partially grown up under suboptimal levels of DFMO (Figure 1-5A). This phenotypic characteristics could thus be associated with the decreased DFMO uptake by the mutant.

The uptake of putrescine is also stimulated in the mutant grown in the presence of DFMO (Figure 1-5B). The stimulation disappears also after a few generations of growth in the absence of DFMO. A similar observation was made on the wild-type procyclic forms grown under partial drug pressure, which suggests that the phenomenon may not be associated with the reduced DFMO uptake in the mutant. These findings can only point to the complexities of polyamine metabolism in *T. brucei* and suggest that more studies will be required before the mechanism of DFMO resistance can be truly understood.

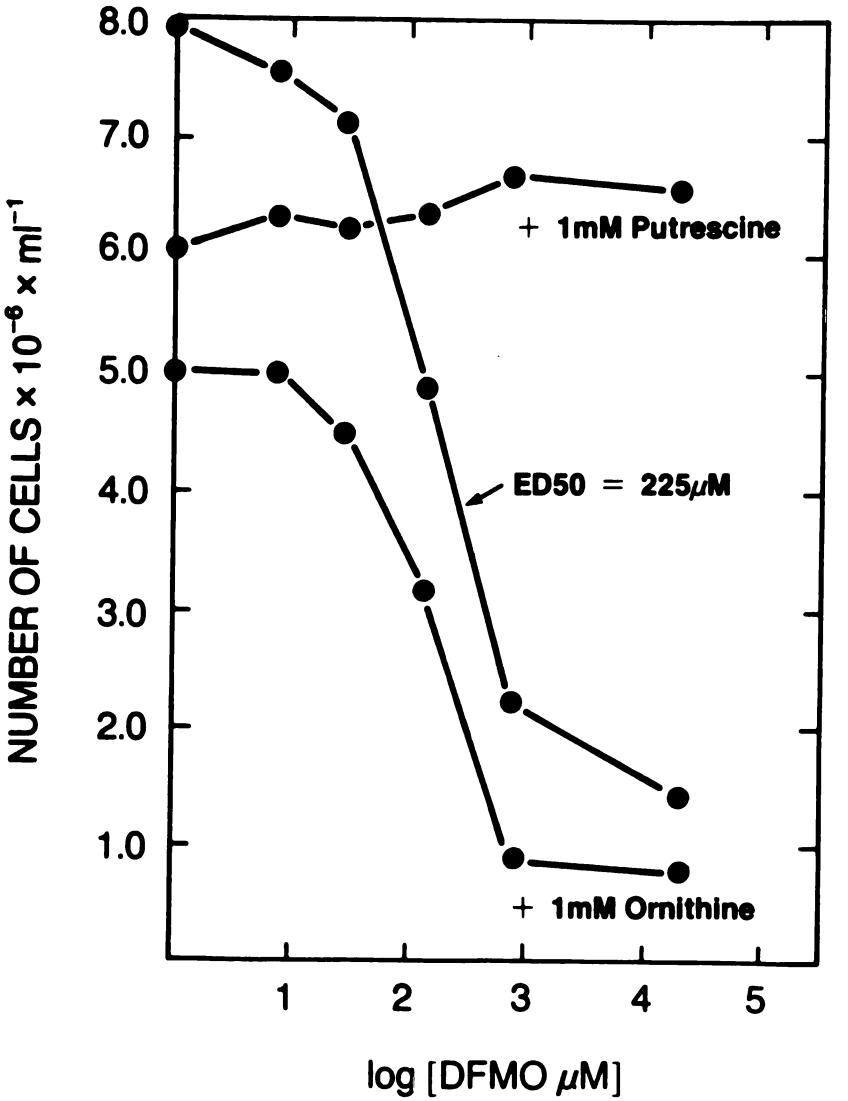

Figure 1-1: The *in vitro* growth inhibition of *T. brucei* 366D procyclic forms by DFMO. Growth was monitored by diluting 0.1 ml of the cell culture in 10 ml PBS and counting the cell number on a Coulter counter.

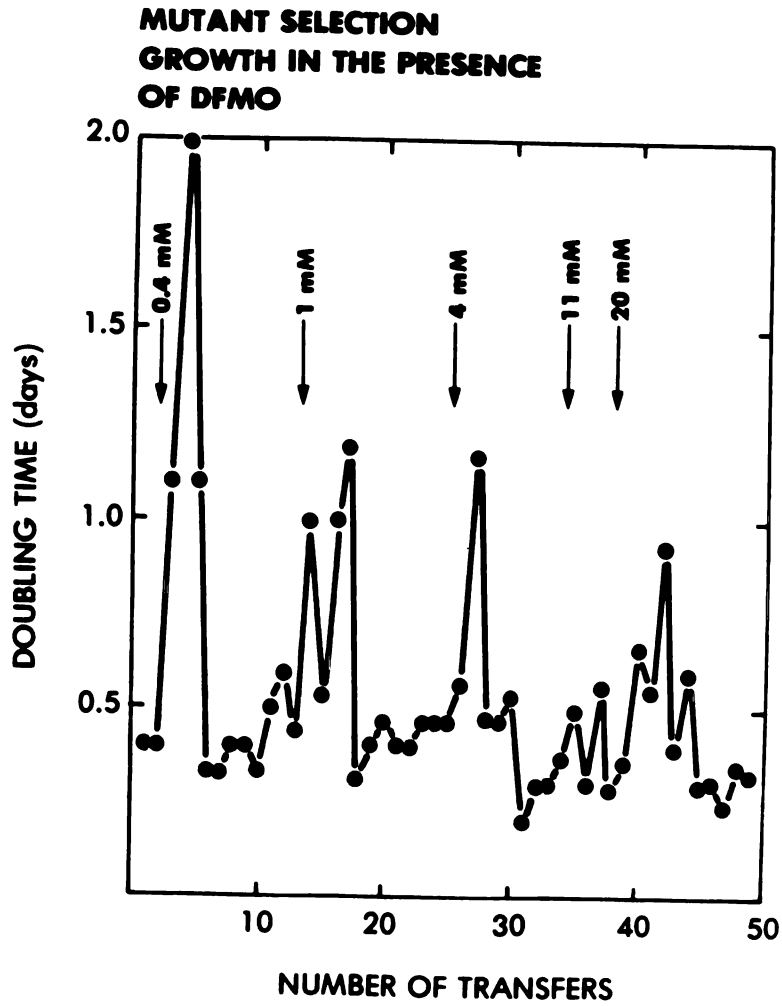

Figure 1-2: Selection of a DFMO resistant mutant *T. brucei* 366D in the procyclic form by serial passages of the *in vitro* culture with increasing concentrations of DFMO in the media.

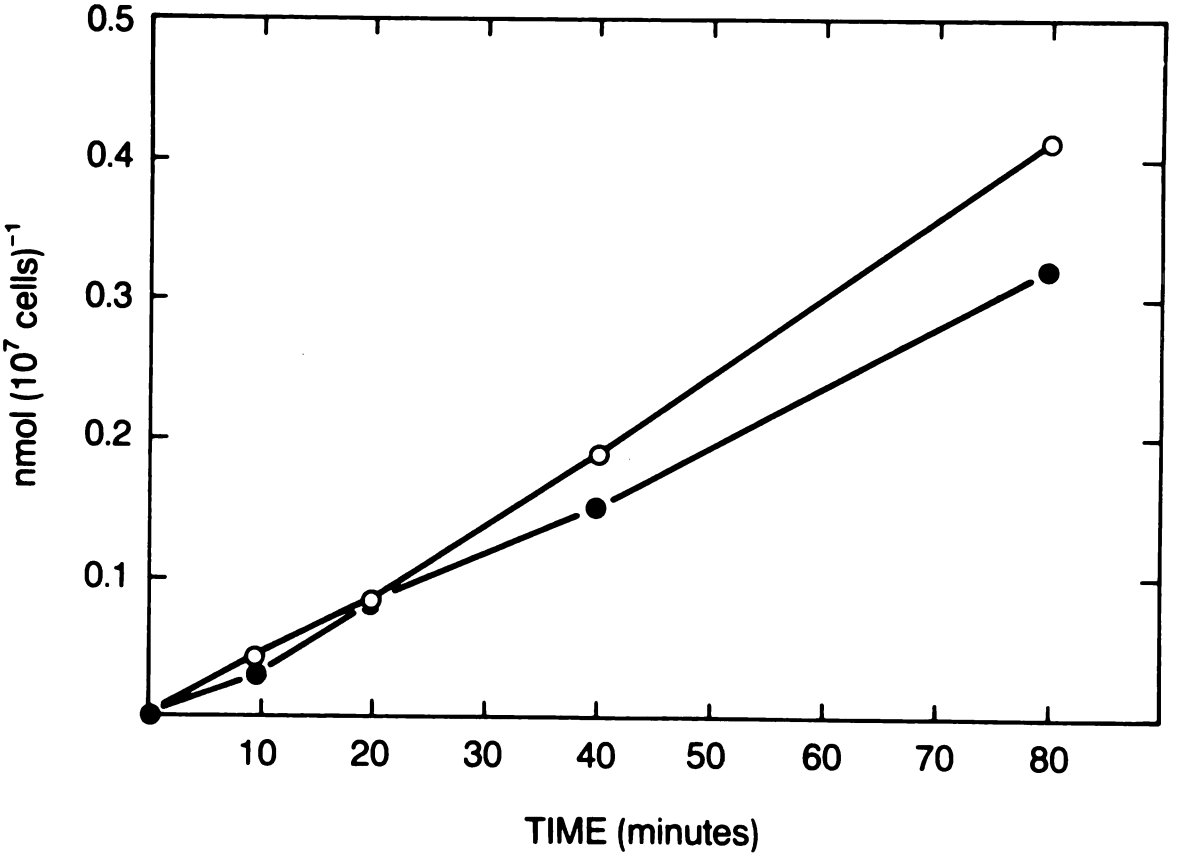

Figure 1-3: Ornithine metabolism in the procyclic forms of T. brucei 366D. Data represent the difference between the levels of incorporated [5-^{14}C] ornithine (54 µM, 59 mCi/mmol) vs levels of incorporated [1-^{14}C] ornithine (54 µM, 59 mCi/mmol) in wild type (●-●) and DFMO- resistant mutant cells (o-o).

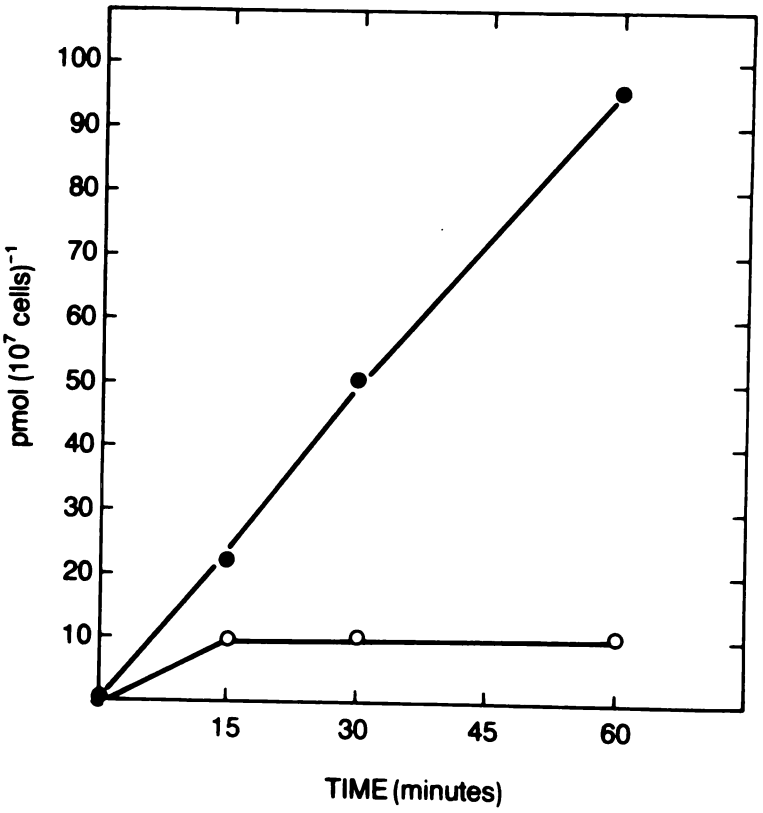

Figure 1-4: The time course of uptake of [5-^{14}C] DFMO (54 μM, 59 mCi/mmol) by wild type (●-●) and DFMO-resistant mutant (o-o) procyclic *T. brucei* 366D at 26 °C.

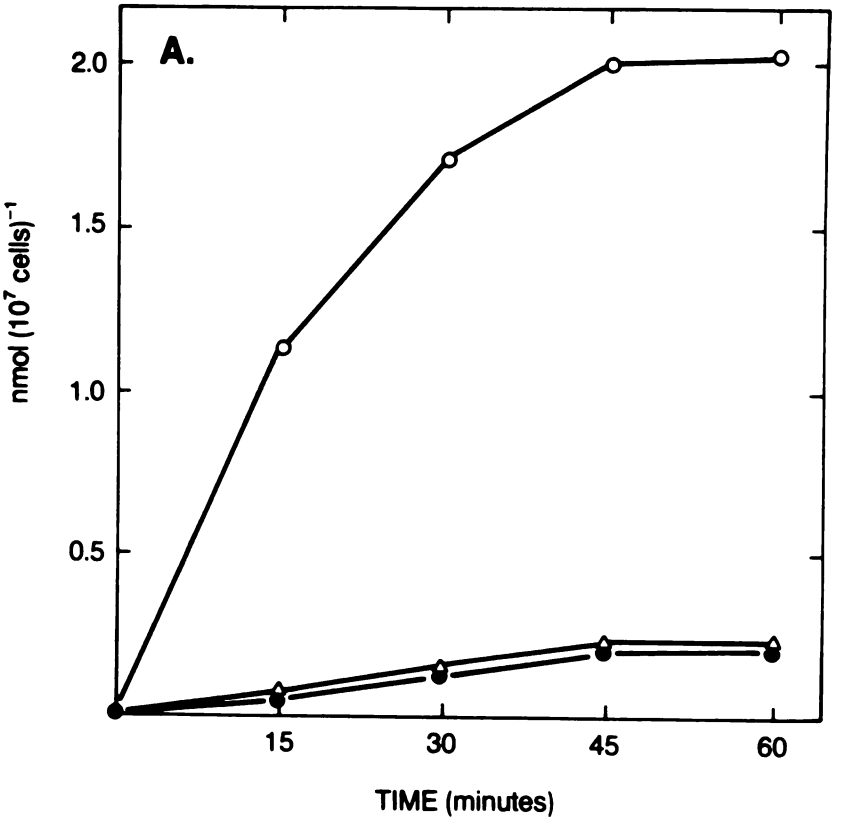

Figure 1-5: A. The time course of uptake of [5-^{14}C] ornithine (54 µM, 59 mCi/mmol) by the *T. brucei* 366D wild-type (●-●) , DFMO-resistant mutant (o-o) and by the wild type grown in the presence of 400 µM DFMO for one generation (Δ-Δ) .

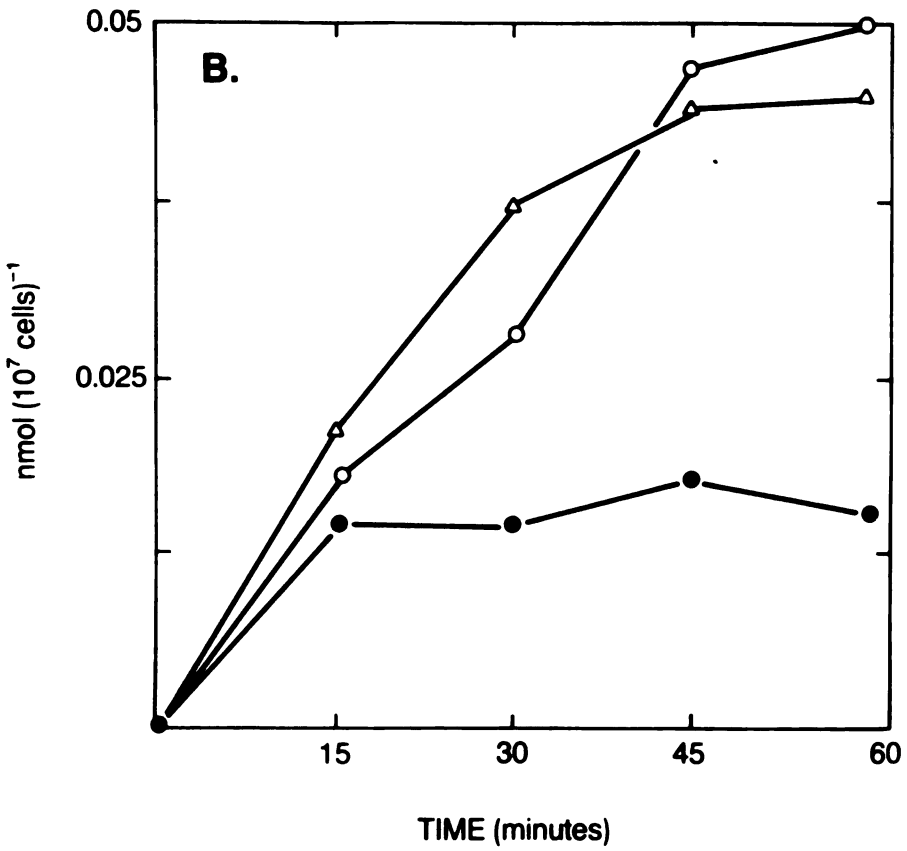

1-5B. The time course of uptake of [1,4-^{14}C] putrescine (54 µM, 118 mCi/mmol) by the *T. brucei* 366D wild-type (●-●), DFMO-resistant mutant (o-o) and by the wild type grown in the presence of 400 µM DFMO for one generation (Δ-Δ).

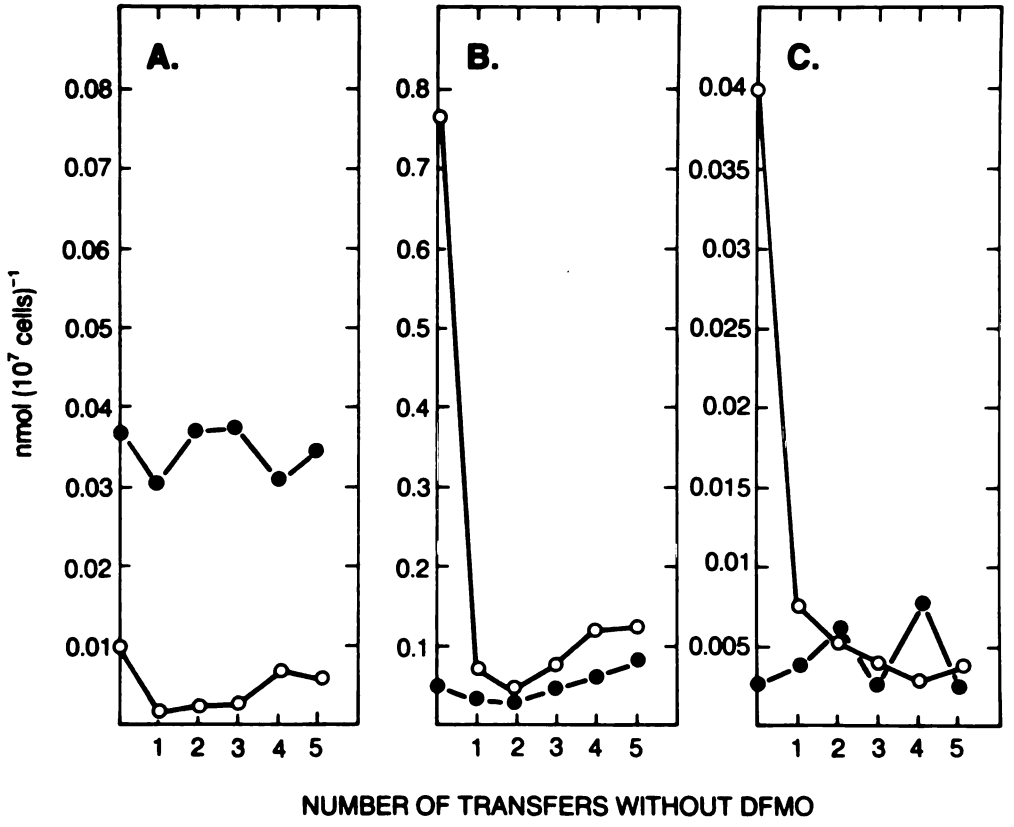

Figure 1-6: *In vitro* stability of the DFMO-resistant *T. brucei* mutant phenotypes in the absence of drug pressure. A. Uptake of [5-^{14}C] DFMO (54 µM) measured 40 min. after the addition of labeled drug. B. Uptake of [5-^{14}C] ornithine(28 µM) measured 20 min. after addition of labelled substrate. C. Uptake of [1,4-^{14}C] putrescine (28 µM) measured 40 min. after the addition of the radioactive compound. T. brucei wild type cells (●-●), DFMO-resistant mutant cells (o-o).

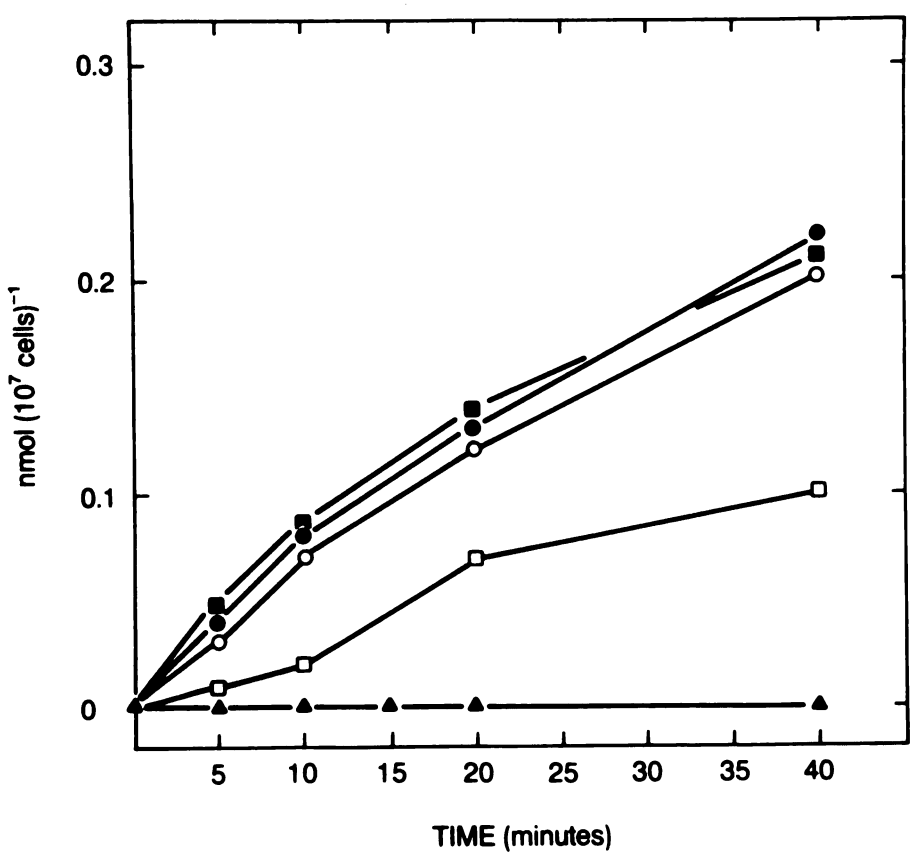

Figure 1-7: The effects of no addition (●-●), 20 mM DFMO (o-o), 20 mM putrescine(◆-◆) , 20 mM arginine (◊-◊) and 20 mM ornithine (▲-▲) on the *in vitro* uptake of [5-^{14}C] ornithine(28 μM) by wild type *T. brucei* 366D procyclic forms.

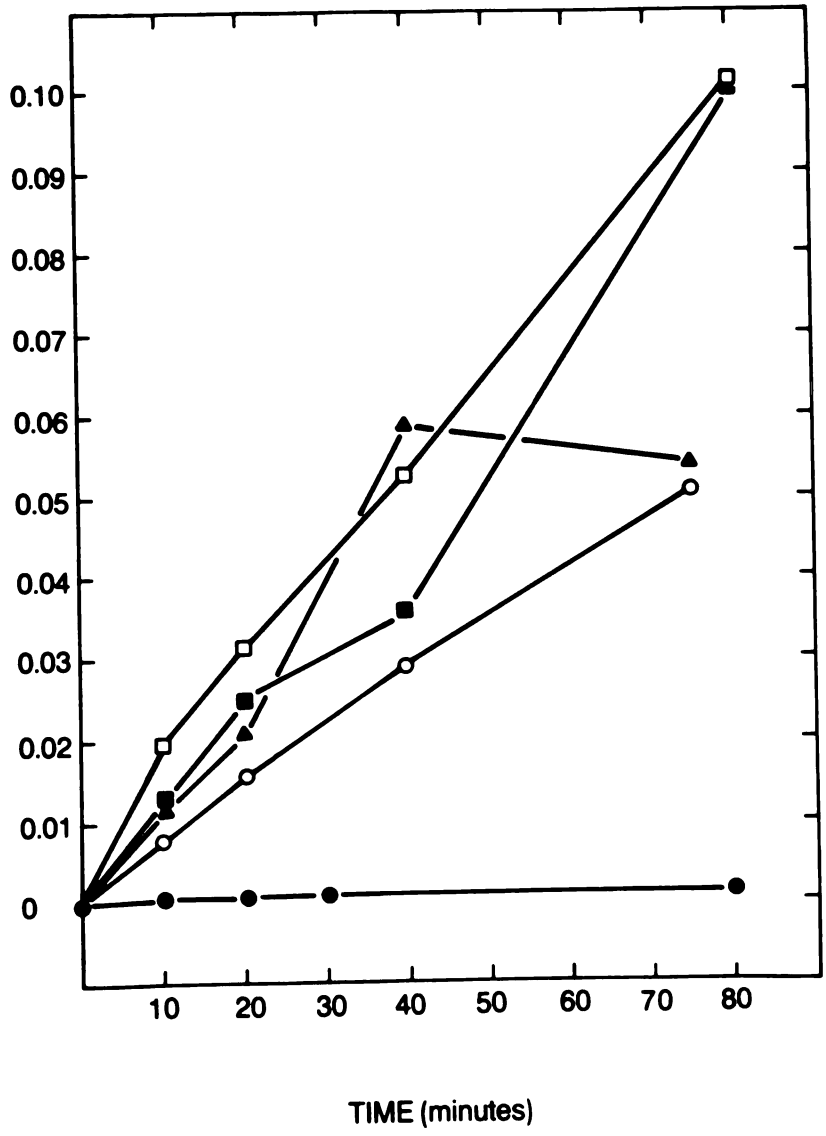

Figure 1-8: The *in vitro* effects of transport inhibitors and temperature changes on [5-^{14}C] DFMO (54 µM, 59 mCi/mmol) uptake in wild-type *T. brucei* procyclic forms. 26°C, no inhibitor (◆–◆); 4°C, no inhibitor (●-●); 26°C, 1 mM Iodoacetamide (▲-▲) ; 26°C, 0.02% azide (o-o); 26°C, 0.5 mM SHAM (◊–◊).

CHAPTER TWO

Cloning and Sequencing of the Ornithine Decarboxylase Gene from *T. brucei*:

Implications for enzyme turnover and selective difluoromethylornithine inhibition.

MATERIALS AND METHODS

Cultures. See Materials and Methods in Chapter one.

Nucleic acid preparations and analyses. *T. brucei* genomic DNA was prepared from $7x10^8$ procyclic cells in 3 ml of 0.5 mM EDTA, 0.5% Sarcosyl and 600 µg proteinase K and incubated at 50°C for 90 min. The DNA was further purified as described (59). A cosmid library of *T. brucei* strain 427 genomic DNA constructed in the vector pc2xB according to the method of Bates and Swift (60) was obtained from Dr. John Boothroyd of the Stanford University School of Medicine. A plasmid pOD20.7 containing the complete mouse ODC cDNA was obtained from Dr. Philip Coffino of the University of California, San Francisco. Cosmid DNA and plasmid DNA for mini screens were prepared by alkaline lysis of 1.5 ml of overnight culture (61). Larger samples of preparative quantities were further purified on a two step CsCl buoyant density gradient (1.47 and 1.80 gm/ml) in a Ti 80 rotor at 65,000 rpm for 5 hr. Total RNA was isolated from $1.4x10^9$ *T. brucei* procyclic forms by the guanidinium isothiocyanate/CsCl method (62,63). Poly(A)$^+$ RNA was separated from the total RNA by chromatography on an oligo(dT)-cellulose column (64).

DNA samples were digested with restriction endonucleases under the specific conditions recommended by the suppliers. DNA fragments were separated by electrophoresis in 0.8% agarose gels, transferred to nitrocellulose filters by the method of Southern (65) and probed with nick translated DNA labeled with [^{32}P]-dGTP and [^{32}P]-dCTP (66). For hybridizations with heterologous probes the blotted filters were incubated overnight at 42°C with 25% formamide, 0.8 M NaCl, 0.05 M NaH_2PO_4, 6 mM EDTA, 5X Denhardt's solution and 100 µg/ml salmon sperm DNA, followed by another overnight incubation with 10^6-10^7 cpm ^{32}P-labeled DNA in the same buffer at 42 °C. The filters were washed briefly two times in 2xSSC (0.3 M NaCl and 0.03 M sodium citrate) plus 0.1% sodium dodecyl sulfate (SDS) at room temperature, followed by one wash in 1x SSC plus 0.1% SDS at 42°C for one hour . For homologous probes the formamide concentration was increased to 50% and the filters were washed for an additional time in 0.1xSSC plus 0.1% SDS at 50°C. For identification of mRNA, purified poly(A)$^+$ RNA was denatured in 2.8% glyoxal, 13.9% dimethyl sulfoxide, 4.1 mM phosphate buffer pH 7.0 at 50°C for 1 hr, and separated by electrophoresis in 1.2% agarose gels. This was transferred immediately to nitrocellulose filters and probed with nick translated DNA.

Subcloning and sequencing of T. brucei ODC gene. The DNA fragment carrying either the entire *T. brucei* ODC gene or a portion of it was cloned into pUC 19 or Bluescript (Stratagene, San Diego, CA) and transformed into an *E.coli* strain dg 98 (obtained from Dr.Charles Craik, University

of California, San Francisco). Single stranded DNA, obtained from Bluescript vectors with the use of a M13 helper phage as described in the bluescript manuel, or CsCl purified double stranded plasmid DNA was used for sequence analysis. The DNA sequence was analyzed by the dideoxy chain termination method with [^{35}S]-dATP as the labeled nucleotide (67). The procedure was modified for double stranded sequencing as described (68) except that the primer annealing and the primer extension were carried out at 50°C. The nucleotide sequence around the Hind III site of the 1.8 kb and 1.0 kb Sst II- Hind III fragments, cloned separately into Bluescript as described, was obtained first. The remaining sequence was obtained for both strands through the use of synthetic oligonucleotide primers and in one area by the creation of a deletion at the Hind III site. Deletions were created with exonuclease III and blunt ends were generated with mung bean nuclease for the subsequent ligation as recommended by Stratagene, San Diego.

[^{35}S-]Methionine incorporation into the proteins of T. brucei procyclic forms. [^{35}S]-Methionine was added to log phase *T. brucei* procyclic 366D *in vitro* culture (3.0x10^{6} cells/ml) at a final concentration of 15.0 µCi/ml. After 10 minutes at 26°C, 50 µg/ml cycloheximide was added to half of the sample. At various time points up to 6 hr., 0.5 ml of the cell culture was removed from the no drug control and the drug-treated sample. Each aliquot was mixed with 0.5 ml of 2N NaOH plus 3.0% H_2O_2, incubated at 37°C for 10 min, added to 4 ml ice cold 25% trichloroacetic acid (TCA) plus 2% casein amino acids, incubated for 30 min on ice, filtered through Whatman GF/B filters and washed with 5% TCA. Radioactivity associated with the filters was measured by scintillation counting.

Preparation of T. brucei crude extracts. Crude extracts were obtained by washing and resuspending freshly harvested *T. brucei* in 50 volumes of 60 mM phosphate buffer pH 7.8, 44 mM NaCl, 1 mM dithiothreitol (DTT), 1 mM EDTA and 0.05 mM pyridoxal phosphate (PSDEP buffer). Cells that were previously incubated in the presence of cycloheximide were washed in PSDEP buffer plus 50 µg/ml cycloheximide prior to resuspension in PSDEP buffer. The cells were freeze-thawed three times in a dry ice-ethanol bath. The suspension was centrifuged in a microfuge for 15 min. to remove cell debris. The ODC activity in the crude extract was monitored as described in Chapter 1.

Materials. Radiolabeled [1-^{14}C]-ornithine (61.1 mCi/mmole), [5-^{14}C]-DFMO (61 mCi/mmole) ,[α-^{32}P] -CTP (800 Ci/mmole), [α-^{32} P] -GTP (800 Ci/mmole) , [alpha thio^{35}S]- ATP (>1000 Ci /mmole) and [^{35}S]-Methionine (1125 Ci/mmole) were obtained from Amersham, Arlington

RESULTS

Size of T. brucei ODC. DFMO has been used previously to specifically label ODC in crude extracts (20). We were able to use this specific labeling to determine the subunit molecular weight of *T. brucei* ODC. Crude extracts, obtained as described in materials and methods, of *T. brucei* bloodstream forms (15 mg protein/ml, 13 ODC activity units/mg protein) were incubated with [5-^{14}C] DFMO (30 μM, 61.1 mCi/mmole) at 37°C for 60 min. The labeled extract (4.0ml) was eluted through a Biogel A 0.5 m column (50cmx1.6cm) with 50 mM Tris pH 7.6, 0.15M NaCl, 4 mM EDTA at 9 ml/hr. A single peak of radioactivity was eluted at an apparent molecular weight of 100,000 for the native *T. brucei* ODC (Figure 2-1A). The peak fractions were pooled, dialyzed against 0.03 M phosphate pH 7.8, lyophilized, redissolved, and samples of 0.5 mg protein were analyzed by SDS 10% polyacrylamide gel electrophoresis (SDS-PAGE) (29) and autoradiography. A single band of radioactivity corresponding to a molecular weight of 45,000 was observed (Figure 2-1B), which may represent the subunit molecular weight of *T. brucei* ODC. Thus, like other phylogenetically diverse ODCs (20), the parasite enzyme may be a dimer of identical subunits.

Restriction analysis of T. brucei genomic DNA. Restriction fragments of *T. brucei* 366D procyclic form genomic DNA, separated in agarose gels and blotted to nitrocellulose filters, were probed with a nick-translated, 1.6 kilobase (kb) fragment of the mouse lymphoma S49 ODC cDNA containing the entire coding region for the enzyme (It was cut from the plasmid pOD 20.7 with PvuII and Taq I, and purified by electroelution from agarose gels). The mouse cDNA hybridized to specific fragments of *T. brucei* genomic DNA (Figure 2- 2). There are two Hind III fragments of 5.3 and 11.0 kb; two EcoRV fragments of 6.2 and 1.6 kb; one Sst II fragment of 2.8kb; one Hinc II fragment of 4.4kb; and one Sst I fragment of 4.5 kb.

Isolation and characterization of the genomic clones of T. brucei ODC. The success in identifying specific *T. brucei* DNA fragments with the mouse cDNA encouraged us to use the same heterologous probe to screen for the *T. brucei* ODC gene cloned into a cosmid library. A total of 7,000 recombinant cosmids were screened on nitrocellulose filters under the hybridization conditions described. Two clones C16 and C22, each hybridized strongly to the mouse cDNA, were selected, purified and digested with restriction enzymes. The DNA fragments were separated by agarose gel electrophoresis, transferred to nitrocellulose filters and hybridized with the mouse cDNA. The two clones differed in their pattern of inserted DNA fragments but had identical patterns of hybridization with the heterologous probe. The results shown for C16 (Figure 2-3) are identical to those obtained for genomic DNA with the exception of the size of the

Sst I fragment which is 5.9 kb in the cosmid clone instead of the 4.5 kb observed in the genomic Southern. The cosmid DNA was isolated from strain 427 whereas the genomic DNA was isolated from strain 366D. No other variations were observed, thus it seems most likely that this is caused by the presence of an additional Sst I site in the 366D strain, an apparent reflection of genetic polymorphism between the two strains. The entire region that hybridizes with the mouse cDNA appears to be confined within the 2.8 kb Sst II fragment. Restriction enzymes Hind III and EcoRV, each of which cut the *T. brucei* ODC gene only once, give different size fragments, suggesting that *T. brucei* does not carry a tandem array of direct repeats of the ODC gene. Sst I, Sst II and Hinc II each generates only a single DNA fragment containing the ODC gene, suggesting that there may be only a single copy of the gene in *T. brucei.*

The 5.9 kb Sst I fragment of clone C16 was subcloned into pUC 19 as described in the Methods section. The restriction map of the 2.8 kb Sst II fragment contained in this clone was constructed and is shown in Figure 2-4. The restriction map for *T. brucei* ODC has nothing in common with the map for the mouse ODC cDNA clone (21). This observation can be most likely explained by the high degree of third base substitutions found in the *T. brucei* DNA sequence when compared to the mouse sequence (see Discussion).

Size of the T. brucei ODC mRNA. Poly(A)$^+$ RNA was isolated from the procyclic forms of *T. brucei* 366D by the described procedures. It was denatured, fractionated by agarose gel electrophoresis, transferred to nitrocellulose filters and probed with the 2.8kb Sst II fragment under the more stringent hybridization conditions described above. A single band of 2.4 kb was observed by autoradiography (Figure 2-5) which may represent the size of mRNA encoding the *T. brucei* ODC.

Nucleotide sequence of the T. brucei ODC gene. The various segments that were sequenced are presented by arrows in Figure 2-4. The entire sequence of the *T. brucei* ODC is presented in Figure 2-6. A single open reading frame of 1,335 nucleotides has been identified . This can be translated into a polypeptide of 445 amino acids with an estimated molecular weight of 49,184 which is in fairly good agreement with the value of 45,000 obtained in Figure 2-1B. The polypeptide, which represents presumably the subunit structure of *T. brucei* ODC, has an extra 20 amino acid N-terminal peptide but lacks a 36 amino acid C-terminal peptide when compared to the mouse ODC. There is 61.5% sequence homology (Figure 2-7) between the *T. brucei* enzyme and the Balb/c mouse ODC when these two terminal regions, which encompass the most striking discrepancies between the two enzymes, are not considered. A similar comparison between the two DNA sequences reveals a 63.6% homology. The pI was predicted from the deduced amino acid sequence to be 5.5.

The turnover rate of T. brucei ODC. Log-phase procyclic forms of *T. brucei* 366D were incubated with [^{35}S]-methionine. The time course of the incorporation of radioactivity into the TCA precipitable fraction suggests active protein synthesis during the incubation period (Figure 2- 8). This protein synthesis was inhibited by the presence of 50 µg/ml cycloheximide (Figure 2- 8). The cellular level of ODC activity was monitored during prolonged incubations of the *T. brucei* procyclic forms with cycloheximide. The results in Figure 2-8 show a constant level of ODC activity in extracts of cells that were incubated with the protein synthesis inhibitor for up to 6 hr. *T. brucei* ODC thus appears to have a half life in excess of six hours.

DISCUSSION

Our investigations on the ODC of *T. brucei* have made use of mouse ODC cDNA to identify the gene encoding the parasite enzyme. This success is not at all surprising in view of the high degree of sequence homology between the residues #35-#410 of the mouse enzyme and the residues #55-#430 in the T. brucei ODC (Figure 2-7). This common region of the two enzymes has 69% identity, with no gaps required for alignment and could constitute the essential portion of the enzyme molecules required for the catalytic function of ODC. This is consistent with observations of the activities of carboxy-terminal truncated mouse ODC's generated by expression of recombinant DNA's in *E. coli.* Vectors encoding enzymes lacking the carboxy terminal 38, 41 or 45 amino acids of native ODC have respectively, 85%, 48%, and 2%, of the activity of an enzyme containing all 461 amino acids of the native enzyme (70). The structural similarity explains the similar kinetic properties of the two enzymes and the similar biochemical susceptibilities toward DFMO (38,39).

An interesting aspect of our findings lies in the significant differences between the two terminal regions of the two enzymes. At their amino termini, the parasite and mammalian enzyme contain, respectively, 54 and 34 amino acid residues outside the 376 amino acid core region of homology. We note that, despite their dissimilarity in size and sequence, the amino terminus of the parasite enzyme begins with met-thr-thr and the amino terminus of the mouse enzyme with met-ser-ser. At their carboxy termini, parasite and mouse enzymes extend 15 and 51 amino acids, respectively, beyond the region of homology. Eukaryotic proteins subject to rapid intracellular degradation have been shown to contain regions that are rich in the amino acids proline, glutamic acid, asparatic acid, serine and threonine (71). Amino acids 423 to 449 of the mouse enzyme are rich in those amino acids. Futhermore, within the core region of homology, the largest contiguous region of non-homology, corresponding to mouse residues 295-307, contains the sequence pro-gly-ser-asp-asp-glu-asp. It has been suggested (71) that these two regions of ODC account for the short intracellular half life of the mouse enzyme. Because the trypanosome ODC lacks the corresponding regions, the hypothesis predicts that it should have a relatively long half life.

This has been both supported and verified by our experimental data presented in Figure 2-8, which implies that intracellular *T. brucei* ODC is very stable and undergoes no detectable turnover. To fully establish that the difference in stability of the mouse and trypanosome enzyme is an intrinsic property of the protein, however, it will be necessary to compare their turnover in a common cellular environment. This could be accomplished following transfection of animal cells with appropriate vectors containing the parasite or mouse gene. Presently, the lack of intracellular turnover of the parasite enzyme apparently distinguishes it from the mammalian ODC,

and may constitute the basis for the antitrypanosomal action of DFMO. The inhibitor may not cause reduction of polyamines in the host where it is continuously removed by the host metabolism and where the inhibited ODC turns over rapidly (20) (half life= 10 - 30 min.) to be replaced by new active enzyme. This enzyme turnover rate is only slightly slower than the rate of enzyme inactivation by DFMO which has been reported to have a half life of 3.1 min. at infinite inhibitor concentration (38) for mouse ODC. In contrast to the mouse enzyme, the *T. brucei* ODC does not turn over at a detectable rate and the decrease in polyamines in DFMO-treated *T. brucei* has been well documented (40). This is the first time, as far as we are aware, that the action of a therapeutic agent may depend on slow turnover of the target enzyme.

The 63.6% nucleotide sequece homology and the lack of resemblance in restriction maps between the mouse cDNA and the *T. brucei* ODC gene has prompted us to examine the third base homology between the two. It was only 39.1% which may explain why the restricion maps are so different. Apparently , the protein sequence of ODC has been largely conserved through evolution, but the long phylogenetic distance between mouse and *T. brucei* may be reflected by the differences among the third bases. On the other hand, however, the recently revealed sequence of *Saccharomyces cerevisiae* gene encoding ODC has shown significant differences from that of the mouse cDNA (25). The open reading frame of the yeast gene encodes 467 amino acids with a sequence bearing only 38.8% homology to the mouse cDNA with extensive gap introductions required for optimum alignment. This makes the close resemblance between the *T. brucei* and the mouse enzyme quite extraordinary in view of the perceived phylogenetic relationships (72) among the three. The possibility of a lateral transfer of a host gene into the parasite must be considered.

No sequence homology to the consensus eukaryotic promotor TATA or CCAAT or to the Pol II promotor sequence TGCA , identified recently in the intergenic region of the *T. brucei* heat shock protein (hsp) 70 gene (73), was found for 150 nucleotides upstream of the start codon. The $(Py)_6$XXXAGG consensus sequence identified as the insertion site of the trans-spliced 35 nucleotide transcript of the mini exon (74) is also absent from this region but may potentially be located further upstream. This possibility is supported by the large size of the *T. brucei* ODC mRNA which is approximately 1 kb larger than required for the protein coding region. The conventional polyadenylation site AATAAA , and the sequence TTTTTATTTT(A), found near the poly (A) tail of the *T. brucei* hsp 70 (73) gene, were both absent for 190 nucleotides downstream of the 3' stop codon.

The treatment of *T. brucei* long-slender bloodstream forms with DFMO depletes putrescine and spermidine from the parasites and transforms the latter to the short-stumpy form (45). It is

likely that natural *T. brucei* transformation from long-slender to short-stumpy forms is also initiated by polyamine depletion, which could be brought about by a decrease of intracellular ODC activity. With the availability of the *T. brucei* ODC gene we will be able to assess if the down regulation of enzyme activity occurs at the transcriptional level, the translational level or if it is caused by enzyme inactivation or degradation.

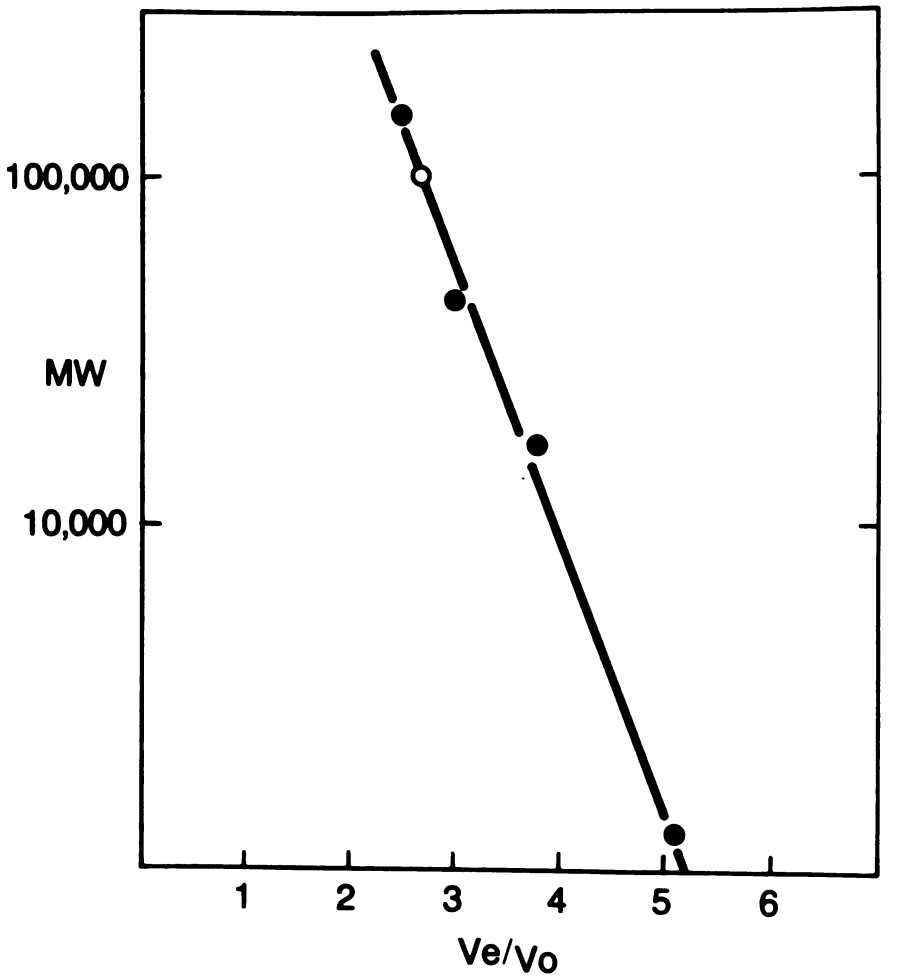

Figure 2-1: *Molecular weight determination of T. brucei ODC* A. Determination of *T. brucei* ODC native molecualr weight. The crude cell extract from blood stream *T. brucei* strain EATRO 110 was labeled with [5-^{14}C]- DFMO and separated on a Biogel A 0.5 m column. The elution profile Ve/Vo (Ve, volumn of elution and Vo, void volumn) vs the molecular weight (MW) of the standards (●, IgG, ovalbumin, myoglobin, vitamin B12) was plotted. Ve/Vo of the peak radioactivity (o) was compared to that of the standard proteins to determine the apparent molecular weight of this peak which presumably corresponds to native *T.brucei* ODC.

Figure 2-1B. *Determination of T. brucei ODC subunit molecular weight.* The peak fraction of radioactivity from the gel filtration column was analyzed by 10% SDS-PAGE and autoradiography. [^{14}C]- labeled protein standards were used as molecular weight markers.

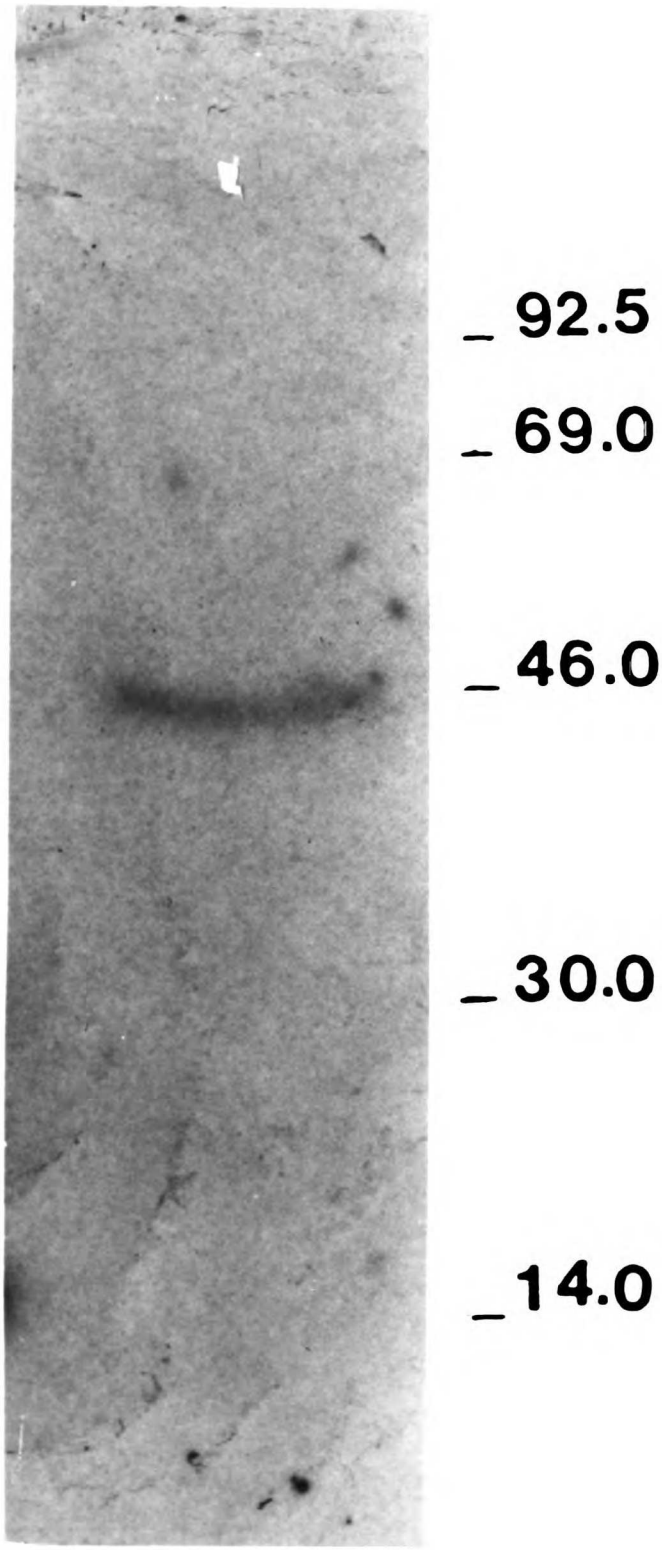
92.5
69.0
46.0
30.0
14.0

Figure 2-2: *Southern blot analysis of T. brucei genomic DNA*. High molecular weight genomic DNA (7ug) from *T. brucei* 366D procyclic forms was digested to completion with A. Hind III, B. EcoRV, C. Sst II, D. Hinc II, E. Sst I. The digested DNA was separated on 0.8% agarose gel, transferred to nitrocellulose and probed with the [^{32}P]- labeled mouse cDNA clone of ODC. Hind III digested lambda DNA was used as markers.

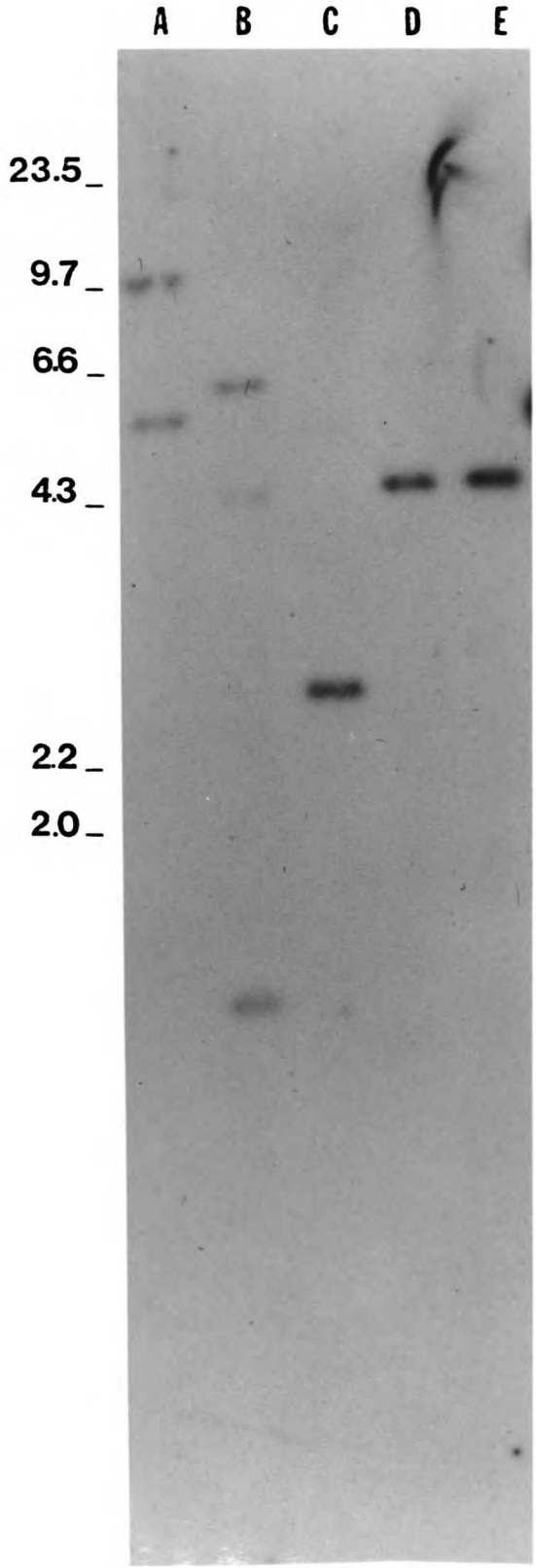
A
B
C
D
E
23.5
9.7
6.6
4.3
2.2
2.0

Figure 2-3: *Southern blot analysis of T. brucei cosmid DNA.* Hind III digested lambda DNA markers (A) and one ug of DNA from cosmid clone C16 digested to completion with B. Hind III C. Sst I D. Sst II E. Hinc II were separated on 0.8% agarose gel and stained with ethidium bromide. b. The DNA was then transfered to nitrocellulose and probed as described in Figure 2-2. Lanes represent the same samples of digested DNA as in (a).

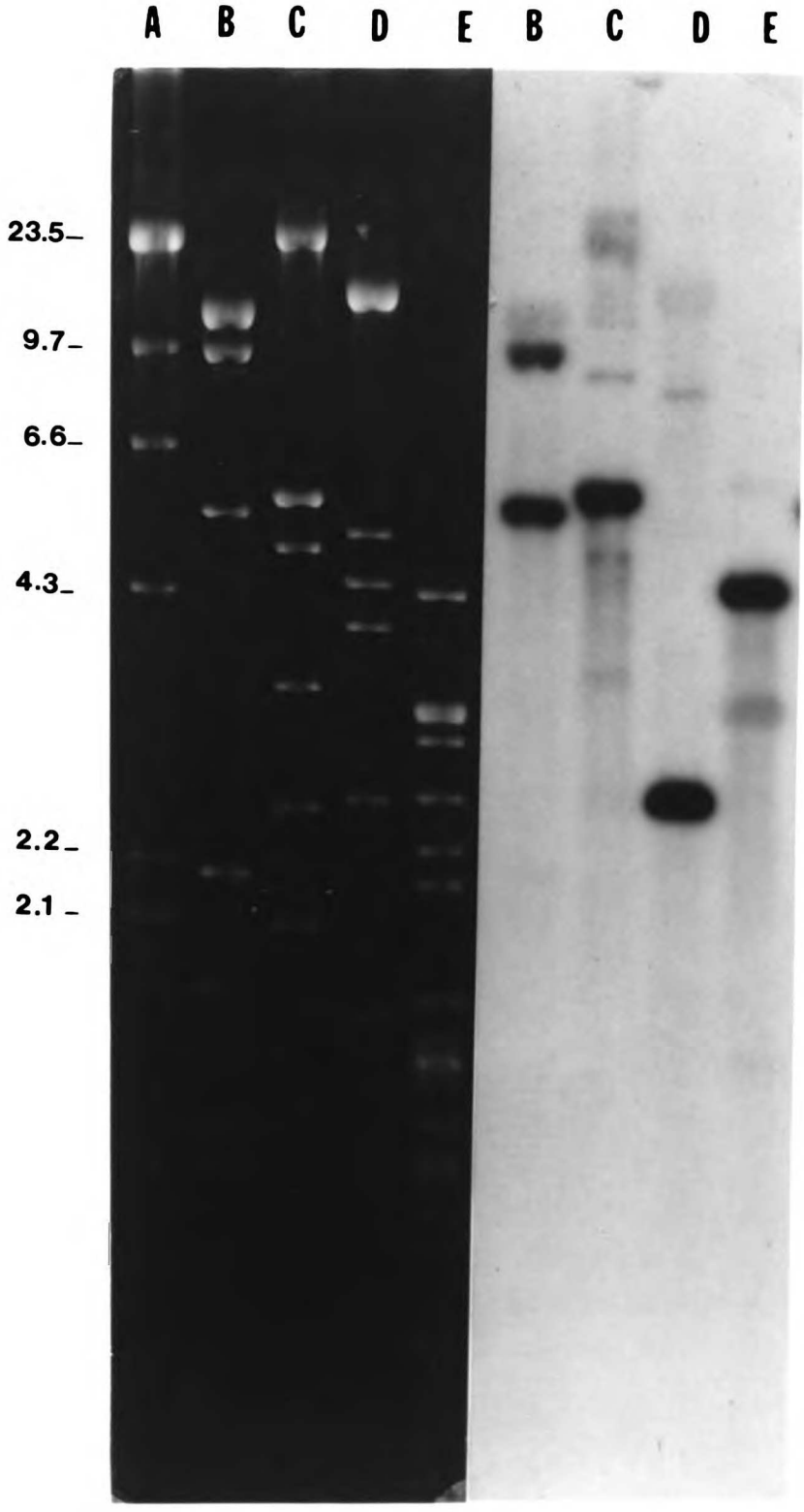
A
B
C
D
E
B
C
D
E
23.5
9.7
6.6
4.3
2.2
2.1

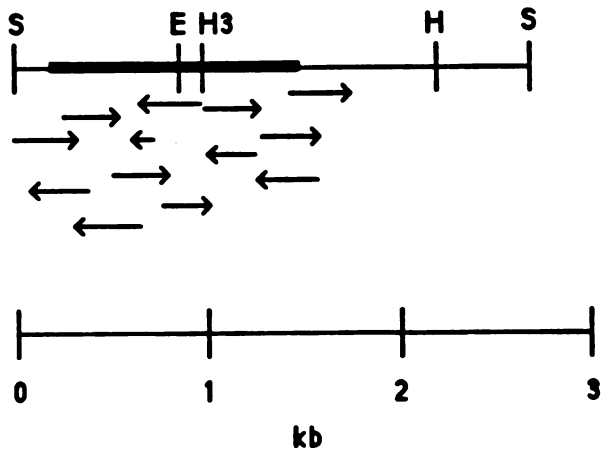

Figure 2-4. *Restriction map of T. brucei ODC.* A partial restriction map of cosmid clone C16 was obtained by Southern analysis of single and double restriction enzyme digests. E=EcoRV, H=Hinc II, S=Sst II, H3=Hind III. The thick bar represents the *T. brucei* ODC structural gene with the 5' end of the mRNA at the left most end. The arrows represent the directions and the fragments that were sequenced.

Figure 2-5. *Northern blot analysis of T. brucei poly (A)$^+$ RNA.* Poly (A)$^+$ RNA (25 ug) denatured in glyoxal/DMSO, separated by 1.2% agarose gel and transferred to nitrocellulose was probed with the [^{32}P]- labeled 2.8Kb Sst II fragment from cosmid clone C16. Rabbit rRNA served as size markers.

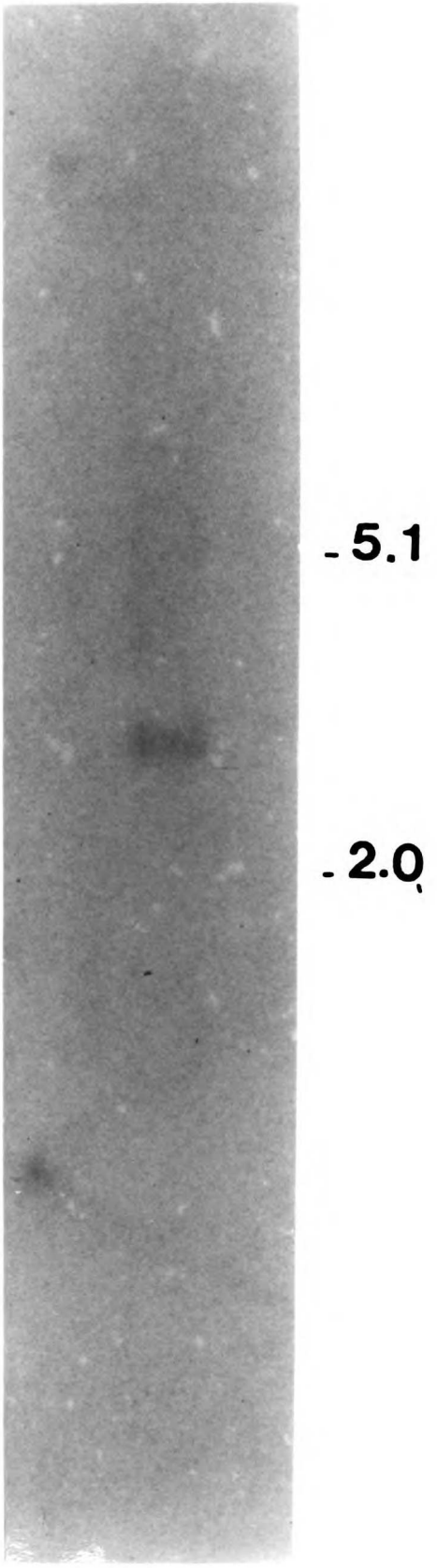
5.1
2.0

```
GCGGGGAGGGCTTTCCTTGCTTCCCAGAAGTATTATGTTTAAACACGCATGTGCGTCGGTAGCAAGCCTGGTAAAATTTGTCTGTACCATTTCCAATGAAGCGGTAGGGAAAGAGGCGG

                                1                                   10                                  20
                            Met Thr Thr Lys Ser Thr Pro Ser Ser Leu Ser Val Asn Cys Leu Val Ala Gln Thr Glu Lys Ser
TACTGGGGAGGGATTAAGCAGTAAGGCAAAT ATG ACC ACC AAA TCA ACC CCC TCT TCT CTC TCT GTG AAT TGT CTT GTA GCA CAA ACG GAG AAA TCT

                            30                                  40                                  50
Met Asp Ile Val Val Asn Asp Asp Leu Ser Cys Arg Phe Leu Glu Gly Phe Asn Thr Arg Asp Ala Leu Cys Lys Lys Ile Ser Met Asn
ATG GAC ATT GTC GTG AAC GAT GAC TTG AGT TGT CGC TTT CTT GAA GGG TTT AAT ACG AGG GAT GCC CTC TGT AAA AAG ATC AGT ATG AAT

                            60                                  70                                  80
Thr Cys Asp Glu Gly Asp Pro Phe Phe Val Ala Asp Leu Gly Asp Ile Val Arg Lys His Glu Thr Trp Lys Lys Cys Leu Pro Arg Val
ACG TGT GAC GAA GGT GAT CCG TTT TTT GTT GCC GAT CTC GGG GAC ATT GTA AGG AAG CAC GAA ACA TGG AAA AAA TGC CTT CCC CGC GTC

                            90                                  100                                 110
Thr Pro Phe Tyr Ala Val Lys Cys Asn Asp Asp Trp Arg Val Leu Gly Thr Leu Ala Ala Leu Gly Thr Gly Phe Asp Cys Ala Ser Asn
ACG CCG TTT TAC GCG GTC AAA TGC AAC GAT GAC TGG CGC GTA CTT GGA ACG CTG GCG GCT CTC GGC ACG GGA TTT GAT TGT GCT AGC AAC

                            120                                 130                                 140
Thr Glu Ile Gln Arg Val Arg Gly Ile Gly Val Pro Pro Glu Lys Ile Ile Tyr Ala Asn Pro Cys Lys Gln Ile Ser His Ile Arg Tyr
ACT GAG ATA CAA CGT GTG AGA GGC ATT GGT GTG CCA CCG GAA AAA ATA ATA TAT GCG AAC CCT TGT AAA CAA ATT TCA CAC ATA CGG TAC

                            150                                 160                                 170
Ala Arg Asp Ser Gly Val Asp Val Met Thr Phe Asp Cys Val Asp Glu Leu Glu Lys Val Ala Lys Thr His Pro Lys Ala Lys Met Val
GCG CGT GAT AGC GGC GTT GAT GTC ATG ACA TTT GAT TGC GTG GAT GAA CTG GAA AAG GTC GCT AAA ACG CAT CCA AAG GCA AAG ATG GTA

                            180                                 190                                 200
Leu Arg Ile Ser Thr Asp Asp Ser Leu Ala Arg Cys Arg Leu Ser Val Lys Phe Gly Ala Lys Val Glu Asp Cys Arg Phe Ile Leu Glu
TTA AGA ATT TCT ACG GAT GAT TCG TTG GCT CGA TGC CGT CTC AGT GTG AAG TTT GGT GCA AAG GTG GAA GAC TGT AGG TTT ATC TTG GAG

                            210                                 220                                 230
Gln Ala Lys Lys Leu Asn Ile Asp Val Thr Gly Val Ser Phe His Val Gly Ser Gly Ser Thr Asp Ala Ser Thr Phe Ala Gln Ala Ile
CAG GCA AAG AAA CTG AAT ATC GAC GTC ACT GGT GTG AGT TTT CAC GTG GGA AGC GGA TCT ACA GAT GCC TCT ACC TTC GCT CAA GCC ATA

                            240                                 250                                 260
Ser Asp Ser Arg Phe Val Phe Asp Met Gly Thr Glu Leu Gly Phe Asn Met His Ile Leu Asp Ile Gly Gly Gly Phe Pro Gly Thr Arg
TCT GAC TCC CGT TTC GTT TTC GAC ATG GGT ACT GAG CTT GGG TTC AAT ATG CAC ATT CTT GAT ATC GGT GGT GGG TTT CCA GGG ACG AGG

                            270                                 280                                 290
Asp Ala Pro Leu Lys Phe Glu Glu Ile Ala Gly Val Ile Asn Asn Ala Leu Glu Lys His Phe Pro Pro Asp Leu Lys Leu Thr Ile Val
GAT GCA CCA CTT AAA TTT GAA GAG ATT GCT GGT GTC ATC AAC AAT GCG CTG GAA AAA CAT TTT CCA CCT GAC CTC AAG CTT ACC ATT GTT

                            300                                 310                                 320
Ala Glu Pro Gly Arg Tyr Tyr Val Ala Ser Ala Phe Thr Leu Ala Val Asn Val Ile Ala Lys Lys Val Thr Pro Gly Val Gln Thr Asp
GCC GAG CCG GGA AGG TAC TAC GTT GCT TCA GCT TTC ACA CTT GCC GTA AAT GTT ATT GCC AAG AAG GTG ACA CCA GGG GTT CAG ACC GAC

                            330                                 340                                 350
Val Gly Ala His Ala Glu Ser Asn Ala Gln Ser Phe Met Tyr Tyr Val Asn Asp Gly Val Tyr Gly Ser Phe Asn Cys Ile Leu Tyr Asp
GTC GGT GCC CAT GCT GAA TCA AAC GCA CAG AGT TTT ATG TAT TAT GTG AAT GAT GGC GTG TAT GGT TCA TTT AAT TGC ATC CTG TAT GAC

                            360                                 370                                 380
His Ala Val Val Arg Pro Leu Pro Gln Arg Glu Pro Ile Pro Asn Glu Lys Leu Tyr Pro Ser Ser Val Trp Gly Pro Thr Cys Asp Gly
CAC GCA GTC GTC AGG CCT TTG CCC CAG AGG GAG CCA ATC CCC AAT GAA AAG CTC TAT CCC TCA AGT GTA TGG GGT CCC ACA TGT GAT GGT

                            390                                 400                                 410
Leu Asp Gln Ile Val Glu Arg Tyr Tyr Leu Pro Glu Met Gln Val Gly Glu Trp Leu Leu Phe Glu Asp Met Gly Ala Tyr Thr Val Val
CTT GAT CAG ATA GTT GAA CGA TAC TAT CTT CCC GAG ATG CAA GTG GGG GAA TGG CTG CTC TTT GAG GAT ATG GGT GCC TAC ACG GTC GTA

                            420                                 430                                 440
Gly Thr Ser Ser Phe Asn Gly Phe Gln Ser Pro Thr Ile Tyr Tyr Val Val Ser Gly Leu Pro Asp His Val Val Arg Glu Leu Lys Ser
GGA ACT TCT TCC TTT AAT GGA TTC CAG AGT CCG ACT ATT TAC TAT GTA GTC TCC GGG CTA CCA GAC CAT GTT GTC CGG GAG TTG AAA AGT

        445
Gln Lys Ser OC
CAA AAA TCA TAA ATGGAAGCGAAGGTGCATAATACGGGCCCAGCTCGTTGGCTCTCTGAGCAATGAAAGAAGGGGCTTTACCACCAGGTGTTGCTTCCTTTGGTAATATATTTGGTC

TGTTCTTGGCCCTGCGTTAGCTTTTTGCCCTTTGTGAGCTTAACGACT

Translated Mol. Weight = 49184.13
```

Figure 2-6. *Nucleotide sequnece of the ODC gene from T. brucei.* The nucleotide sequence was determined by the dideoxy sequencing method and the amino acid sequence was deduced from the 1,335 nucleotide open reading frame.

```
tb    1                                                        MTTKSTPSSLSVNCLVAQTE

         21                  40                  60                  80
tb   21 KSMDIVVNDDLSCRFLEGFNTRDALCKKISMNTCDEGDPFFVADLGDIVRKHETWKKCLPRVTPFYAVKCND
         *       *                *       *  * * *******  **  * * **************
M     1 MSSFTKDEFDCHILDEGFTAKDILDQKINEVSSSDDKDAFYVADLGDILKKHLRWLKALPRVTPFYAVKCND

                100                 120                 140                 160
tb   93 DWRVLGTLAALGTGFDCASNTEIQRVRGIGVPPEKIIYANPCKQISHIRYARDSGVDVMTFDCVDELEKVAK
              **** ******** **** * * *** *  ******** * * **   **  ****   ** ***
M    73 SRAIVSTLAAIGTGFDCASKTEIQLVQGLGVPAERVIYANPCKQVSQIKYAASNGVQMMTFDSEIELMKVAR

                        180                 200                 220
tb  165 THPKAKMVLRISTDDSLARCRLSVKFGAKVEDCRFILEQAKKLNIDVTGVSFHVGSGSTDASTFAQAISDSR
         ***** **** **** * *********     *  ** ** ***** ********* **  ** ** ** *
M   145 AHPKAKLVLRIATDDSKAVCRLSVKFGATLKTSRLLLERAKELNIDVIGVSFHVGSGCTDPDTFVQAVSDAR

            240                 260                 280                 300
tb  237 FVFDMGTELGFNMHILDIGGGFPGTRDAPLKFEEIAGVINNALEKHFPPDLKLTIVAEPGRYYVASAFTLAV
         **** ** ** ** *********  *  ******  *** ** * ** *    * ****************
M   217 CVFDMATEVGFSMHLLDIGGGFPGSEDTKLKFEEITSVINPALDKYFPSDSGVRIIAEPGRYYVASAFTLAV

                    320                 340                 360
tb  309 NVIAKKVTPGVQTDVGAHAESNAQSFMYYVNDGVYGSFNCILYDHAVVRPLPQREPIPNEKLYPSSVWGPTC
        * ****     *       *** * ********************** *  * *  * * ** * ** *****
M   289 NIIAKKTVWKEQPGSDDEDESNEQTFMYYVNDGVYGSFNCILYDHAHVKALLQKRPKPDEKYYSSSIWGPTC

        381                 400                 420                 440
tb  381 DGLDQIVERYYLPEMQVGEWLLFEDMGAYTVVGTSSFNGFQSPTIYYVVSGLPDHVVRELKSQKS
        **** ****  **** ** * *** ******   * ***** * **** *           *
M   361 DGLDRIVERCNLPEMHVGDWMLFENMGAYTVAAASTFNGFQRPNIYYVMSRPMWQLMKQIQSHGFPPEVEEQ

M   433 DDGTLPMSCAQESGMDRHPAACASARINV
```

Figure 2-7. *Comparison of the amino acid sequences between T. brucei ODC and the mouse ODC.* Identical segments between the *T. brucei* sequence (Tb) and the mouse sequence (M) are marked by stars (*).

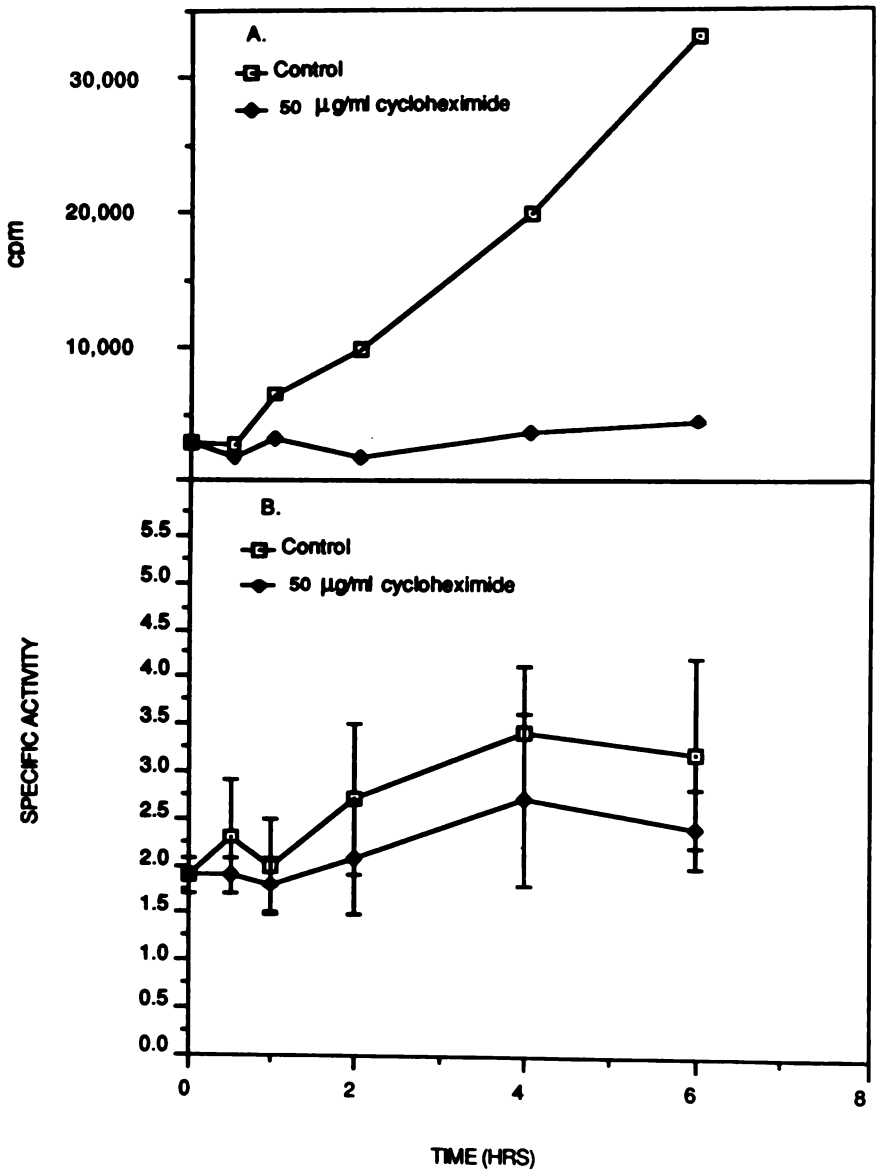

Figure 2-8. *Measurement of the turnover rate of T. brucei ODC.* A. [^{35}S]-methionine incorporation into *T. brucei* procyclic cells. ◊—◊ , no drug control; ♦—♦ , incubated in the presence of 50 µg/ml cycloheximide. B. ODC activity (nmoles CO_2/hr/mg protein). ◊— ◊,no drug control; ♦—♦ , incubated in the presence of 50 µg/ml cycloheximide.

CHAPTER THREE

Purification and Characterization of Ornithine Decarboxylase from *Trypanosoma brucei*

MATERIALS AND METHODS

Trypanosome isolation: *T.brucei* monomorphic strain Eatro 110 bloodstream forms were isolated as described in Chapter one. Approximately 10^{11} long slender bloodstream trypomastigotes were obtained from 30 rats by this procedure and were used for the purification of ODC.

Enzyme purification. A. Crude Extract: The purified trypanosomes were suspended in 110 ml of buffer A (25 mM Tris-HCl pH 7.5, 0.1 mM EDTA, 2 mM DTT) plus 1 mM leupeptin and 1 mM phenylmethylsulfonyl fluoride (PMSF), and sonicated for 15 sec bursts until no intact cells remained. The crude homogenate was spun at 27,000 x g for 20 min. The supernatant was centrifuged again at 125,000 x g for 1.5 hr and the pellet discarded.

B. Ammonium sulfate fractionation: The supernatant from the high speed centrifugation was precipitated with ammonium sulfate. The 25-55% fraction contained the majority of the ODC activity. The pellet was dissolved in 5 ml buffer A plus 0.02% Brij 35, applied to a 40 ml Sephadex G25 column and eluted with the same buffer to remove the excessive ammonium sulfate.

C. Pyridoxamine phosphate affinity column chromatography: The column was prepared by incubating 1 g of pyridoxamine phosphate dissolved in 25 ml of 0.1 M HEPES pH 7.5 with the entire contents of a 25 ml bottle of Affigel 10 (Biorad, Richmond, CA) at 4°C overnight. The mixture was made 0.1 M in ethanolamine HCl pH 8.0 and incubated at 4°C for an additional hour. Approximately 1.3 umoles of pyridoxamine were bound to one ml bed volume of gel, corresponding to a reaction efficiency of 9%.

The eluent from the G-25 column was applied to the pyridoxamine affinity gel in a 1.6x15 cm column preequilibrated with buffer A plus 0.02% Brij 35, at a flow rate of 10 ml/hr. The column was washed with Buffer A plus 0.02% Brij 35 at a rate of 3 ml/hr for 10 hrs. The bound ODC activity was then eluted with the above buffer plus 0.05 mM pyridoxal phosphate at a flow rate of 10 ml/hr. Approximately 50% of the ODC activity failed to be adsorbed to the column on the first passage. This flow through was reloaded onto the same column and the bound ODC was eluted as before. The ODC containing fractions eluted with pyridoxal phosphate from both passages were pooled.

D. Ion Exchange column chromatography: Eighty mM NaCl was added to the pooled material from section C and this was then loaded onto a Mono Q column (Pharmacia) at a flow rate of 0.5 ml/min. The sodium chloride was required to prevent pyridoxal phosphate from adhering to the column. The column was washed with 10 ml buffer A plus 0.02% Brij 35, 0.05 mM pyridoxal

phosphate and 80 mM NaCl. A linear gradient of 10 ml from 80 mM NaCl to 300 mM NaCl was used to elute the enzyme.

E. Gel filtration: A portion (10%) of the ODC activity recovered from the mono Q column was applied to a Superose 6 column(Pharmacia) at a flow rate of 0.5 ml/min. The column was equilibrated and washed with 25 mM Tris-HCl pH 7.5, 0.15 M NaCl and 2 mM DTT. Biorad gel filtration standards were used to calibrate the column(thyroglobulin, 670 kdal; IgG, 158 kdal; ovalbumin, 44 kdal; myoglobin, 17 kdal; and vitamin B12, 1.4 kdal).

The ODC assay. ODC activity was monitored by trapping $^{14}CO_2$ as described in Chapter one with several modifications. L-[1^{14}C] ornithine (1 mM, 1 mCi/mmol) was used as the labeled substrate. For enzyme samples purified beyond the ammonium sulfate step, 1 mg/ml bovine serum albumin (BSA) was also included. Enzyme was added to start the reaction. The reactions were carried out in 13 x 100 mm test tubes stoppered with serum caps at 37°C. The reaction was stopped by the injection of 1 ml 40% TCA through the serum cap. The filter paper was removed and the radioactivity measured by scintillation counting. The assay was linear up to 30 min with 0.001-0.02 µg of the protein sample purified beyond the Mono Q ion exchange column chromatography step. One unit of activity is defined as 1 nmol CO_2/hr.

Kinetic analysis. The K_m for ornithine was measured by varying the concentration of ornithine in the above assay procedure with one modification. A 60 mM phosphate buffer pH 7.2 was used in place of glycylglycine because the latter had inhibitory effects on the enzyme at low ornithine concentrations. DFMO kinetic analysis was performed as follows. Enzyme samples were incubated with different concentrations of DFMO in 25 mM Tris-HCl pH 7.5, 2 mM DTT, 0.05 mM pyridoxal phosphate and 1 mg/ml BSA for varying lengths of time at 30°C. At each sampling time a 10 µl aliquot was removed from the incubation mixture, added to 0.48 ml of assay mixture minus radiolabeled ornithine and kept on ice . Controls were done by adding DFMO at the appropriate concentration to assay mixture that already contained the enzyme on ice. Radiolabeled ornithine was added to each reaction after the pre-incubation had been completed. Samples were capped as described above, incubated at 37°C for 15 min and the ODC activity was monitored as before. The reaction was stopped by the addition of 1 ml 80% TCA through the cap.

Protein determination and sodium dodecylsulfate polyacrylamide gel electrophoresis(SDS-PAGE). Protein concentrations were determined by the Bradford method (76) using the Biorad reagent and IgG as a standard. For samples with protein levels too low to be detected by this

method, the protein concentrations were estimated by comparison to standards on SDS-PAGE stained with CoomasSie blue and quantitated with an LKB laser densitometer. SDS-PAGE was performed in 10% gels as described (69). Protein standards were purchased from Biorad(phosphorylase b, 92.5 kdal; BSA, 66.2 kdal;ovalbumin, 45 kdal;, carbonic anhydrase, 31 kdal; soybean trypsin inhibitor; 21.5 kdal and lysozme, 14.4 kdal). Gels were stained with Coomasie blue.

DFMO labeling of ODC. Approximately 1 µg of mono Q purified ODC was incubated for 1 hr with 0.13 mCi of DL-[5-^{14}C] DFMO at 37°C. The protein was precipitated and washed with 5% TCA with *Micrococcus lysodeikticas* protein as a carrier. The pellet was analyzed by SDS-PAGE followed by audoradiography of the gel, which had first been treated with enhancer and dried. The band with radioactivity was cut out and measured by scintallation counting.

Determination of isoelectric point(pI). The pI measurement was performed on a Mono P(Pharmacia) chromatofocusing column. The start buffer was 25 mM Bis-Tris pH 6.5, 0.02% Brij 35 and 2 mM DTT. The elution buffer was Polybuffer 74(Pharmacia) pH 4.0, 0.02% Brij 35 and 2 mM DTT. The column was run at a flow rate of 1 ml/min for 40 min to complete the gradient. Collected samples were neutralized immediately with 10%(v/v) 1 M Tris-HCl pH 7.5 plus 0.5 mM pyridoxal phosphate after elution and examined for ODC activity.

Materials. D,L-[1-^{14}C]ornithine(61.1 mCi/mmol) and D,L-[5-^{14}C]DFMO(61 mCi/mmol) were obtained from Amersham. D,L-DFMO was a gift from Dr. P.P. McCann, Merrill Dow.

RESULTS AND DISCUSSION

Enzyme Purification. The procedure used to purify the *T. brucei* ODC was a modification of the procedure used previously to purify mouse kidney ODC (77). The protocol, summarized in Table 3-1, resulted in a 107,000 fold purification with an overall recovery of 17%. The final specific activity is 2.7 x 10^6 nmoles CO_2/hr/mg protein. This indicates that ODC constitutes at most 0.001% of the total cell protein in *T. brucei.* The final specific activity is very similar to the value of 3.0 x 10^6 reported for purified mouse kidney ODC(77). When 5 -^{14}C DFMO was used to label the purified ODC, the radioactivity bound to the enzyme allows another measure of the quantity of ODC . The ratio of ODC activity/DFMO bound thus gives an alternate measure of the specific activity of pure *T. brucei* ODC. When this was done for Mono Q purified ODC 1.9 x 10^5 units//nmol DFMO/subunit bound was obtained which corresponds to a specific activity of 4.4 x 10^6 units/mg. This is in good agreement with the value(4.5 x 10^6 units/mg) obtained for Chinese hamster ovary cell ODC labeled to ^{3}H-DFMO by a similar procedure(78). The profile for a typical pyridoxamine phosphate affinity column elution is shown in Figure 3-1. Since very little protein other than ODC was bound to the column, it resulted in a major purification of ODC. The difficulty, however, is that the capacity of the column for binding ODC was low and two passes over the column were required to recover the majority of the active ODC. Mono Q column chromatography (Figure 3-2) provided both a major increase in enzyme purity and a convenient way to concentrate the sample. Recovery from this column was nearly quantitative. ODC was eluted from the Superose 6 column at a position corresponding to a molecular weight of 90 kdal (Figure 3-3), which is in good agreement with our previous result (75). Only 10% of the total sample was loaded onto this column in our present study. It should be possible, however, to load a much more concentrated sample to achieve further purification of a larger quantity of ODC.

This sequence of purification steps resulted in purification of *T. brucei* ODC to near homogeneity , as shown by SDS PAGE analysis of the purified protein sample(Figure 3-4). [5-^{14}C]-DFMO labeling of the mono Q purified protein prior to SDS-PAGE, followed by autoradiography, gave a single band at 45 kdal corresponding exactly to the major protein band observed when the gel was stained with Coomasie blue.

Enzyme Characterization. The K_m for ornithine was measured using the ODC sample that had been purified through the Mono Q step. The apparent K_m for ornithine at a pyridoxal phosphate concentration of 50 μM is 244 μM as determined by Lineweaver Burk analysis (Figure 3-5) with a

V_{max} of 1.6 x10^4 nmol CO_2/min/mg.. The K_m value is 2 fold higher than the K_m observed previously in crude trypanosome extracts (37). The inactivation of ODC by DFMO was time dependent (Figure 3-6). The halflife of inactivation at an infinite concentration of DFMO can be extrapolated to 5.8 min(Figure 3-6) at an incubation temperature of 30°C. The K_I determined by this study was 179 µM, in good agreement with the values reported from crude *T. brucei* extracts(38).

When applied to a mono P chromatofocusing column the major peak of ODC activity elutes at a pH value of 5.O (Figure 3-7), which is in good agreement with the pI of 5.5 predicted from the deduced amino acid sequence (75). Two minor peaks at 6.4 and 5.7 were also observed. The significance of these peaks is unknown. However, a similar result is obtained when *T. brucei* ODC that has been expressed in *E. coli* and purified, was applied to the column by a similar procedure (Chapter 4). This suggests that the heterogeneity in pI values may be a result of protein structural modifications during purification rather than multiple forms of the enzyme generated by posttranslational modifications in the trypanosome.

When the properties of this purified *T. brucei* ODC are compared with those known for mouse ODC (79,39), close similarities between the two enzymes are observed(Table 3-2). *T. brucei* ODC has a lower molecular weight than the mouse enzyme, as had been previously predicted from the genomic sequence(75). The close similarities in the catalytic properties between the mouse and parasite enzyme are not surprising considering the degree of homology at the amino acid level(75). This illustrates that differences in catalytic properties between host and pathogen enzymes are not necessarily required for an enzyme to be an effective chemotherapeutic target. As reported previously, the selective toxicity of DFMO on the parasite may instead be the result of differences in the turnover rate of the two enzymes (75). Thus, when one searches for chemotherapeutic targets no potentially exploitable difference between the host and the infectious agent should be overlooked.

We have described a working procedure for the purification of *T. brucei* ODC to near homogeneity. The quantities of enzyme that can be obtained from this procedure are,however, too low for more extensive enzyme characterizations. Expression of the cloned ODC gene and purification of the recombinant enzyme by a similar procedure should provide much larger quantities of this important enzyme for further studies.

Table 3-1
Native *T. brucei* ODC Purification Scheme

Step	Specific Activity	Total Activity	Total protein (mg)	Volume (ml)	%Recovery	Fold Purified
Crude Extracts	25.2	3.4×10^4	1375	110	-	-
Ammonium Sulfate	45.6	3.6×10^4	825	22	100	1.8
Pyridoxamine Phosphate Affinity	35,880	1.2×10^4	0.4	67	35	1420
Mono Q	0.4×10^6	1.2×10^4	0.03	6.5	35	16,000
*Gel Filtration	2.7×10^6	$.06 \times 10^4$	0.001	1.5	17	107,000

* 0nly 10% of protein from step 4 was loaded in step 5. Activity is measured in nmol CO_2/hr .

Table 3-2
Comparison of *T. brucei* ODC with Mouse Kidney ODC

	T.brucei	Mouse*
A. Kinetic properties		
$K_m$orn(μM)	244	75
K_IDFMO(μM)	178	39
B. Physical properties		
subunit MW(kdal)	45	53
native MW(kdal)	90	100
isoelectric point	5.0	4.8

*Information derived from reference #19 and #39.

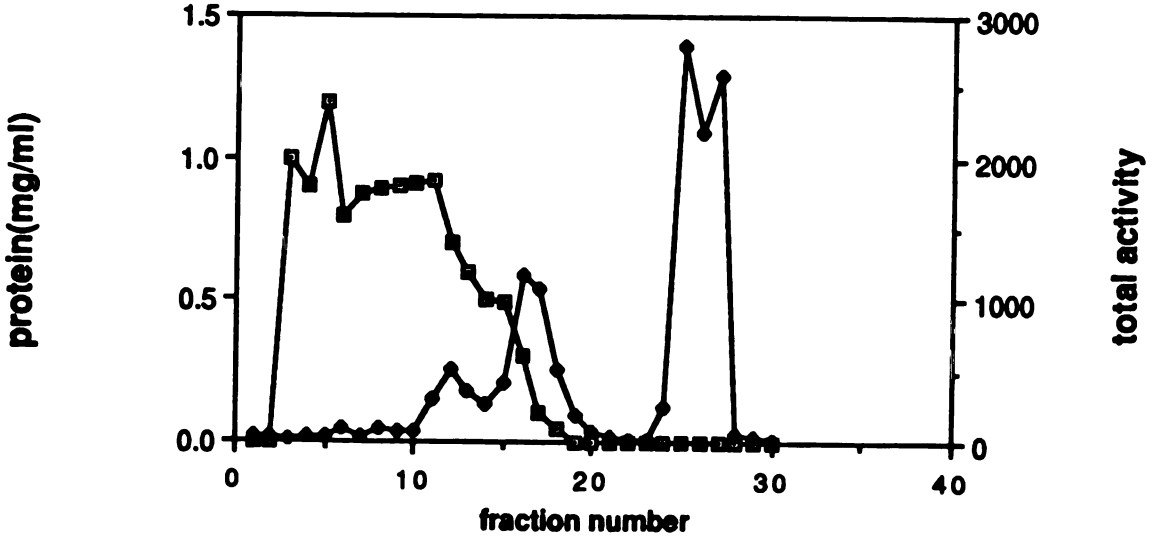

Figure 3-1: *Pyridoxamine phosphate affinity column elution profile.* ◊-◊, protein concentration in mg/ml, ♦-♦, ODC activity in nmol CO_2/hr/fraction.

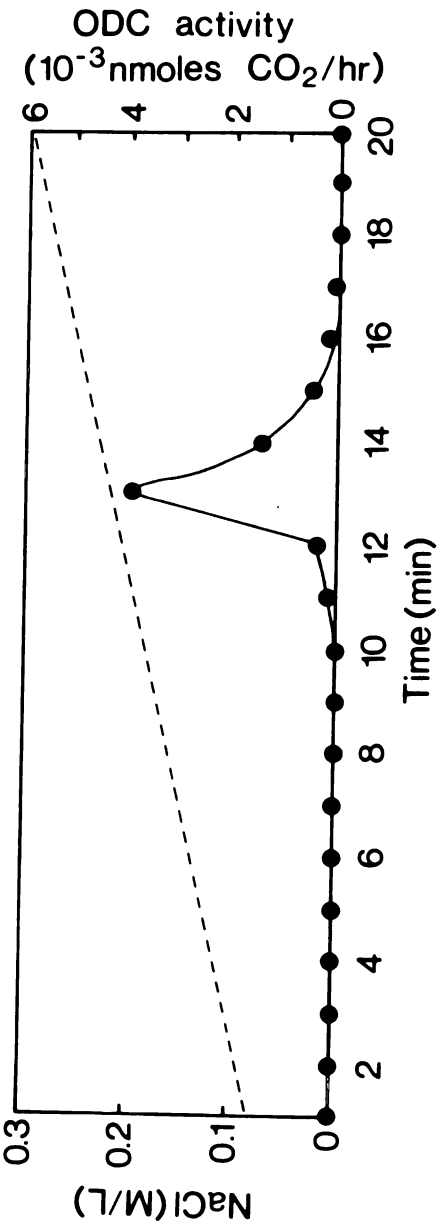

Figure 3-2: ***Mono Q, anion exchange column chromatography elution profile.*** **- -, sodium chloride concentration, ●-● ODC activity in nmol CO_2/hr/fraction.**

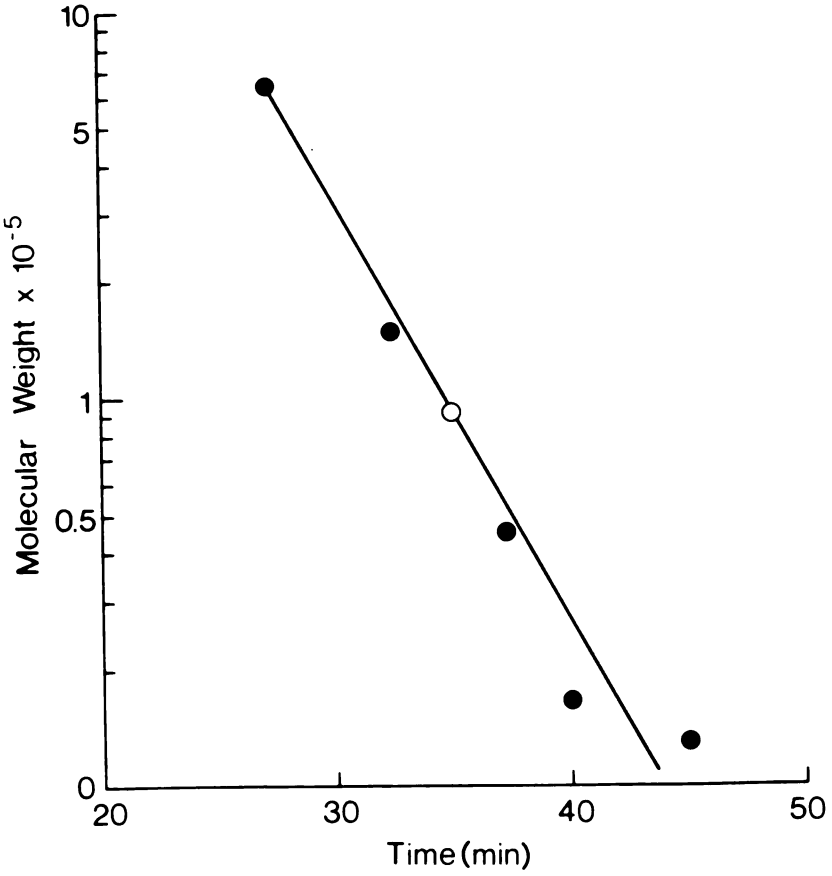

Figure 3-3: *Native Molecular weight determination.* Partially purified ODC was mixed with Biorad standards and applied to a Superose 6 gel filtration column at a flow rate of 0.5 ml/min. Fractions collected every 0.2 min were checked for ODC activity. The elution time of the Biorad standards was plotted versus the molecular weight of the standards(●,thyroglobulin, IgG,ovalbumin , myoglobin and vitamin B12) and the elution time of the ODC activity peak(o) was compared to that of the standard proteins.

Figure 3-4: *SDS-PAGE analysis of purified T. brucei ODC.* Lane A, molecular weight markers (phosphorylase b, 92.5 kdal; BSA, 66.2 kdal;ovalbumin, 45 kdal;, carbonic anhydrase, 31 kdal; soybean trypsin inhibitor; 21.5 kdal and lysozme, 14.4 kdal); lane B crude *T. brucei* extract; lane C, *T. brucei* ODC purified through the mono Q step ; Lane D, *T. brucei* ODC purified through the gel filtration step; Lane E, an autoradiogram of lane C, ODC had been labeled with [5-^{14}C]DFMO prior to loading on the gel. The gel was stained with Coomassie blue.

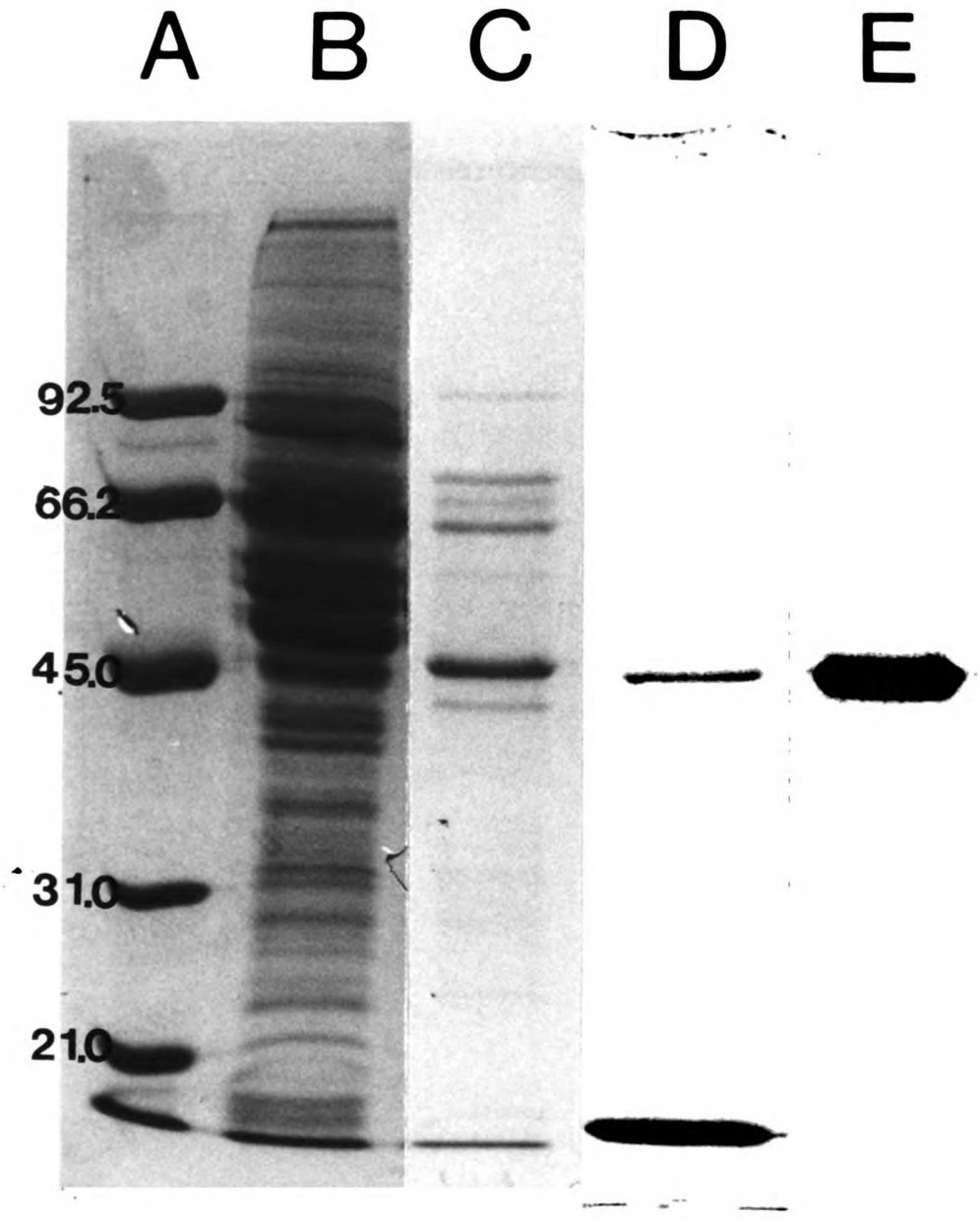
A
B
C
D
E
92.5
66.2
45.0
31.0
21.0

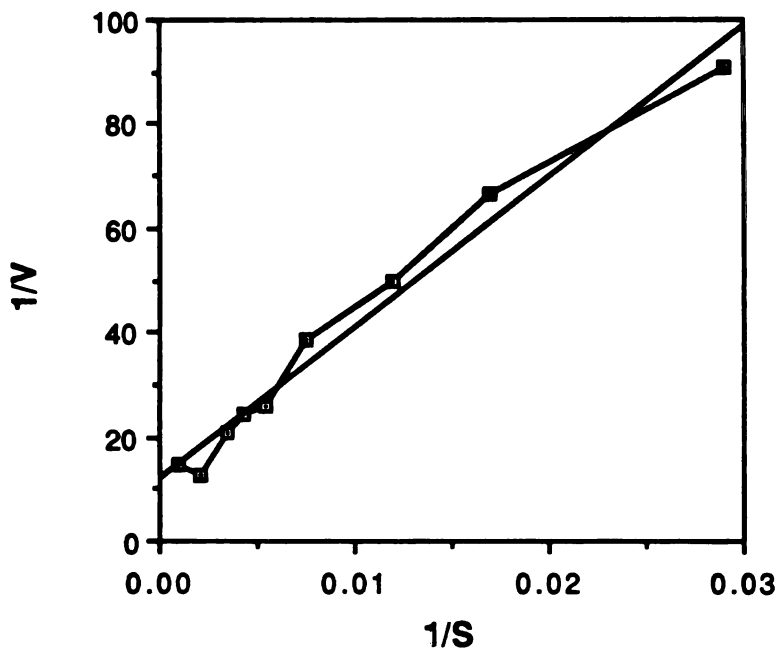

Figure 3-5: *Determination of the K_m for ornithine.* Lineweaver Burk analysis of the dependence of the ODC catalyzed reaction rate(V, velocity nmol/min) on substrate concentration(S, L-ornithine concentration μM). ϕ-ϕ represents actual data points and the solid line represents the best fit line. The K_m for ornithine was calculated to be 244 μM from the best fit line y = 11.9 + 2894.7x.

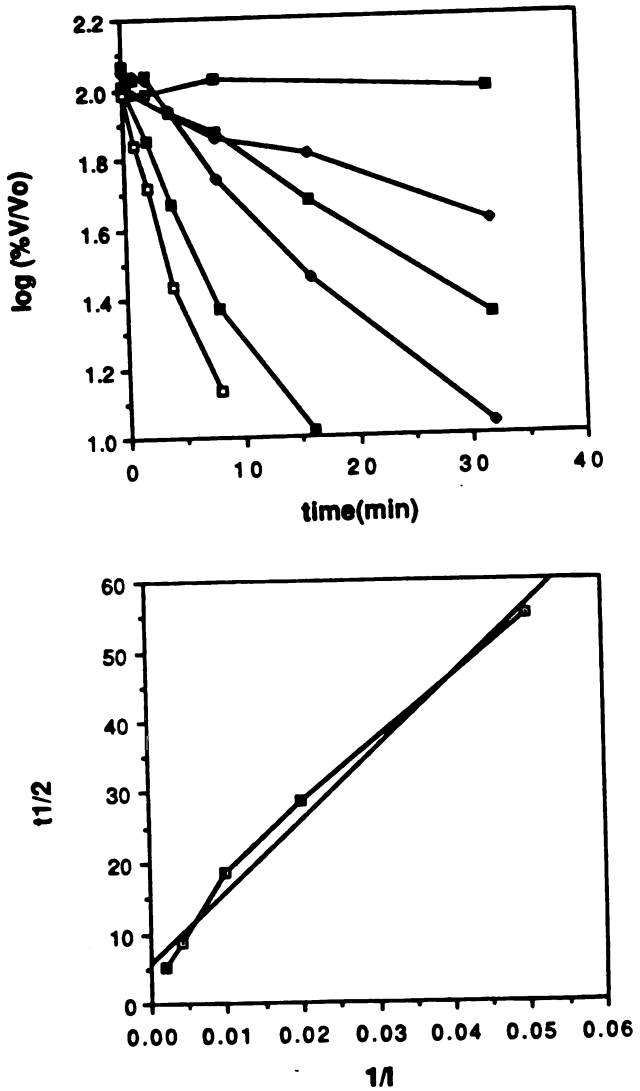

Figure 3-6: A. *Time dependence of DFMO inactivation of purified T. brucei ODC, Log(activity) vs time of inactivation.* ◊-◊, no DFMO control; ●-●, 20 μM DFMO; ♦-♦, 50 μM DFMO; ●-●, 100 μM DFMO; ♦-♦, 250 μM DFMO; and ◊-◊, 500 μM DFMO. B. Plot of halflife(t1/2). vs reciprocal value of DFMO concentration(1/I),■-■ represents actual data and the solid line represents the best fit line. $T_{1/2}$ was calculated for each DFMO concentration (I, μM)using the equation for exponential decay. From this plot the K_I for DFMO(-1/x-intercept) was determined to be 179 μM and the $t_{1/2}$ at infinite concentration(y-intercept) of DFMO was determined to be 5.8 min.

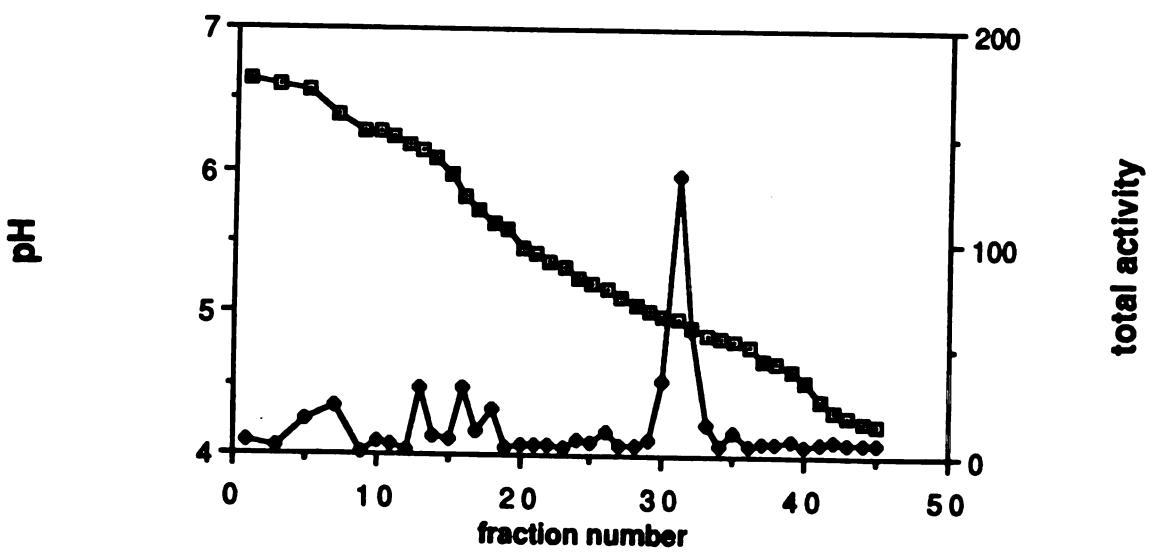

Figure 3-7: *Determination of the Isoelectric point of T. brucei ODC.* Purified ODC was loaded onto a mono P chromatofocusing column. The elution profile of ODC activity, ◆-◆ was compared to the pH ,■-■ of the fraction.

CHAPTER FOUR

Expression of *Trypanosoma brucei* Ornithine Decarboxylase Gene in *E. coli*: Purification and characterization of the recombinant enzyme.

Materials and Methods

Nucleic acid preparation and DNA sequencing. Single stranded DNA was obtained from Bluescript vectors with the use of M13 helper phage DNA as described in chapter 2. Plasmid DNA for mini screens was purified by the alkaline lysis method from 1.5 ml of overnight culture and larger samples of preparative quantities were further purified by CsCl buoyant density gradient centrifugation as described in Chapter 2. DNA sequencing was performed by the dideoxy chain termination method(67) with [^{35}S]-dATP as the labeled nucleotide. The procedure was modified for double stranded DNA as described in chapter 2. Oligonucleotides complementary to the appropriate regions of the *T. brucei* ODC gene were used to prime the sequencing reactions.

In vitro transcription ,translation and immunoprecipitation.

In vitro transcription of the plus strand of the *T. brucei* ODC gene was performed as described (Promega,Madison WI). Briefly, 5 µg plasmid pBHS2.2 (full length *T. brucei* gene (75) cloned into a 2.2 kb SSTII-Hinc II fragment into the (-) bluescript vector (Stragagene, San Diego)) was linearized with Hinc II and reacted with 10 units T7 polymerase, 0.5 mM ATP, CTP, UTP, 0.05 mM GTP 0.5 mM GpppG(Pharmacia), 60 units RNasin(Promega) and buffer as described for 60 min at 40°C. RQ1 DNase(Promega) was then used to remove the DNA template. Approximately 1 µg of the synthesized RNA was translated using a rabbit reticulocyte lysate system(Promega) . RNA, the rabbit reticulocyte lysate, 25 units RNasin, 1 mM amino acid mix(- methionine) and 50 µCi [^{35}S]- methionine(1200 Ci/mmol) were incubated together for one hr at 30°C. The protein thus synthesized was then immunoprecipitated with a rabbit anti-mouse ODC antiserum (provided by Dr. Olli Janne) and formalin-killed *Staphlyococcus aureas* cells. One tenth of the *in vitro* translation mixture was incubated for 1 hr at 4°C with non immune rabbit serum and the formalin treated *S. aureas* cells suspended in buffer B(PBS with 1% NP40, and 10 mM methionine). The mixture was centrifuged and the pellet discarded. The supernatant was incubated with 5 µl rabbit anti-mouse ODC overnight at 4 °C, followed by a one hr incubation at 4°C in the presence of *S. aureas* cells. The mixture was centrifuged and the pellet was washed 2 times in buffer B. SDS-PAGE sample buffer was added , the pellet was boiled for 10 min and the supernatant analysed on SDS-PAGE.

Site directed mutagenesis of the T. brucei ODC gene. A ScaI site was created between the initiating ATG and the second amino acid codon ACC. Mutagenesis was done using the double primer method (80). A. Primer extension and ligation: A twenty four nucleotide primer 5'-P-

AAGGCAAATAG*T*ACT*ACCAAATCA-3' was annealed at 55°C for 5 min to single stranded pBHS2.2. A second primer was annealed simultaneously to bases 1272-1289 in the *T. brucei* ODC genomic sequence(75). The primers were simultaneously extended with Klenow and ligated at 15°C overnight. Annealing and strand synthesis were carried out in 50 mM Tris pH 8.0, 20 mM KCl, 7 mM $MgCl_2$, 0.1 mM EDTA and 10 mM β– mercaptoethanol. The reaction contained 20 pmoles of each primer, one pmol template, 9 units Klenow, 6 units T4 DNA ligase, 0.15 mM dGTP, dTTP, dCTP, 0.05 mM dATP and 0.05 mM rATP in 20 µl. The ligation mixture was then used to transform *E. coli* strain dg98. B. Screening: Colonies were lifted and hybridized to nitrocellulose filters as described(81). Filters were prehybridized overnight at 50°C in 6X SSC(0.9M NaCl and 0.09 M sodium citrate pH 7.0), 10X Denhardt's,50 µg/ml salmon sperm DNA and 1 mM ATP followed by one hour at 65°C in fresh prehybridization buffer. Ten pmole of the 24 nucleotide mutagenic primer was phosphorylated with [γ^{32}P]-ATP using T_4 polynucleotide kinase, added to 5 ml of prehybridization buffer and hybridized to the filters at 42°C overnight. Filters were then washed sequentially in 6X SSC, 0.1% SDS first at 50°C (the melting temperature (T_m) of the mutagenic primer annealing to wild type template) and in 6° increments to 62°C (the Tm of the mutagenic primer annealing to the identical sequence). Colonies that continued to hybridize to the primer at 62°C were picked and screened for the presence of the Sca I site. Those containing the new ScaI site were sequenced .

Cloning of T. brucei ODC gene into the expression vector. The expression vector pCQV2 (82) was digested with BamH1 followed by mung bean nuclease to expose the initiating ATG (82). The vector was then blunt end ligated to the 1.8 kb ScaI fragment containing the entire ODC gene minus its initiating ATG to make the final *T. brucei* ODC gene expression vector . The recombinants were used to transform *E. coli* strain HT289(83), plated on LB amp plates and incubated overnight at 32°C.

Bacterial growth and heat shock induction of ODC gene expression. Either LB broth or minimal media containing 0.5 mM putrescine was inoculated with the *E. coli* strain HT289 containing the appropriate plasmid and grown up at 32°C overnight. A 1/10 dilution into fresh media was made and cells were grown at 32°C until the OD_{595} reached 0.6. The cells were then slowly added to an equal volume of media, preheated and maintained at 42°C over a 5 min period, incubated at 42°C for an additional 10 min to allow the temperature of the culture to reach 42°C, and finally grown at 39°C until the OD_{595} was again 0.6.

Pulse chase experiments with [^{35}S]-methionine. Cultures were grown as described above in minimal media. After 10 min of incubation at 39°C 0.03µM [^{35}S]- methionine(1125Ci/mmol) was added to the culture. After an additional 2 min at 39°C cold methionine to a final concentration of

1 mM was added and the incubation continued. Aliquots(0.5 ml) were removed at various time points and stored on ice until all time points were taken. Cells were pelleted, resuspended in 100µl 0.06 M sodium phosphate pH 7.8, 0.15M NaCl, 2 mM DTT and 1 mM EDTA and sonicated. A10 µl sample from each time point was analyzed by SDS-PAGE and autoradiograpy.

Purification and characterization of ODC. The methods for the purification and characterization of ODC, the ODC assay , enzyme kinetic analysis, DFMO labeling, protein determination, SDS-PAGE, isoelectric point determination and native molecular weight determination were described in Chapter 3.

Materials. D,L-[1-^{14}C]ornithine(61.1 mCi/mmol) and D,L-[5-^{14}C]DFMO(61 mCi/mmol) were obtained from Amersham. [^{35}S]- Methionine(1200 Ci/mmol) was obtained from New England Nuclear. D,L-DFMO was a gift from P.P. McCann, Merrill Dow.

Results

In vitro transcription and translation of the T. brucei ODC gene: Before proceeding with the complicated cloning steps required to insert the cloned *T. brucei* ODC gene into an expression vector we wanted to verify that the clone (75) indeed coded for authentic *T. brucei* ODC and that the predicted translation initiation site was correct . In vitro transcription of the *T. brucei* ODC gene using the T_7 promotor and T_7 polymerase, followed by in vitro translation in a rabbit reticulocyte system resulted in the production of a 45 kdal protein(Figure 4-1), corresponding to the molecular weight of full size *T. brucei* ODC subunit(75). The 45 kdal protein could be immunoprecipitated by the rabbit anti-mouse ODC but not by the non immune serum(Figure 4-1), implying strongly that the cloned gene encodes full length *T. brucei* ODC.

Site directed mutagenesis of the T. brucei ODC gene: The 5' region upstream of the genomic sequence coding for *T. brucei* ODC (the SSTII site 150 base upstream of the initiating ATG) contained no unique restriction sites (75). This made the task of cloning the gene into an *E. coli* expression vector, with a suitable alignment with the promotor, difficult. Through the creation of a blunt ended cleavage site between the first and second codons it became possible to ligate the *T. brucei* ODC gene to any upstream sequence required for expression. Mutagenesis to replace the sequence ATGACC with AGTACT was performed using the mutagenic primer shown in Figure 4-2. A change in the DNA sequence of the second codon, which encodes threonine, was required to create the desired Sca I cleavage site, but the new sequence also codes for threonine and thus should retain the original protein structure. The ODC coding region of clone pBsca19 was sequenced in its entirety and was found to contain the three base changes that created the Scal site but no other alterations.

Cloning and expression of the T.brucei ODC gene in the pCQV2 expression vector.

pCQV2 contains the lamda phage P_R promotor which has the advantage of being a very strong, inducible promotor capable of producing protein to levels of up to 10% of the total cellular protein. The P_R promotor is under the control of a heat sensitive repressor (82) which inhibits transcription from the P_R promotor at 32°C but not at 42°C (82). The vector also contains the initiating ATG codon conveniently placed within a Bam H1 site. *T. brucei* ODC was cloned into pCQV2 at this site and introduced into a polyamine deficient strain of *E. coli* , HT289 (83), that requires an exogenous source of putrescine for growth. This strain lacks *E. coli* ODC as well as several other key polyamine biosynthetic enzymes making it easy for us to screen for the production of active *T. brucei* ODC. One clone pQtODC.8 which contained the *T. brucei* ODC gene ligated in frame with the initiating ATG from the expression vector was chosen for further

study. pQtODC.12, a clone with the opposite orientation was also picked to serve as a control. pQtODC.8 was able to complement the growth of HT289 when plated on minimal media at 42°C in the absence of putrescine while pQtODC.12 was not(data not shown). pQtODC.8 was sequenced in the region of the initiating ATG and was found to contain the desired construction illustrated in Figure 4-2.

pQtODC.8 and pQtODC.12 transformed *E. coli* HT289 were grown up and heat induced, and the ODC activity in crude extracts from these preparations was measured(Table 4-1). ODC activity was negligible at both 32°C and at 42°C in HT289 cells that had not been transformed or in pQtODC.12 transformed cells. When cells containing pQtODC.8 were grown at 32°C very little ODC activity was observed. However, when these cells were heat induced at 42°C, ODC activity increased over 60 fold. To ensure that the enzyme being synthesized was not being simultaneously degraded inside *E. coli*, cells containing pQtODC.8 and pQtODC.12 were pulse labeled with [^{35}S]- methionine and the fate of labeled ODC throughout a 60 min chase with cold methionine(Figure 4-3) was followed by SDS-PAGE and autoradiography. A protein band of 45 kdal corresponding to the subunit molecular weight of *T. brucei* ODC(75) was visible in SDS-PAGE only when cells containing pQtODC.8 had been heat induced at 42°C. This band did not change in intensity throughout the one hr chase with cold methionine suggesting that we had achieved stable production of *T. brucei* ODC in *E. coli*. Several other bands were also seen in cells incubated at 42°C that were not present at 32°C. They were present in both pQtODC.8 and pQtODC.12 transformed cells and thus, maybe bacterial heat shock proteins.

Purification of T. brucei ODC from pQtODC.8 transformed E. coli HT289 cells. The purification procedure was a truncated version of that used to purify authentic *T. brucei* ODC from long slender *T. brucei* strain Eatro 110 bloodstream trypomastigotes (Chapter 3). The enzyme purification, summarized in Table 4-2, resulted in a 2200 fold purification with an overall recovery of 13% from the first batch of bacteral culture. The final specific activity is 3.2 x 10^6 nmoles/hr/mg protein. The profile of a typical pyridoxamine phosphate affinity column elution is shown in Figure 4-4. This step in conjunction with the ammonium sulfate precipitation resulted in purification of the recombinant enzyme to near homogeneity. The mono Q column(Figure 4-5) provided an additional purification step,as well as a way to concentrate the sample, and resulted in purification of *T. brucei* ODC to homogeneity as shown by SDS-PAGE analysis(Figure 4-6). In the second preparation the initial specific enzyme activity was much higher (Table 4-2), and the same purification can be achieved without the Mono Q column chrmatography step. A 500 fold purification to homogeneity, reflecting an original enzyme content of 0.2% of the total protien,

resulted in a yield of 34%. This would allow 1 mg of pure enzyme from 25 liters of bacterial culture (Table 4-2).

[5-^{14}C] -DFMO labeling of the purified protein prior to SDS-PAGE analysis and autoradiography gave a single band that corresponded precisely to the position of the Coomasie stained band at 45 kdal(Figure 4-6). It also migrated identically to the partially purified authentic *T. brucei* ODC(Figure 4-6). There is no possibility that this protein could be of *E. coli* origin because; (a) *E. coli* HT289 lacks ODC; (b) *E. coli* ODC does not bind DFMO (20); and (c) *E. coli* ODC has a subunit molecular weight of 86 kdal (20).

Characterization of recombinant T. brucei ODC and comparison with the authentic T. brucei ODC.

The specific activity of the purified recombinant ODC was 3.2 x 10^6 nmoles/hr/mg protein which is in good agreement with the specific activity of 2.7 x 10^6 nmoles/hr/mg protein obtained for purified authentic *T. brucei* ODC(Chapter 3). A separate measurement of the specific activity can be obtained by labeling the purified enzyme with [5-^{14}C] DFMO. The amount of DFMO incorporated into the protein can be used as an alternative way to calculate the concentration of ODC in solution. The ratio of ODC activity (nmol $C0_2$/hr) to nmol of DFMO bound per subunit was 2.2 x 10^5 units/nmol DFMO. This corresponds to a specific activity of 4.3x10^6 units/mg, which is in good agreement with the value of 4.4 x 10^6 units/mg found for authentic *T. brucei* ODC(Chapter 3). The value is somewhat higher than that obtained by estimating protein concentration from Coomasie stained gels but is within experimental error of the two techniques.

The apparent native molecular weight of the recombinant ODC was measured by gel filtration on a Superose 6 column and found to be 92 kdal(Figure 4-7). The recombinant enzyme like the authentic enzyme, which had a native molecular weight of 90 kdal in a similar experiment(Chapter 3) , thus appears to exist as a dimer of two identical subunits.

The K_m for ornithine was found to be 303 µM for the recombinant enzyme in the presence of 50 µM pyridoxal phosphate (Figure 4-8) and the V_{max} was 6.0 x 10^4 nmol CO_2/min/mg protein. DFMO was a time dependent inhibitor of the enzyme (Figure 4-9A) with a $T_{1/2}$ at infinite DFMO concentration of 3.9 min. at 30°C and a K_I of 154 µM(Figure 4-9B). The kinetic results agree well with those obtained previously for the authentic *T. brucei* ODC(Table 4-3).

The isoelectric point of the recombinant protein was measured on a mono P chromatafocusing column. The major peak of ODC elutes at a pH of 5.0(Figure 4-10) with two smaller peaks appearing at pH 6.4 and 5.7. A similar profile was observed for authentic *T. brucei* ODC(Chapter 4-3).

Discussion

E. coli expression of the *T. brucei* ODC gene and the purification of the recombinant enzyme described in this chapter allows for the production of approximately 40 μg of purified recombinant ODC / liter of *E. coli* culture. Based on the final specific activity of purified ODC and the original values in the crude extracts of different batches of bacterial cultures, we can estimate that 0.05-0.2% of the cellular protein in the transformed, induced *E. coli* HT289 cell is *T. brucei* ODC. This is a considerable improvementof 50-200 fold over the bloodstream long-slender *T. brucei* trypomastigote where slightly less than 0.001% of the total cell protein is ODC.

In addition to the simple method for obtaining large amounts of purified *T. brucei* ODC, this expression system also produces an active enzyme with no apparent differences from the authentic *T. brucei* enzyme. The native(90 kdal) and subunit(45 kdal) molecular weights of the authentic and recombinant enzymes are identical, implying that the recombinant protein had been correctly folded and aggregated to form a dimer of two identical subunits. The kinetic properties of the two proteins are virtually indistinguishable suggesting that there is no major difference in their catalytic function. The similar pI values observed for the two proteins imply that specific post translational modification of ODC does not play a significant role in the trypanosome .

Synthesis of recombinant protein at the level of 5-10% of total cell protein were reported for β-galactosidase and small T antigen using the same expression vector, pCQV2 in *E. coli*(82). The expression level observed for *T. brucei* ODC gene, though much lower, is quite comparable to the level(4700 nmol CO_2/hr/mg protein) of expression of mouse ODC cDNA in the same system(84). *T. brucei* ODC appears stable in *E. coli* HT289, thus protein degradation does not appear to be a factor in the lower yield of *T. brucei* ODC . A cause that commonly contributes to problems in eukaryotic protein production in bacterial cells is poor protein solubility(85). This does not appear to be a significant problem in the production of active *T. brucei* ODC, but the possibility that a fraction of the ODC produced is in an insoluble form cannot be ruled out. SDS-PAGE analysis of the total cellular protein after [^{35}S]-methionine pulse labeling (Figure4-3) supports the conclusion that *T. brucei* ODC does not represent more than 1% of the cell protein, a value not very different from the estimated 0.2% for soluble active enzyme.

Analysis of the codon usage in *T. brucei* ODC gene reveals that the preferred codons fall into the class of weakly expressed *E. coli* genes. Codons which are considered modulating codons, rarely found in highly expressed *E. coli* genes, occur with fair frequency in the *T. brucei* ODC gene. Where NNU is the preferred codon over NNC for pro,ala,and gly in highly expressed *E. coli*

genes(86), usage of NNU is preferred only for gly in the parasite gene. While NNC is preferred for phe, ile, tyr, asn, his, asp, cyt and ser in highly expressed *E. coli* genes(86), NNC is preferred only for his in the *T. brucei* ODC gene (75). The modulating codons(AUA,CGA,CGG,AGA,AGG,CUA, and GGA), which are believed to regulate the rate of translation are all found frequently in the *T. brucei* ODC gene. Thus, it may be that the *T. brucei* gene carries signals that target it for low level expression in *E. coli* preventing the synthesis of *T. brucei* proteins at high levels. If this is the case, neither modifications to the present system nor a change to another *E. coli* expression system will provide a significantly higher yield of *T. brucei* ODC. Expression in a yeast system might provide a viable alternative with the potential to increase the level of expression above what is obtained in the present system.

Despite these considerations the procedure described in this paper will allow for the purification of milligram quantities of the recombinant *T. brucei* ODC, apparently identical to the authentic trypanosome enzyme. The protein will be a useful model for drug design, particularly if it can be crystallized and further characterized. It will also provide a readily available source of pure protein that will aide in further studies of ODC regulation and the role of polyamines in *T. brucei* development.

Table 4-1
Induction of ODC Activity in Transformed HT289 Cells

clone	temperature(°C)	specific activity (nmol CO_2/hr/mg)
pQtODC.8	32	24
pQtODC.8	42	1660
pQtODC.12	32	0.8
pQtODC.12	42	0.2
HT289, no plasmid	32	0.4
dg98, no plasmid	32	7.0

Table 4-2
Recombinant *T. brucei* ODC Purification Scheme

Step	Specific Activity	Total Activity	Total Protein (mg)	Volume (ml)	%Recovery	Fold Purified
Crude Extracts						
1.	1460	2.6×10^5	190	20	-	-
2.	5840	3.8×10^5	64	13	-	-
Ammonium Sulfate						
1.	3900	1.8×10^5	50	8	71	2.7
2.	9800	1.8×10^5	16	8	50	2.0
Pyridoxamine Phosphate Affinity						
1.	2×10^6	$.4 \times 10^5$	.02	57	15	1375
2.	2.8×10^6	1.4×10^5	.04	40	34	500
Mono Q						
1.	3.2×10^6	$.32 \times 10^5$	.01	10	13	2200

Activity is measured in nmol CO_2/hr. Numbers 1 and 2 represent two different batches of heat-induced bacterial cultures.

Table 4-3
Comparison of Recombinant and Native *T. brucei* ODC

	Recombinant	Native
A. Kinetic properties		
$K_m$orn(μM)	303	244
K_IDFMO(μM)	154	178
$T_{1/2}$DFMO(min) (at 30°C)	3.9	5.8
Specific Activity of Purified Enzyme (nmol CO_2/hr/mg)	3.2×10^6	2.7×10^6
B. Physical properties		
subunit MW(kdal)	45	45
native MW(kdal)	92	90
isoelectric point	5.0	5.0

Figure 4-1: *In vitro translation and immunoprecipitation of T. brucei ODC. T. brucei* ODC was translated in a rabbit reticulocyte lysate system from RNA transcribed *in vitro* as described in Materials and Methods. Lane M, ^{14}C molecular weight markers(phosphorylase b,92.5 kdal;bovine serum albumin,69; ovalbumin, 46; carbonic anhydrase, 30; and lysozyme, 14) lane TL, total in vitro translation products; lane NI, in vitro translation products immunoprecipitated with non immune serum; lane I, in vitro translation products immunoprecipitated with rabbit anti-mouse ODC.

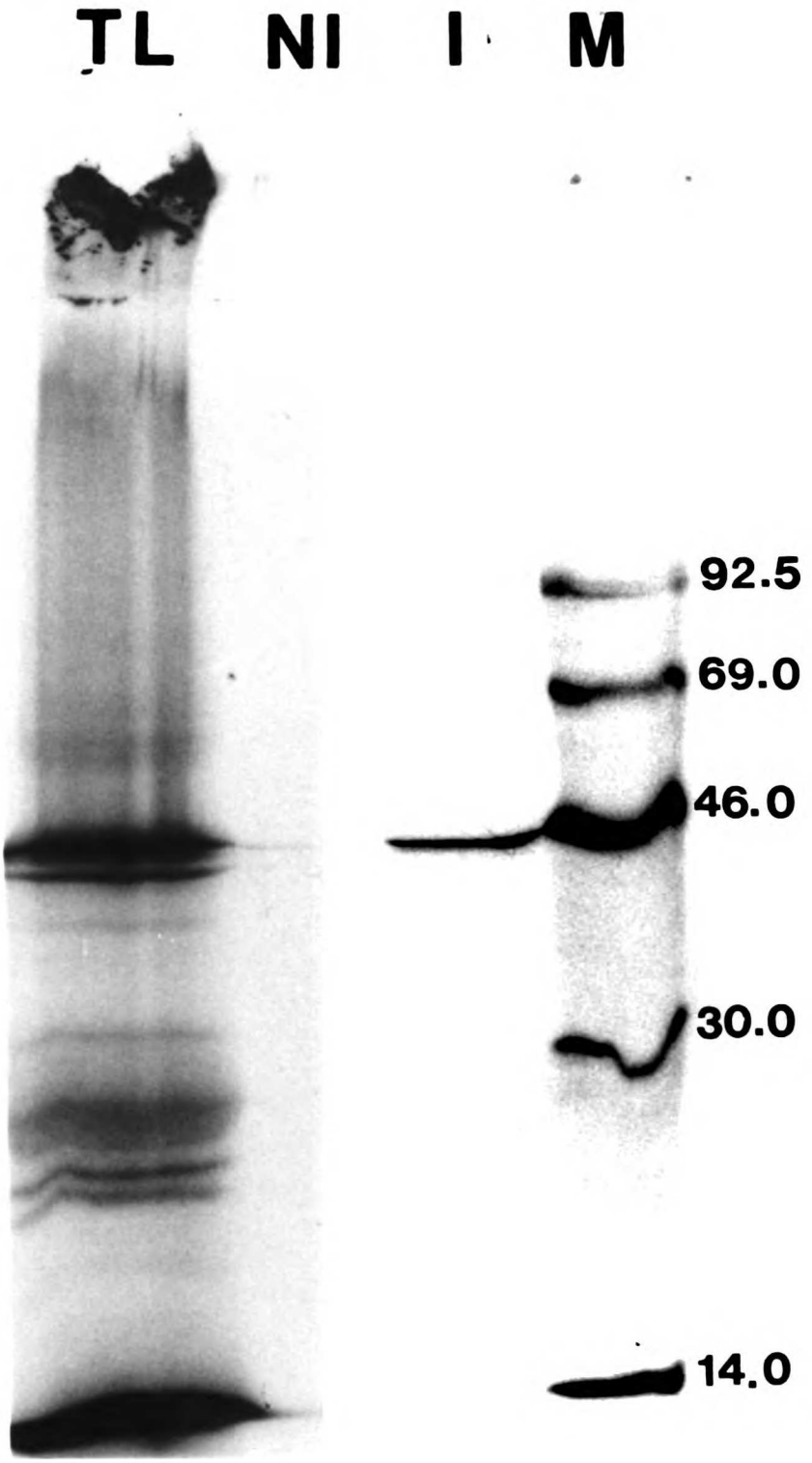
TL
NI
I
M
92.5
69.0
46.0
30.0
14.0

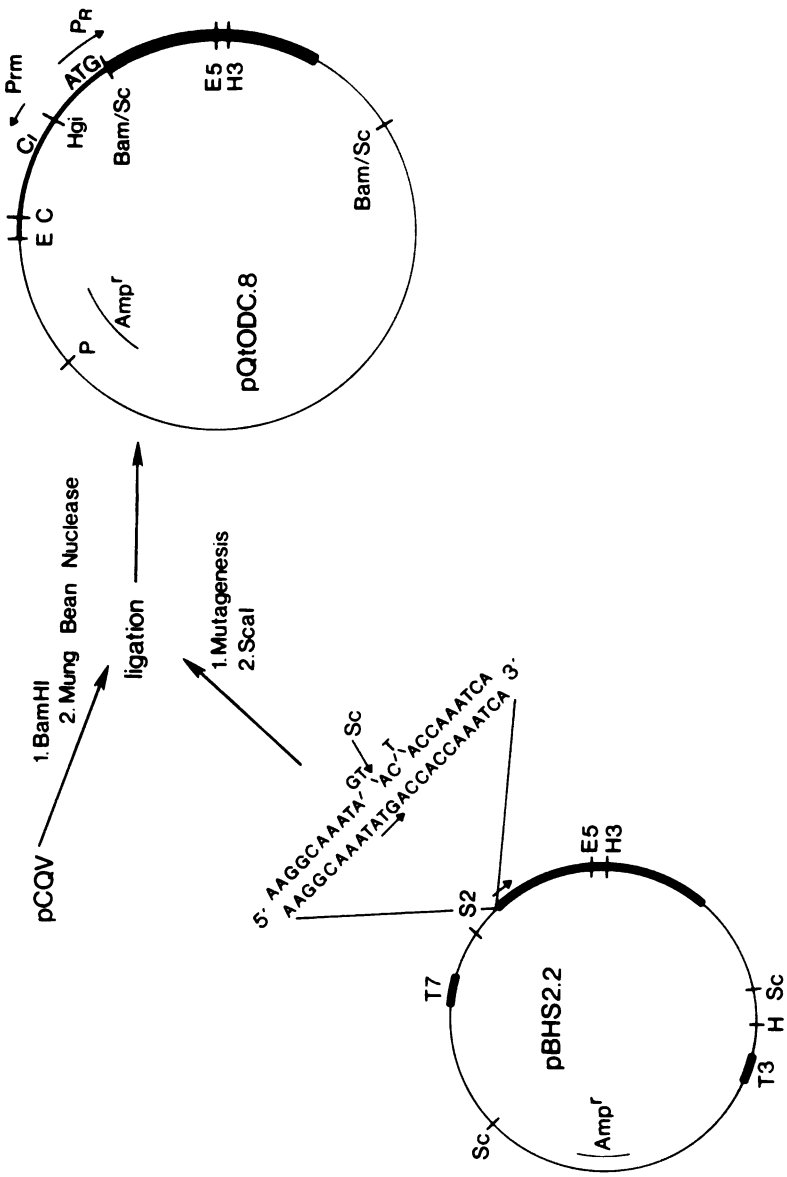

Figure 4-2: *Construction of ODC expression vector pQtODC.8.* A Sca I site was created in pBHS2.2 using the mutagenic primer drawn above the plasmid. Sca I digestion of the mutagenized plasmid gives a 1.8 kb fragment that was ligated to pCQV treated with BamH1 and mung bean nuclease, to yield pQtODC.8. Sc = ScaI, H3 = HindIII, E5 = EcoR5, H = Hinc II, Bam = Bam H1, The dark bar represents the *T. brucei* ODC structural gene.

Figure 4-3: *Turnover of T. brucei ODC produced in E. Coli HT289 cells.* HT289 cells containing either pQtODC.8 or pQtODC.12 were pulse labeled with 0.03 μM [^{35}S]- methionine followed by a chase with 1 mM cold methionine for varying time intervals. Lane A,J [^{14}C]- molecular weight markers (see figure 4-1); Lane B, [5^{14}C]-DFMO labeled ODC; lane C, pQtODC.12, 1 min pulse with [^{35}S]-methionine, 39°C; lane D, pQtODC.12, 1 min chase, 39°C; lane E, pQtODC.8, 1 min pulse , 32°C; lane F, pQtODC.8, 1 min pulse, 39°C; lane G, pQtODC.8, 1 min chase, 39°C; lane H, pQtODC.8, 5 min chase, 39 ^{o}C; lane I, pQtODC.8, 30 min chase, 39°C.

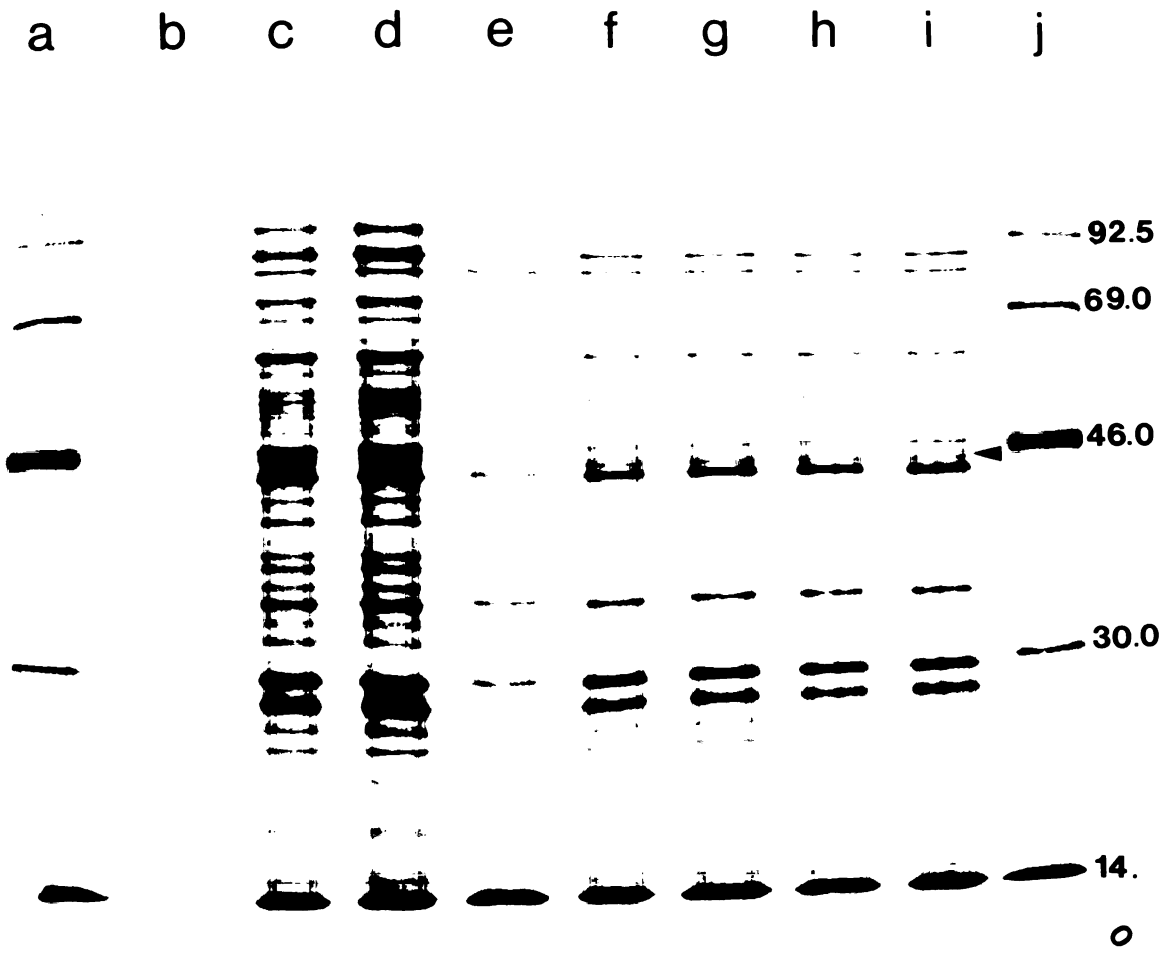
a
b
c
d
e
f
g
h
i
j
92.5
69.0
46.0
30.0
14.
0

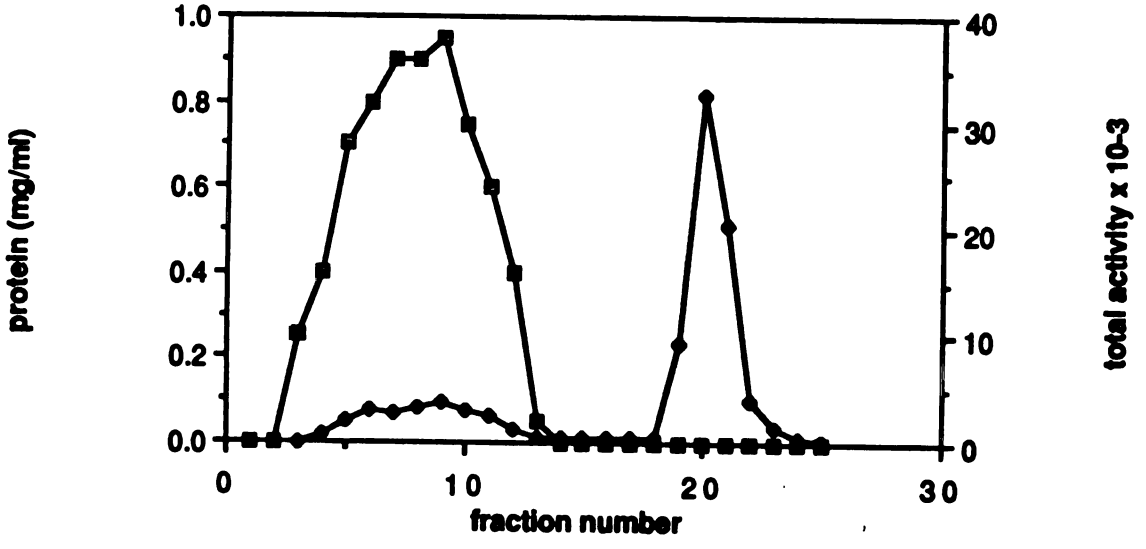

Figure 4-4: *Pyridoxamine phosphate affinity column elution profile.* ◊-◊, protein concentration in mg/ml, ◆-◆, ODC activity in nmol CO_2/hr/fraction.

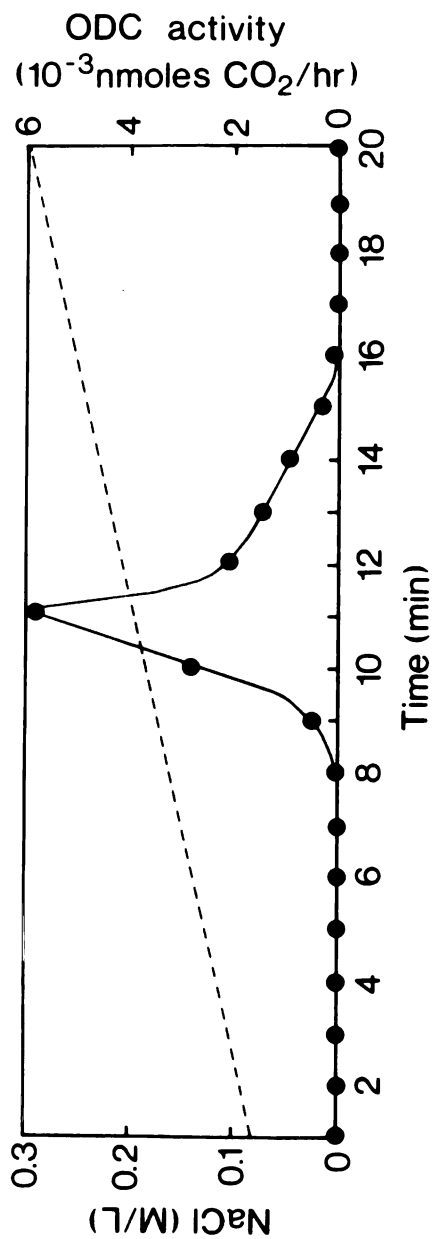

Figure 4-5: *Mono Q, anion exchange column elution profile.* - -, sodium chloride concentration, ●-● ODC activity.

Figure 4-6: *SDS-PAGE analysis of purified authentic and recombinant T. brucei ODC.* Lane A, authentic *T. brucei* ODC purified through the mono Q step ; Lane B, an autoradiogram of lane A, ODC had been labeled with [5-^{14}C]DFMO prior to loading onto the gel; lane C, an autoradiogram of lane D, ODC had been labeled with [5-^{14}C]DFMO prior to loading onto the gel; lane D, recombinant *T. brucei* ODC purified through the mono Q step; lane E, recombinant *T. brucei* ODC purified through the pyridoxamine phosphate affinity column step; lane F, recombinant *T. brucei* ODC purified through the ammonium sulfate fractionation step, lane G, crude extract, induced HT289 cells containing pQtODC.8; lane H, molecular weight (markers phosphorylase b, 92.5 kdal; BSA, 66.2 kdal;ovalbumin, 45 kdal;, carbonic anhydrase, 31 kdal; soybean trypsin inhibitor; 21.5 kdal and lysozme, 14.4 kdal). The gel was stained with Coomassie blue.

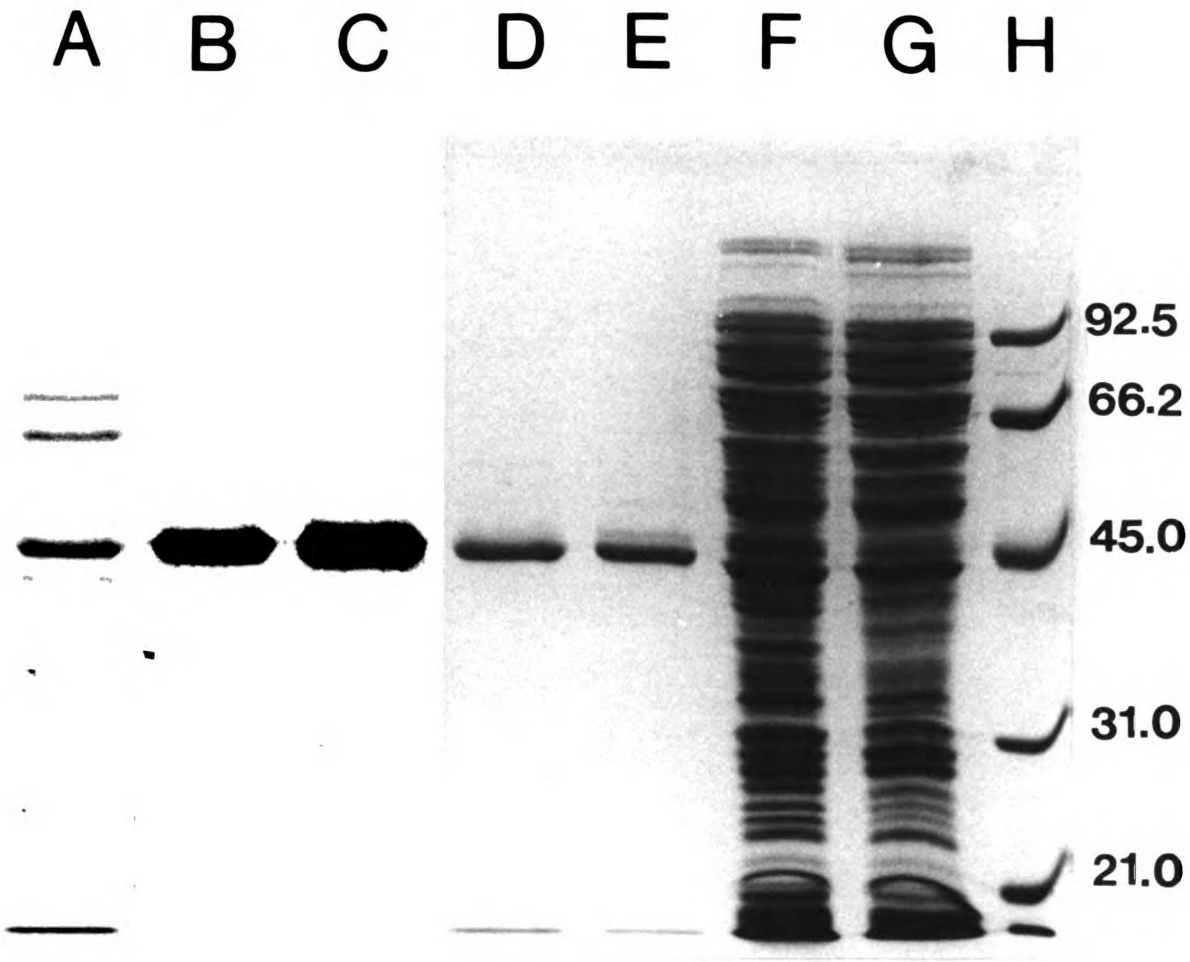
A
B
C
D
E
F
G
H
92.5
66.2
45.0
31.0
21.0

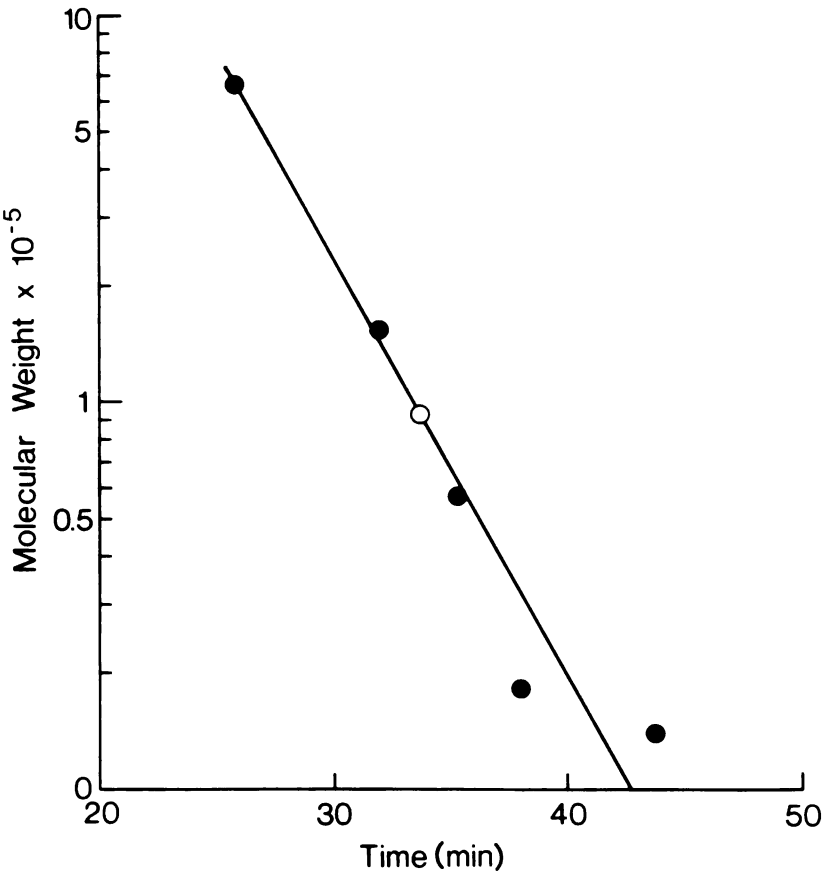

Figure 4-7: *Native molecular weight determination.* Purified ODC was mixed with Biorad standards and applied to a Superose 6 gel filtration column at a flow rate of 0.5 ml/min. Fractions collected every 0.2 min were checked for ODC activity. The elution time of the Biorad standards was plotted versus the molecular weight of the standards(●,Thyroglobulin, IgG,ovalbumin , myoglobin and vitamin B12) and the elution time of the peak ODC activity(o) was compared to that of the standard proteins.

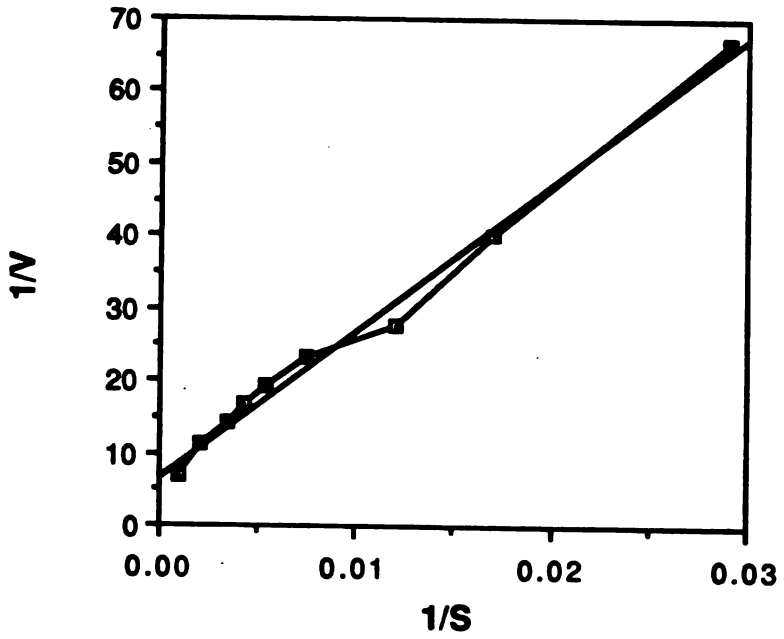

Figure 4-8: *Determination of the K_m for ornithine.* Lineweaver Burk analysis of the dependence of recombinant ODC catalyzed reaction rate(V, velocity nmol/min) on substrate concentration(S, L-ornithine concentration μM). ◊-◊ represents actual data points and the solid line represents the best fit line. The K_m for ornithine was calculated to be 303 μM from the best fit line y = 6.7 + 2028.3x..

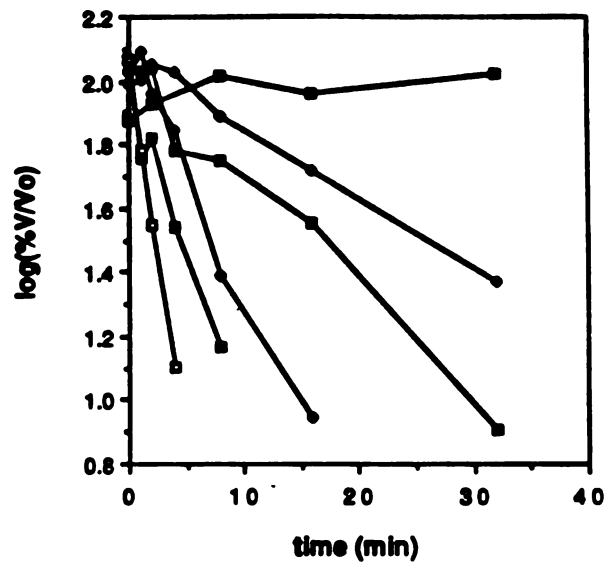

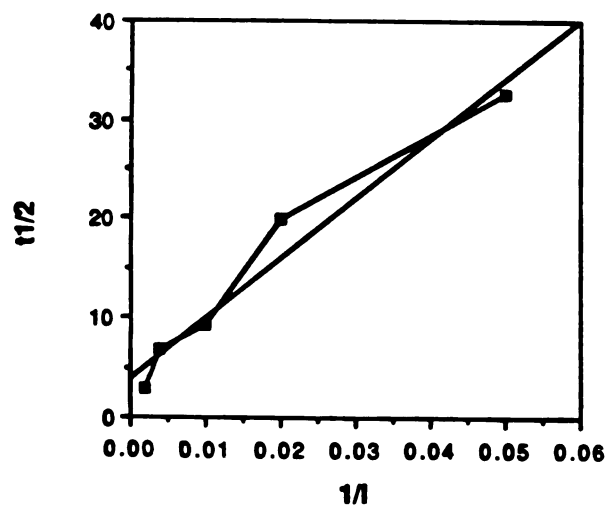

Figure 4-9: A. *Time dependence of DFMO inactivation of purified recombinant T. brucei ODC.* Log(activity) vs time of inactivation. ◊-◊, no DFMO control; ●-●, 20 μM DFMO; ♦-♦, 50 μM DFMO; ●-●, 100 μM DFMO; ♦-♦, 250 μM DFMO; and ◊-◊, 500 μM DFMO. B. *Determination of the K_I for DFMO.* Plot of halflife(t1/2). vs 1/I, ◊-◊ represents actual data and the solid line represents the best fit line. $T_{1/2}$ was calculated for each DFMO concentration (I, μM)using the equation for exponential decay. From this plot the K_I for DFMO(-1/x-intercept) was determined to be 154 μM and the $t_{1/2}$ at infinite concentration(y-intercept) of DFMO was determined to be 3.9 min.

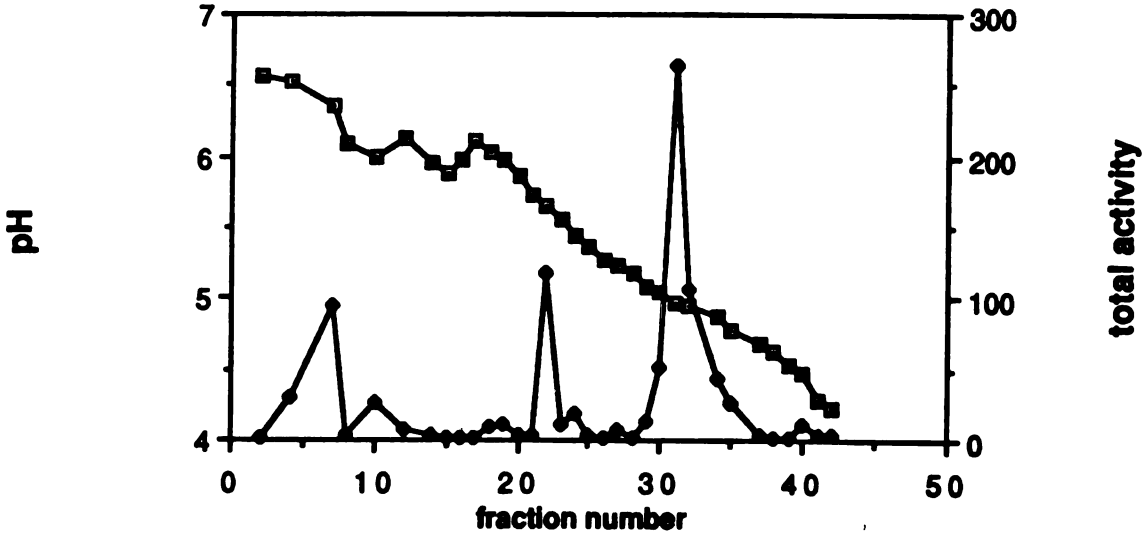

Figure 4-10: *Determination of the Isoelectric point of recombinant T. brucei ODC.* Purified ODC was loaded onto a mono P chromatofocusing column. The elution profile of ODC activity, ◆-◆ was compared to the pH ,◆-◆ of the fraction.

Conclusion

The major goals that were outlined in the introduction have been achieved. We were able to characterize *T. brucei* ODC at both the genomic level, through cloning and sequencing of the *T. brucei* ODC gene, and at the protein level through purification and characterization of *T. brucei* ODC from bloodstream trypomastigotes. In addition we were able to express the *T. brucei* ODC gene in *E. coli*, purify to apparent homogeneity the recombinant enzyme and show that it appears identical to the authentic *T. brucei* ODC.

As a result of this work we were able to postulate a mechanism for the selective toxicity of DFMO on the parasite over the mammalian host. As discussed in Chapter 2, mammalian ODC has a rapid intracellular turnover rate of 15-30 min and mammalian ODC contains two PEST regions which are predicted to play a role in rapid intracellular turnover of eukaryotic proteins. Through sequencing of the *T. brucei* ODC gene we were able to show that the PEST regions are not found in *T. brucei* ODC, predicting that the parasite enzyme would not be rapidly turned over. This hypothesis was verified *in vivo* ; we found that(Chapter 2) *T. brucei* ODC did not turnover during a 6 hr study. Thus, DFMO may be more toxic to the trypanosome because its ODC is stable whereas the mammalian enzyme is rapidly degraded and replenished thus diminishing the effects of DFMO inhibition. There are two aspects of this work that would be valuable to pursue . First though our data support the PEST hypothesis, it does not fully prove the validity of the PEST sequences as markers for rapid intracellular turnover. The trypanosome may simply not recognize the same signals for protein turnover as the mammalian cell, resulting in the observed differences in protein stability. The PEST hypothesis could be further tested by expressing the trypanosome ODC gene in a mammalian cell line and verifying whether it indeed is not rapidly turned over. This work is currently in progress. The postulate that the lack of *T. brucei* ODC turnover forms the basis for selective DFMO toxicity toward the parasite is likewise not proven. Unfortunately, the obvious experiments are not genetically feasible; (a) the selection of an ODC deficient strain of *T. brucei* that could be transformed with mouse ODC would not be easy ; and (b) foreign DNA has not yet been successfully introduced into *T. brucei*. Thus, these experiments will have to wait until genetic manipulation of the *T. brucei* genome becomes more advanced.

This work has also provided the tools that will be necessary in pursuing ODC regulation and the role of polyamines in *T. brucei* growth and differentiation. This information may lead to the discovery of alternative chemotherapeutic targets. The cloned DNA will provide a way to follow

levels of transcription during *T. brucei* growth and differentiation as well as during external manipulations of the parasite environment. The availability of large quantities of purified *T. brucei* ODC through the *E. coli* geneexpression system will also be essential to these types of studies because it will now be feasible to obtain antibody to *T. brucei* ODC, a useful tool for characterizing protein changes during growth and differentiation.

Lastly, the *E. coli* gene expression system will allow enough *T. brucei* ODC to be purified for this protein to become a model for studies on rational drug design, particularly if the crystal structure can be elucidated.

References

1) Katz, M., Despommier, D.D. and Gwadz, R.W. (1982) in *Parasitic Diseases* , 166-172,Springer-Verlag New York, inc.

2) Vickerman, K. (1985) *British Medical Bulletin*, 41, 105-114.

3) Greenwood, B.M. (1982), in *Cecil Textbook of Medicine,*1725-1728, Wyngaarden, J.B. and Smith, L.H. editors, W.B. Saunders Co.

4) Bacchi, C.J., Nathan, H.C., Hutner, S.H., McCann, P.P. and Sjoerdsma, A. (1980), *Science* 210, 332-334.

5) Sjoerdsma, A. and Schechter, P.J. (1984) *Clin Pharmacol Therap* 35, 287-300; Van Nieuwenhove, S., Schechter, P.J., Declercq, J. Bone, G., Burke, J. and Sjoerdsma, A.(1985) *Trans Roy Soc Trop Med Hyg* 79, 692-698; Taelman, H., Schechter, P.J., Marcelis, L., Sonnet, J., Kazyumba, G., Dasnoy, J., Haegele, K.D., Sjoerdsma, A., and Wery, M. (1987) *American Journal of Medicine* 82, 607-614.

6) Borst, P., Fase-Fowler, F., Frasch, A.C., Hoeijmakers, J.H. and Weijers, P.J. (1980) *Mol. Biochem. Parasitol.* 1, 221-246.

7) Wang, C.C. (1984) *J Med Chem Perspective* 27, 1-9.

8) Ross and Thomoson (1910), *Proc R Soc London (Biol) Sci* 82:411-415.

9) Turner, M.J.(1985), *Britich Medical Bulletin*, 41, 137-143.

10) Ferguson, M.A.J., Duszenko, M.,Lamont, G.S., Overath, P. and Cross, G.A.M. *J. Biol. Chem.* 261, 356-362.

11) Cross, G.A.M. (1987), *Cell* 48,179-181.

12) Fox, J.A., Duszenko, M., Ferguson, M.A.J., Low, M.G. and Cross, G.A.M. (1986) *J. Biol. Chem.* 261, 15767-15711.

13) Metcalf, P., Blum, M., Freymann, D., Turner, M. and Wiley, D.C. *Nature* 325, 84-86.

14) Van der Ploeg, L.H.T. (1987) *Cell* 51, 159-161.

15) Van der Ploeg, L.H.T. (1986) *Cell* 47, 479-480.

16) Johnson, P.J., Kooter, J.M. and Borst, P. (1987) *Cell* 51, 273-281.

17) Clayton, C.E. (1988), *Genetic Engineering*, in press.

18) Michels, P.A.M. (1986) *J. Mol. Evol.* 24, 45-52.

19) Russel, D.H. (1985) *Drug Metabolism Reviews* 16, 1-88.

20) Tabor, C.W. and Tabor, H. (1984) *Ann. Rev. Biochem.* 53, 749-790.

21) Gupta, M. and Coffino, P. (1985) *J. Biol. Chem.* 260, 2941-2944.

22) Kontula, K.K., Torkkeli, T.K., Bardin, C.W. and Janne, O.A. (1984) *Proc. Natl. Acad. Sci. USA* 81, 731-735.

23) Kahana, C. and Nathans, D. (1985) *Proc. Natl. Acad. Sci. USA* 82, 1673-1677.

24) Hivkok, N.J., Seppanen, P.J., Gunsalus, G.L. and Janne, O.A. (1987) *DNA*, 6, 179-187.

25) Fonzi, W. and Sypherd, P.S. (1987) *J. Biol. Chem.* 262, 10127-10133.

26) Chen, E.L. and Coffino, P. (1988), *Nuc. Acids Res.*, in press.

27) Heby, O. (1981) *Differentiation* 19, 1-20.

28) Isomaa, V.V., Pajunen, A.E.I., Bardin, C. W. and Janne, O.A. (1983) *J. Biol. Chem.* 258, 6735-6740.

29) Rose-John, S., Rincke, G. and Marks, F. (1987) *BBRC* 147, 219-225.

30) McConlogue, L., Dana, S.L. and Coffino, P. (1986) *Mol. and Cell. Biol.* 6, 2865-2871.

31) Persson, L., Holm, I. and Heby, O. (1986) *FEBS* 205, 175-178.

32) Holtta, E. and Pohjanpelto, P. (1986) *J. Biol. Chem.* 261, 9502-9508.

33) Glass, J.R. and Gerner, E.W. (1986) *Biochem. J.* 236, 351-357.

34) Tabor, C.W. and Tabor, H. (1985) *Microbiological Reviews* 49, 81-99.

35) Slotkin, T. A. and Bartolome, J. (1986) *Brain Research Bulletin* 17, 307-320.

36) Bacchi, C.J. (1981) *J. Protozool.* 28, 20-27.

37) Garofalo, J., Bacchi, C.J., McLaughlin, S.D., Mocdenhaupt, D., Trueba, G. and Hutner, S.H. (1982) *J. Protozool* 29, 389-394.

38) Bitonti, A.J., Bacchi, C.J., McCann, P.P. and Sjoerdsma, A. (1985) *Biochem. Pharmacol.* 34, 1773-1777.

39) Metcalf,B.W., Bey, P., Danzin, C., Jung, M.J., Casara, P., and Vevert, J.P. (1978) *J. Am. Chem.Soc.* 100, 2551-2553.

40) Bacchi, C.J., Garofalo, J., Mockenhaupt, D., McCann, P.P., Diekema, K.A., Pegg, A.E., Nathan, H.C., Mullaney, E.A., Chunosoff, L., Sjoerdsma, A., and Hutner, S.H. (1983) *Mol. Biochem. Parasitol.* 7, 209-225.

41) de Gee, A.L.W., McCann, P.P. and Mansfield, J.M. (1983) *J. Parasitol.* 69, 818-822.

42) Nathan, H.C., Bacchi, C.J., Hutner, S.H., Rescigno, D., McCann, P.P., and Sjoerdsma, A. (1981) *Biochem. Pharmacol.* 30, 3010-3013.

43) Fairlamb, A.H., Blackburn, P., Ulrich, P., Chait, B.T. and Cerami, A. (1985) *Science*, 227, 1485-1487; Fairlamb, A.H., Henderson, G.B., Bacchi, C.J. and Cerami, A. (1987) *Mol. Biochem. Parasitol.* 24, 185-191.

44) Feagin, J.E., Jasmer, D.P. and Stuart, K. (1986) *Mol. Biochem. Parasitol.* 20, 207-214.

45) Giffin, B.F., McCann, P.P., Bitonti, A.J. and Bacchi, C.J. (1986), *J. Protozool.* 33, 238-243.

46) Aman, R.A., Kenyon, G.L., and Wang C.C. (1985) *J. Biol. Chem.* , 260, 6966-6973.

47) Simpson, L. (1978) *J. Parasitol.* 64, 360.

48) Simpson, A.M., Hughes, D. and Simpson, L. (1985) *J. Protozool* , 32, 672-677.

49) Lowry, O.H., Rosenbrough, H.J., Farr, A.L. and Randall, R.J. (1951) *J. Biol. Chem.* 193, 265-275.

50) Janne, J. and Williams-Ashman, H.G. (1971) *J. Biol.Chem.* 216, 1725-1732.

51) Bitonti, A.J., Bacchi, C. J., McCann, P.P. and Sjoerdsma, A. (1986) *Biochem. Pharmacol.* 35,351-354.

52) Ghiotto, V., Brun, R., Jenni, L. and Hecker, H. (1979) *Exp. Parasitol.* 48, 447-456.

53) Midgley, M. (1983) *J. Gen. Microbiol.* 129, 2677-2679.

54) Visser, N. and Opperdoes, F.R. (1980) *Eur . J. Biochem.* 103, 623-632.

55) Carlsen, S.A., Till, J.E. and Ling, V. (1976) *Biocim. Biophys. Acta* 455, 900-912.

56) Gros, P., Neriah, Y.B., Croop, J.M. and Housman, D.E. (1986) *Nature* 323, 728-731.

57) Gros, P., Croop, J. and Housman, D. (1986) *Cell*, 47, 371-380.

58) Chen, C., Chin, J.E., Ueda, K., Clark, D.P., Pastan, I., Gottesman, M.M. and Roninson, I.B. (1986) *Cell* 47, 381-389.

59) Blin, N. and Stafford, D.W. (1976) *Nucleic Acid Res.* , 3, 2303-2308.

60) Bates,P.F. and Swift, R.A. (1981) *Gene* , 26, 137-146.

61) Maniatis, T., Fritsch, E.F., and Sambrook, J. (1982) *Molecular Cloning A Laboratory Manual* , 368-369.

62) Glisin, V., Crkvenjakov, R., and Byus, C. (1974) *Biochemistry* ,13, 2633-2637.

63) Ullrich, A. , Shine, J., Chirgwin, J., Pictet, R., Tisher, E., Rutter, W.J. , and Goodman, H.M. (1977) *Science* ,196 ,1313-1319.

64) Aviv, H. and Leder, P. (1972) *Proc. Natl. Acad. Sci. USA* , 69, 1408-1412.

65) Southern (1975) *J. Mol. Biol.* ,98, 503-517.

66) Rigby, P.W.J., Dieckmann, M., Rhodes, C., and Berg, P. (1977) *J. Mol. Biol.* ,113, 237-251.

67) Sanger, F. and Coulson,A.R. (1978) *FEBS Lett.*, 87,107-110.

68) Hattori, M. and Sakaki, Y. (1986) *Anal. Biochem.* ,152, 232-238.

69) Laemmli, U.K. (1970) *Nature* ,227, 680-685.

70) Macrae, M. and Coffino, P. (1987) *Mol. Cell. Biol.*, 7, 564-567.

71) Rogers, S. Wells, R., and Rechsteiner, M. (1986) *Science* ,234,364-368.

72) Sogin, M.L., Elwood, H.J., and Gunderson, J.H. (1986) *Proc. Natl. Acad. Sci. USA* , 83, 1383-13387.

73) Glass, D.J., Polvere, R.I. and Van der Ploeg, L.H.T. (1986) *Mol. Cell. Biol.*, 6, 4657-4666.

74) Miller, S.I., Landfear, S.M. and Wirth, D.F. (1986) *Nucleic Acid Res.*, 14, 7341-7360.

75) Phillips, M.A., Coffino, P. and Wang, C.C. (1987) *J. Biol. Chem.* 262, 8721-8727.

76) Bradford, M. (1976) *Anal. Biochem.*, 72, 248.

77) Seely, J.E. and Pegg, A.E. (1983) *Methods in Enzymology* 94, 158-161.

78) Choi, J.H. and Scheffler, I.E. (1983), *J. Biol. Chem.* 258, 12601-12608.

79) Seely, J.E., Poso, H. and Pegg, A.E. (1982), *Biochemistry*,21, 3394-3399.

80) Norris, K., Norris, F., Christiansen, L. and Fiil, N. (1983) *Nucleic Acids Res.* 11, 5103-5112.

81) Maniatis, T., Fritsch, E.F., and Sambrook, J. (1982) *Molecular Cloning A Laboratory Manual*, 313-314.

82) Queen, C. (1983) *J. Mol. and Appl. Gen.* 2, 1-10.

83) Tabor, H., Tabor, C.W., Cohn, M.S., and Hafner, E.W. (1981) *J. Bacteriol.* 147, 702-704.

84) Macrae, M. and Coffino, P. (1987) *Mol. Cell. Biol.* 7, 564-567.

85) Schoemaker, J.M., Brasnett, A.H. and Marston, F.A.O. (1985) *EMBO Journal* 4, 775-780.

86) Grosjean, H. and Fiers, W. (1982) *Gene* 18, 199-209.

87) Michels, P.M., Poliszczak, A., Osinga, K.A., Misset, O., Van Beeumen, J.,Wierenga, R.K., Borst, P. and Opperdoes, F.R. (1986) *EMBO J.* 5, 1049-1056; Osinga, K.A., Swinkels, B.W., Gibson, W.C., Borst, P., Veeneman, G.H., Van Boom, J.H., Michels P., and Opperdoes, F.R. (1985) *EMBO J.* 4, 3811-3817; Swinkels, B.W., Gibson, W.C., Osinga, K.A., Kramer, R., Veeneman, G.H., Van Beem, J.H., and Borst, P. (1986) *EMBO J.* 5, 1291-1298; Clayton, C.E., (1986) *EMBO J.* 4, 2997-3003.

88) Tschudi, C., Young, A.S., Ruben, L., Patton, C.L. and Richards, F.F. (1985) Proc. Natl. Acad. Sci., USA 82, 3998-4002.

89) Gibson, W.C. and Borst, P. (1986) *Mol. Biochem. Parasitol.* 18, 127-140; Kimmel, B.E., Samson, S., Wu, J., Hirschberg, R. and Yarbrough, L.R. (1985) Gene 35, 237-248.

OF CALIFORNIA, UNIVERSITY OF CALIFORNIA

FOR REFERENCE

NOT TO BE TAKEN FROM THE ROOM

BRODART CAT. NO. 23 012 PRINTED IN U.S.A.